12-2018

GENETIC EVOLUTION AND PROGNOSTIC DETERMINANTS OF PANCREATIC CANCER ON LONGITUDINAL LIQUID BIOPSIES

Vincent Bernard

Follow this and additional works at: https://digitalcommons.library.tmc.edu/utgsbs_dissertations

Part of the Gastroenterology Commons, Genomics Commons, and the Oncology Commons

**GENETIC EVOLUTION AND PROGNOSTIC DETERMINANTS OF PANCREATIC CANCER
ON LONGITUDINAL LIQUID BIOPSIES**

By

Vincent Bernard Pagan, MS

APPROVED:

_____
Anirban Maitra, MBBS
Supervisory Committee Chair

_____
Russell Broaddus, MD/PhD

_____
Stephen Hahn, MD

_____
Nicholas Navin, PhD

_____
Cullen Taniguchi, MD/PhD

_____
Eduardo Vilar-Sanchez, MD/PhD

_____

APPROVED

_____
Dean, The University of Texas

MD Anderson Cancer Center UTHealth Graduate School of Biomedical Sciences

GENETIC EVOLUTION AND PROGNOSTIC DETERMINANTS OF PANCREATIC CANCER ON LONGITUDINAL LIQUID BIOPSIES

A

DISSERTATION

Presented to the Faculty of

The University of Texas

MD Anderson Cancer Center UTHealth

Graduate School of Biomedical Sciences

in Partial Fulfillment

of the Requirements

for the Degree of

DOCTOR OF PHILOSOPHY

By

Vincent Bernard Pagan, MS

Houston, Texas

December, 2018

Dedication

To my wife, Marimar de la Cruz Bonilla, the Milas, and my parents, Lillibeth Pagan and Victor

Bernard.

Acknowledgments

I would like to start by saying thank you to my mentor, Dr. Anirban Maitra, for giving me the opportunity to work in his lab. He has provided me invaluable mentorship and experiences in not just research, but also in career and personal related aspects of science. He has given me the tools to pursue an independent career in science and ultimately becoming a better person who is empathetic to those individuals that are the reason we do what we do in the lab, the patients and their families. He has supported my career aspirations, and unconditionally had my back through every step of this process. I am thankful to have had a PhD advisor such as Dr. Maitra who has given me the time and freedom to grow as a scientist and an individual.

I thank my advisory committee members (Drs. Nicholas Navin, Russell Broaddus, Stephen Hahn, Eduardo Vilar-Sanchez, Cullen Taniguchi, and Jason Fleming) for taking time out of their busy schedules to provide exceptional advice and direction during the past several years. I would like to particularly thank Dr. Russell Broaddus, who has always puts trainees as his priority. He has provided me with numerous opportunities for career support and advancement and is someone who's advice I will always trust. I would also like to thank Dr. Cullen Taniguchi for his candid guidance which have given me significant perspective in becoming a physician scientist, and of course Astros tickets.

I am grateful to all the members of the Maitra lab (old and new). I have learned so much from you all. Particularly Anthony San Lucas, who took me under is wing and was an incredible postodoctoral fellow and day to day mentor. You always found, and even now find time to help with questions and anything I need. You introduced me to many tools that I've used for this dissertation and continue to use today. You are a stellar mentor and I hope others get the opportunity to learn from you as much as I did. I would like to thank our newest members, Paola Guerrero, Alex Semaan, and Jonathan Huang, you guys have made my life so much easier

during the past year by providing me support on my projects and taking on an incredible amount of responsibilities in the lab. You guys have made my life in the lab a lot more enjoyable.

I would like to thank my parents, Lillibeth Pagan and Victor Bernard. You have provided me unconditional love and support throughout all these years. It saddens my that my father will not be able to witness what years of this support have yielded in me due to his Alzheimer's, but know that I appreciate everything you have done for me. And to my mother, as a caregiver, I admire the sacrifices you've had to make in order to make sure I had every opportunity I needed to succeed, not just now, but throughout my life. I can't imagine how the past several years have been for you as an Alzheimer's caregiver, but know that this work would not have been possible without the values you have instilled in me.

Finally, I would like to thank my wife, Marimar de la Cruz Bonilla. You've taught me the importance of having a work like balance, however probable/improbable that may be at times. You always looked out for me, and have been my #1 fan throughout this whole process. You've challenged me mentally every part of the way throughout these PhD years which makes me have no doubt that you will be a stellar physician scientist. I'm incredibly proud of what you've been able to achieve, and look forward to you becoming a role model to other minority women in science, as you are to me. These past 8 years as a MD/PhD student have been an incredibly experience with you and of course Mila and Maia.

GENETIC EVOLUTION AND PROGNOSTIC DETERMINANTS OF PANCREATIC CANCER ON LONGITUDINAL LIQUID BIOPSIES

Vincent Bernard Pagan, MS

Advisory Professor: Anirban Maitra, MBBS

Pancreatic ductal adenocarcinoma (PDAC) has one of the lowest 5-year survival rates amongst solid tumors. As early detection of PDAC is unusual and typically incidental, most patients present with locally advanced and metastatic disease where effective therapeutic strategies remain a significant unmet need. Specifically, surrogate biomarkers for tumor monitoring of PDAC may lead to improved elucidation of clinical actionability and prognostic potential. On the other hand, tumor tissue is rarely sampled in patients presenting with *de novo* or recurrent metastatic PDAC, apart from a fine needle aspiration or a core needle biopsy performed for diagnosis. This precludes the opportunity for elucidating molecular underpinnings of cancer recurrence, chemoresistance, and therapeutic decision-making in advanced disease patients over the course of their therapy. For this reason, we aim to use so called "liquid biopsies" in the form of circulating nucleic acids and exosomes as a strategy that is amenable to longitudinal, relatively non-invasive sampling. Circulating tumor DNA and circulating exosomes contain genetic cargo representative of the neoplastic cells from which they are released and can serve as a reliable surrogate of the patient's tumor DNA, enabling a new way of interrogating cancers. We demonstrate that serial quantitative measurements of these tumor nucleic acid sources in circulation can provide clinically relevant predictive and prognostic information in pancreatic cancer patients, including anticipation of impending disease progression and putative mechanisms of resistance to ongoing therapy. We also describe our ability to specifically capture tumor material in circulation following a comprehensive characterization of the pancreatic cancer exosomal "surfaceome". By leveraging an immune-capture approach paired with ultrasensitive molecular barcoding techniques, we are able to increase our sensitivity of detection of rare

molecules in circulation that are derived from the tumor. Ultimately, this has implications for stratification of patients into therapeutic "buckets" through a personalized approach that may lead to greater survival benefits in PDAC.

Chapter 3 – Liquid biopsies for detection of early stage pancreatic cancer 44

Chapter 4 – Predictive and prognostic utility of liquid biopsies in pancreatic cancer

Chapter 5 – Whole genome, exome, and transcriptome profiling of liquid biopsies

List of Figures

List of Tables

Chapter 1 – Introduction

Chapter 1 – Introduction

Pancreatic Cancer

Although rare (2% of cancer cases), pancreatic ductal adenocarcinoma (PDAC) is the fourth leading cause of cancer-related deaths in this country. In contrast to the decline of cancer related deaths from other malignancies, the alarming rise in incidence of PDAC is projected to make it the second leading cause of cancer related death by 2030 (1). The relatively equal incidence and mortality rates in PDAC have led to its dire prognosis, with a 5-year survival rate of only 4% (2). The lethality of PDAC is attributed in part to the lack of early detection, with the majority of patients (~85%) presenting with locally advanced or metastatic disease. Diagnosis at these late stages is due to the absence of specific symptoms and clinical findings due to its retroperitoneal location, and a lack of serological tests that are sufficiently sensitive and specific. In addition, the therapeutic landscape of PDAC is limited, with Gemcitabine and FOLFIRINOX (folinic acid, fluorouracil, irinotecan, and oxaliplatin) being the two main regimens with low overall response rates. The main oncogenic driver mutation, observed in >90% of PDAC, *KRAS* (v-Kiras2 Kirsten rat sarcoma viral oncogene homolog) has also compounded its poor survival rate due to its "undruggability"; although chemotherapeutic strategies may exist in certain targetable cases as discussed below.

Advances in next generation sequencing (NGS) technologies have allowed for a detailed insight into the genomic landscape of PDAC, in order to better understand how molecular alterations contribute to disease initiation and progression. In particular, dissecting the molecular events involved in the progression of PDAC from pancreatic intraepithelial neoplasia (PanINs) lesions to invasive carcinoma, are being achieved with possible implications to targeted therapeutic approaches.

Multi-step progression of PDAC

The progression of PDAC from a normal cell to an invasive adenocarcinoma involves the accumulation of inherited and/or acquired mutations throughout the span of up to approximately 20 years (3). This highlights the importance of exploiting this window of progression to develop new screening methods to provide curative surgical approaches. This progression involves the evolution of histologically recognized precursor lesions known as pancreatic intraepithelial neoplasias (PanINs). As of date of this publication, the categorization of PanIN is divided into low grade (PanIN-1A and 1B), intermediate (PanIN-2), and high-grade PanIN-3)(4), although there is an emerging consensus in the clinical research community to move to a simplified two-tier classification of "low" grade (PanIn-1 and -2) and "high" grade PanINs (PanIN-3). This is based on observations that, while PanIN-1 and-2 lesions can be found even in the absence of cancer, PanIN-3 is almost never found without concomitant invasive neoplasia. Genetic alterations can be grouped into those that arise in precursor lesions and are usually, albeit not always, found in the concomitant PDAC, *versus* those that arise during subclonal evolution of the infiltrating carcinoma resulting in genetic heterogeneity.

One of the earliest genetic events involved in PDAC pathogenesis is an activating point mutation in the *KRAS* oncogene, an oncogenic driver mutation found in more than 90% of all PDACs. Subsequent genetic aberrations include inactivation of tumor suppressor genes including *CDKN2A*, *TP53*, and *SMAD4*, which encode for p16^{INK4A}, p53, and Smad4, respectively, and contribute to the histological evolution of these precursor lesions. Together, these four alterations comprise the "big four" in PDAC, although many other recurrent somatic mutations are found in lower frequencies (5-10%) of cases, including those that afflict particular functional pathways in the cancer cell, such as DNA damage repair or chromatin regulation.

Among the population of noninvasive precursor lesions, it is also important to recognize intraductal papillary mucinous neoplasms (IPMNs) and mucinous cystic neoplasms (MCNs). Although histologically distinct from the microscopic PanIN lesions, these cystic precursor lesions share similar diver mutations including point mutations in the KRAS oncogene(5), and inactivating mutations in p53 and p16, with SMAD4 loss typically not being found in IPMNs (6,

7). Among the unique drivers found in both IPMNs and MCNs, are inactivating mutations in *RNF43*, encoding for an ubiquitin ligase that has a role in WNT signaling inhibition(5). IPMNs also contain point mutations in the *GNAS* gene, which result in constitutively active guanine nucleotide-binding protein due to loss of intrinsic GTPase activity preventing hydrolysis of GTP (8).

KRAS

Under physiological conditions, activation of Ras protein is induced through growth factor receptor signaling, which promotes Ras activity through transitory binding to GTP. This results in the interaction of Ras with a variety of downstream effectors that govern proliferation, cell division, survival, and gene expression such as the RAF-mitogen-activated protein kinase and phosphoinositide 3-kinase pathways (9). Through an intrinsic GTPase mechanism and GTPase-activating proteins, Ras can then hydrolyze GTP to GDP to inactivate itself. It is this intrinsic GTPase activity that is altered in the activating point mutation of *KRAS,* which results in an inability to hydrolyze GTP allowing for a constitutively active protein that no longer relies on external stimuli. The most common "hotspot" mutation in the *KRAS* oncogene occurs at codon 12, followed by codon 13, and less frequently codon 61; emerging genomic data suggests that the specific codon involved might have an impact on disease prognosis, underscoring differences in Ras function (10, 11).

Telomere shortening

Telomeres are repetitive nucleoprotein complexes found at the end chromosomes that have a role in genomic stability by protecting against chromosomal degradation and chromosome end fusion. In PDAC, shortened telomeres lengths that potentially lead to chromosomal abnormalities can be detected in early lesions such as IPMNs and nearly universally in all PanINs

(12). Genomic instability of this kind will typically lead to cell death unless cells are able to inactivate tumor suppressor mechanisms as described below.

CDKN2A

The most commonly mutated tumor suppressor in PDAC (~95%) is an inactivation of *cyclin-dependent kinase inhibitor 2A* gene (*CDKN2A*), encoding for the cell cycle checkpoint protein, p16[INK4A](13). Inactivation of CDKN2A in PDAC can occur via several different mechanisms, including mutation, genomic deletions, and promoter hypermethylation resulting in epigenetic silencing. (14). The encoded protein p16[INK4A] functions as a cyclin-dependent kinase inhibitor, specifically of CDK4 and CDK6 thereby preventing the phosphorylation of the retinoblastoma protein and blocking G1-S transition(15). Loss of this protein thus results in unregulated cell cycle transition.

TP53

Aberrations of *TP53*, which encodes for p53, are typically a later event in the multi-progression of PDAC, often arising in PanIN-3 lesions, and is mutated in up to 70% of tumors(16). As the master guardian of the genome, p53 is involved in cell cycle arrest, DNA repair, blocking of angiogenesis, and induction of apoptosis in response to DNA damage or environmental stressors. Loss of this protein allows for DNA damage and external stressors to go unchecked, thereby promoting genomic instability and aberrant proliferation.

SMAD4

SMAD4 (DPC4, SMAD family member 4 gene), which encodes for the Smad4 protein, is inactivated in approximately 50% of PDACs as a late event in its progression (PanIN-3 – Carcinoma) (17). As a downstream effector of transforming growth factor-β (TGF- β), loss of SMAD4 activity leads to tumor promotion by relieving the growth inhibitory effect of TGF- β signaling (18).

Clinical Relevance of Core PDAC Mutations

Although pancreatic cancers have been shown to harbor an average of 63 genetic mutations, the genomic landscape of PDAC is faithfully represented by these four genomic mutations (KRAS, CDKN2A, TP53, and SMAD4)(10). The high degree of mutational concordance at these four loci between primary and metastatic sites of individual cancers (19) suggests these are so-called founder mutations. This describes a mutation present in all samples from a single patient, thus sharing a common ancestor, which likely originated during PanIN progression (3, 12). Of note, PDACs continue to accumulate genetic alterations through subclonal evolution throughout their natural history, the vast majority of which are so-called "passenger" mutations that have little functional impact on progression, while a minor fraction are so-called "progressor" mutations, and do have a deleterious consequence on disease progression. In any case, a variable combination of the "big four" is altered in most PDAC cases, with nearly all cancers showing at least *KRAS* mutations in conjunction with one or more of the three tumor suppressors. Yachida et. al. describe correlations of the status of these 4 genes to disease progression, metastatic failure, and overall survival, with patients with 3-4 of these mutated driver genes demonstrating worse overall survival (19). When looking at the genes individually, there is no significant difference in outcome in patients with *KRAS* and *CDKN2A* mutations, but *TP53* and *SMAD4* mutations were evidently associated with widespread metastatic disease and worse clinical outcomes (20, 21). In particular, SMAD4 status in PDAC (measured using immunohistochemical expression for the Smad4 protein) is being used to provide guidance towards tailoring treatment with systemic chemotherapy, as patients with Smad4-null tumors are most likely to develop widely metastatic disease. (22).

Germline Variants

With estimates of 10% of PDAC patients having a family history of the disease, elucidation of the PDAC genome has also contributed towards risk assessment and early detection in the

context of familial pancreatic cancers(23, 24). Among hereditary pancreatic cancer susceptibility genes, *STK11/LKB1*, associated with Peutz-Jegher syndrome, is correlated with one of the highest risks of familial pancreatic cancers with approximately 132x relative lifetime risk (25). *PRSS1* and *SPINK1* germline mutations are seen hereditary pancreatitis families with a 50-80x relative lifetime risk, or 30-44% risk, of developing PDAC (26-28). *P16/CDKN2A* germline mutations, associated with familial atypical multiple mole melanoma syndrome (FAMMM), entails a 38x (17% lifetime risk) increased risk of developing PDAC (29). Additional germline variants associated with increased PDAC risk are clustered into defects of DNA repair pathways. This includes members of the Fanconi anemia pathway such as FANC-C, FANC-G, and PALB2, whose encoded proteins interact with that of BRCA2, and are associated to young onset pancreatic cancer (30). BRCA1/BRCA2 mutations, which are associated with familial breast and ovarian cancers, have a 3.5-10x estimated relative risk (31-33). Lynch syndrome, caused by mutations in DNA mismatch repair (MMR) genes, MLH1, MSH2, MSH6 or PMS2, have an estimated 3.68% lifetime risk (34). Patients with ATM (Ataxia telangiectasia mutated) germline mutations have also demonstrated a predisposition for PDAC (35). Further elucidation of additional genes associated with familial PDAC may have implications for risk assessment and surveillance in affected family members. Detection of these germline mutations in patients is also important in the context of therapy as a way to exploit synthetic lethal interactions in the case of DNA repair pathways as described below.

Core Signaling pathways in pancreatic cancer

Large scale sequencing efforts have uncovered novel mutated genes in PDAC, as well as revealing multiple core signaling pathways that are affected throughout its carcinogenesis. In 2008, Jones et. al. performed polymerase chain reaction (PCR)-based exome sequencing of primary and metastatic tumors (10). Their data supported the role of the 4 main genetic drivers in pancreatic cancer, KRAS, CDKN2A, TP53, SMAD4, and identified genetic alterations in many other critical pathways recognized as "hallmarks of cancer", at least some of which appear to

have a prognostic influence in subsequent studies (11, 36). The core "hallmarks of pancreatic cancer" pathways that appear to be targeted in PDAC are highlighted in **Table 1** with some salient examples of genes mutated in each pathway.

Table 1: Core hallmarks of pancreatic cancer pathways

Apoptosis	**CASP10, VCP, CAD**
DNA damage control	**TP53, RANBP2, EP300**
Regulation of G1/S phase transition	**CDKN2A, FBXW7, APC2**
Hedgehog signaling	**GLI1, GLI3, BMPR2**
Homophilic cell adhesion	**CDH1, CDH2, CDH10, PCDH15**
Integrin signaling	**ITGA4, ITHA9, LAMA1, FN1**
C-Jun N-terminal kinase signaling	**MAP4K3, TNF, ATF2**
KRAS signaling	**KRAS, MAP2K4, RASGRP3**
Regulation of invasion	**ADAM11, ADAM12, DPP6, MEP1A**
Small GTPase-dependent	**PLXNB1, AGHGEF7, PLCB3, RP1**
TGF-B signaling	**SMAD4, SMAD3, TGFBR2, BMPR2**
Wnt/Notch signaling	**MYC, GATA6, WNT9A, MAP2, TCF4**

The altered genes in these respective pathways varied among separate patient tumors, such as the TGF-B pathway being altered by a *SMAD4* mutation in one patient *versus* a *BMPR2*

mutation in another, but the pathway in itself is often altered among samples. With this new global view of the PDAC genome as a set of a specific and limited number of pathways involved, we can begin to simplify the genetic heterogeneity that is intrinsic to these tumors and develop strategies to target the physiological effects of the mutations rater than the specific mutations themselves. By targeting key nodes involved in these pathways, such as the impaired ability to repair DNA, or altered cell cycle control, we may be able to circumvent the inevitable resistance that these tumors develop following targeted gene therapies.

In 2012 Biankin et. al. performed next generation sequencing of whole exomes and copy number analysis of primary resected PDAC from 142 patients, under the umbrella of the International Cancer Genome Consortium (ICGC) (37). This study reaffirmed the core signaling pathways identified by Jones et. al. (10), and also discovered novel mutated genes in these core signaling pathways including those involved in DNA damage repair (ATM), which is also shown to have a role in familial PDAC. Novel gene signatures were also identified in axon guidance pathway genes (SLIT/ROBO signaling) which are known to have a role in neuronal migration and positioning during embryogenesis with potential implications in cancer cell survival, growth, invasion and angiogenesis (38). Deregulation of these axon guidance genes was shown to have a role in tumor initiation and progression in the context of PDAC. Particularly, low ROBO2 or high ROBO3 expression was seen to be associated to poor patient survival. High expression of Semaphorin signaling molecules, specifically SEMA3A and PLXNA1 were also determined to be associated with poor patient survival. The ICGC team's methodology provided them the opportunity to identify potential novel drivers of pancreatic cancer, and new nodal signaling targets involving axon guidance, where therapeutics are currently developed for neuronal regeneration after injury (39). Again, we see the importance of developing therapeutics based on molecular phenotypes as further elucidation of genetic heterogeneity provides a cumbersome picture of pancreatic cancer.

In 2015, the next iteration of the ICGC PDAC dataset was published by Waddell et. al, who performed whole genome sequencing and copy number variation analysis of 100 PDACs, and

demonstrated chromosomal rearrangements that led to genetic aberrations(40). These structural rearrangements led to gene deletions, amplifications and fusions that are associated with driving carcinogenesis while presenting opportunities for clinical actionability and biomarkers of therapeutic response for platinum based chemotherapies. This led to the classification of PDACs into 4 subtypes based on structural rearrangement profiles **(Table 2).**

Table 2: PDAC structural rearrangements profiles

Stable	Small number of structural rearrangements (<50) with defects in cell cycle characterized by aneuploidy.
Locally rearranged	Presence of intra-chromosomal rearrangements classified as complex: leading to chromothripsis or breakage-fusion-bridge cycles; or focal copy number gains in genes such as KRAS, SOX9, GATA6 and potential therapeutic targets like ERBB2, MET, CDK6, PIK3CA, and PIK3R3.
Scattered	Chromosomal aberrations due to structural rearrangements (50-200) throughout the genome.
Unstable	Widespread structural rearrangements (>200) with genomic instability pointing towards somatic or germline deleterious mutations in DNA maintenance pathways (e.g. BRCA1, BRCA2, and PALB2) which suggest sensitivity to DNA damaging agents. A subset of these patients who were treated with platinum based therapy at tumor recurrence demonstrated robust or exceptional responses.

In addition to the classic "big four" and alterations in genes whose products are involved in DNA maintenance, the Waddell et al study highlighted the emerging importance of chromatin regulatory genes in the pathogenesis of PDAC. In particular, mutations of genes whose encoded proteins are involved in histone modification (*MLL2, MLL3, KDM6A*) and SWI/SNF genes that regulate how DNA is packaged in nucleosomes. (*ARID1A*, *ARID2*) emerged as a family of driver genes with unequivocal significance in PDAC. A recent whole exome study of resected PDAC patients by Sausen et. al. found strikingly favorable impact of harboring MLL2 or MLL3 mutations in the corresponding tumor, although the functional basis for this observation is still being elucidated (36). Inactivation of other tumor suppressors such as ROBO1, ROBO2, SLIT2, and RNF43 also demonstrate the role of aberrant WNT signaling in PDAC, as well as the potential for sensitivity that these mutations may confer to WNT inhibitors (41).

Overall, the recent series of exome studies in PDAC have suggested that a major mechanism of genomic instability and damage in pancreatic cancer involves structural variations and their potential clinical relevance. This supports the role of platinum based regimens such as FOLFIRINOX in a subgroup of patients that are both able to tolerate the regimen and contain a signature of impaired DNA maintenance pathways due to an unstable structural rearrangement phenotype within their tumors. It may also provide a model for patient stratification for PARP-1 inhibitor therapy as current clinical trials are predominantly restricted to patient populations with BRCA1 and BRCA2 germline defects. This new model also allows for a surrogate measure of defects in DNA maintenance where there may be a larger population that may benefit from such therapies who have non-BRCA pathway gene mutations, but whose unstable tumor subtype suggests sensitivity to DNA damaging agents.

More recently, Bailey et. al. have used exome and RNA profiling on 450 PDAC samples in the ICGC cohort to define 4 subtypes of PDAC based on differential gene expression signatures with distinct biological underpinnings: Squamous, Pancreatic Progenitor, ADEX (aberrantly differentiated endocrine exocrine) and Immunogenic (*unpublished data, Biankin et al personal communication*). While each of these molecular subtypes is enriched in a particular histological

variant (for example, the nom de plume for Squamous subtype arising from its enrichment of adenosquamous carcinomas in this subset), the intent of this expression signature is to tease out biological distinctions that might underlie PDACs that look identical at the morphological level. Not surprisingly, as is being increasingly noted across pan-cancer profiling datasets, there exists striking molecular similarities between subtypes across cancer types than within subtypes in a single cancer. Thus, the squamous subtype of PDAC has greater similarities to the so-called basal type cancers observed in head and neck and triple negative breast cancers (characterized by a overriding p63-driven signature) than to the other three PDAC subtypes.

Among clinical actionability in these subtypes, MYC amplifications have been found to be associated to the adenosquamous subtype with a correlation to poor survival (11). Also, appreciable differences in roles of the immune system can be identified, which may lead to exploiting immunotherapeutic strategies. In the case of the squamous subtype, a loss of cytotoxic T cells was associated with an increase in Toll-like receptors, CD4+ T cells and macrophages, as well as high expression of CTLA4 and PD1 immunosuppressive pathways. Stratification based on these subtypes may thus assist in clinical trial patient selection for therapeutics such as PD1 and CTLA4 checkpoint inhibitors to decipher their potential role in this disease.

Many of these recent global sequencing efforts provide a biomarker-based approach in order to identify surrogates for prognostic and therapeutic stratification. As most of the sequencing data provided was performed on patients with surgically resectable primary tumors *versus* those undergoing recurrence or falling into the locally advanced or metastatic category, the complete picture of PDAC remains limited to a small subset of patients (~15%). Still, these efforts provide proof of concept on how measures of aberrant molecular mechanisms may inform clinical actionaibility using next generation sequencing techniques.

New promising strategies involving liquid biopsies are being developed as noninvasive methods of disease detection and monitoring (42, 43). Specifically, through the use of circulating tumor DNA (ctDNA) that is released in the blood by primary and metastatic tumors, one can theoretically obtain a full representation of the tumor heterogeneity that is present within each

patient. Sausen et. al. demonstrated that somatic mutation calling can be made from ctDNA in PDAC patients to determine presence of subclinical, residual or recurrent disease following surgical resection. Detection of this ctDNA was correlated to disease progression that even predated standard computed tomography imaging by an average of 6 months, suggesting that there may be an ability to treat subclinical disease before it is overtly clinically evident based on imaging (36). Using ultrasensitive digital PCR techniques, ctDNA was detected in 43% of surgically resectable (i.e. lower stage) PDAC patients at the time of diagnosis. Although this study did not examine pre-diagnostic samples in patients prior to a clinical manifestation of disease, nonetheless, it provides a potential screening approach through which high-risk patients, such as those with family history or germline mutations, can undergo non-invasive surveillance for the emergence of PDAC in time for curative surgical options.

Liquid biopsy has also shown promise in being able to genomically characterize tumors, and predict chemotherapy response and resistance using next generation techniques through both ctDNA and circulating tumor cells (CTCs) (44-46). One can thus begin to imagine how tumor evolution and the emergence of new dominant clones can be identified using these methods to guide therapeutic decisions in real time.

Using genomic sequencing to guide therapy

The genetic heterogeneity of PDAC as presented above is unequivocally one of the many significant contributors to the intrinsic and acquired resistance that is characteristic of these cancers (47). Targeting of subclonal populations will only lead to transient effects on tumor burden, thus new strategies are required for therapeutic targeting of core pathways that are induced by founder events. By targeting convergent phenotypes that can be elucidated through genome sequencing of patient tumors, genomic information has the potential to guide individual patient therapies and outcomes (48, 49).

In patients with familial PDAC, information of deleterious germline variants may provide some success in the cases of gene mutations in double strand break repair pathways by using therapeutics aimed at compromising additional DNA repair mechanisms such as platinum based

therapies, mitomycin C, and PARP-1 (poly (ADP-ribose) polymerase 1) inhibitors(50-52). By exploiting synthetic lethal approaches, which result in cancer-specific cell death through exploitation of cancer-specific molecular aberrations, one can target base excision repair through PARP-1 inhibition, leading the accumulation of chaotic DNA damage (53-55).

The ideal gene target in PDAC is Ras itself as it is the main oncogenic driver in more than 90% of these tumors, but efforts have so far proven ineffective (56, 57). Synthetic lethality screens for *KRAS* have not been successful, but there has been some data suggesting possible targeting of its downstream effectors such as the MEK-ERK MAPK and AKT (protein kinase B) signaling pathway (58); unfortunately, recent clinical trials have shown unacceptable levels of toxicities in humans when two downstream Ras effectors are inhibited (59). In the small subset of PDAC identified as harboring wild type KRAS, sequencing studies have found mutations in genes encoding RAS effector proteins including *PIK3CA* and *BRAF* (11). In this small subset of cases, targeted therapies using BRAF and PI3 kinase inhibitors may beneficial.

Further work still remains to be done to determine all key components that drive PDAC. Exploiting nodal signaling pathways vs. attacking genetic heterogeneity head on, may be the best strategy in overcoming the advantages pancreatic cancers have over current treatment regimens. For now, stratification of subsets of patients based on defined molecular markers into clinical trials may prove beneficial in demonstrating the effectiveness of targeted therapies in these populations.

Clinically relevant concepts in pancreatic cancer

While early diagnosis of PDAC remains is an unequivocal unmet need, the clinical reality is that 85% of patients present with locally advanced or distant metastatic (Stage 3 or 4) disease, rendering their cancers inoperable. The standard of care for clinical follow up in PDAC patients, for both *de novo* advanced and recurrent tumors, is to use imaging and one biochemical marker (CA19-9). The reasons for this are manifold, including the difficulties of repeatedly sampling a

visceral site, the costs involved for an inpatient biopsy (easily in the range of $10,000 in most academic centers), and the lack of insurance reimbursement for tissue acquisition beyond the initial diagnostic workup. As a result, patients with *de novo* advanced or recurrent disease are treated empirically, with minimal insights into genomic underpinnings of treatment failure, in contrast to diseases like lung cancer or melanoma, where tissue accessibility has allowed elegant mapping of secondary mutations. In passing, it is also worth noting that the paucity of tissues from advanced PDAC patients is an important reason why the pioneering exome sequencing studies in PDAC, as well as the ongoing TCGA effort, are almost entirely focused on surgically resected tumors.

Given the visceral location of the pancreas, the only biomarker strategy amenable to widespread application in the community and to repeated sampling for monitoring treatment progress, is one that is **blood-based**, since direct tissue biopsy involves skillful and expensive medical procedures not applicable for general population screening or monitoring. In terms of currently available blood-based biomarkers for PDAC, measurement of the glycoprotein CA19-9 is the only FDA approved assay for diagnosis and monitoring. However, in *symptomatic* patients, CA19-9 only has a sensitivity and specificity that ranges in the 70-90%. Thus, it is clearly suboptimal for diagnosis in asymptomatic patients, which is the eventual target population of interest for early detection. While a multitude of blood-based protein biomarkers have been tested in research settings for PDAC, none have yet made it to the clinic besides CA19-9. In many instances, this is because they are unable to significantly improve the performance of CA19-9, while in other scenarios, confounding variables such as chronic pancreatitis or other non-neoplastic entities lead to false positives and obfuscate the results. Recently, there has been an increasing reliance on using mutant DNA in serum as a cancer biomarker. The reliance on mutant DNA over aberrantly expressed proteins stems from the recognition that somatic mutations are pathognomonic of neoplasia, and circulating mutant DNA has not been reported in patients with benign tumors or non-neoplastic conditions. Cancers release large quantities of

cell free DNA (cfDNA) from their mutant genomes into the circulation, and even though much of this cleaved into fragments 150bp or less by nucleases, sensitive PCR assays can be designed for detecting "hot spot" mutations in genes such as *KRAS, PIK3CA, BRAF,* etc.. This is quite pertinent for PDAC, where >95% of patients have *KRAS* mutations in their tumors. Nonetheless, a recent study that combined isolation of cfDNA in PDAC patients with a bead-based digital PCR technology identified *KRAS* mutations in 75% of patients with advanced disease, but only in 48% with localized tumors Thus, clearly, while cfDNA has great promise, there is substantial room for improvement in assay parameters for patients most likely to benefit from early detection. Another limitation of cfDNA, from the context of genomic characterization of advanced tumors, is the extensively fragmented nature of the nucleic acids, which precludes its use in most next generation sequencing (NGS) platforms. **Thus, an ideal "liquid biopsy" biomarker strategy for early detection and treatment monitoring in PDAC would**: *(a)* be feasible for application using blood samples (1-2 vials) in a Point-of-Care Test (POCT) setting; *(b)* be paired with ultra-sensitive and quantitative detection of mutant DNA for purposes of early detection and treatment/recurrence monitoring; and *(c)* provide high quality nucleic acids amenable to NGS. We this in mind, **we hypothesize** that liquid biopsies in the form of cfDNA and exosomal derived DNA are a reliable surrogate of the tumor genome in PDAC patients, and can be a biospecimen of choice for early detection, serial disease monitoring, and therapeutic stratification, without the need for tissue acquisition. We aim to identify mutant DNA in liquid biopsies from patients with surgically resectable and metastatic PDAC in order to query the actionable exome of PDAC for therapy guidance.

Exosomes and other extracellular vesicles

Exosomes are extracellular vesicles (EVs) exhibiting a diameter of 40-120 nm, conceived endogenously through the multivesicular endosome pathway and released to the extracellular space via fusion with the plasma membrane (60, 61). Microvesicles (MVs) are a class of larger EVs with a diameter ranging from 0.2 to 1 μm and originate from the budding and fission at

special "lipid raft" domains of the plasma membrane (62). A methodology to reliably enrich for exosomes, but not microvesicles, currently does not exist, as there are significant overlap between size, shape, density and cell marker profiles (63). Both are molecular vehicles reported to transfer a variety of biochemical cargo, including protein products, RNA transcripts, microRNAs, and fragmented DNA, but beyond their distinct biogenesis pathways and relative diameters, the two are difficult to delineate, and as a result, are frequently used interchangeably in literature (64-67). For the purpose of this chapter, we will use the term exosome to refer specifically to the population of small EVs produced through the multivesicular endosome biogenesis pathway.

Double-Stranded Genomic DNA in Circulating Exosomes

Circulating exosomes are known to facilitate intercellular communication through the exchange of numerous biochemical products such as proteins, lipids, mRNA transcripts, miRNA, and DNA of both chromosomal and mitochondrial origin (68). The recent identification of double-stranded high molecular weight genomic DNA within circulating exosomes has proven to be an exciting discovery in the context of cancer liquid biopsies with translational implications for early detection, diagnosis, monitoring, and prognostic and therapeutic stratification of solid tumors, including deep seated visceral cancers. Specifically, exosome-derived DNA (exoDNA) may have a role in precision medicine, whereby molecular profiling of exoDNA may lead to the identification of effective therapeutic strategies based on the molecular makeup of a patient's underlying cancer from which the exosomes have been released into circulation. Similar in concept to the use of circulating tumor DNA (ctDNA), exoDNA allows for the profiling of an additional liquid biopsy compartment, whereby tumor profiling is possible through a minimally invasive approach compared to more invasive tumor biopsy procedures, thus allowing for repeated biopsy samples taken throughout disease treatment and progression.

The presence of chromosomal DNA cargo within exosomes was validated in exosomes isolated from healthy human plasma and from the culture supernatants of HEK293 human embryonic kidney cells and K562 human leukemia cells (69). In this study, isolated exosomes were treated with DNase to ascertain that the isolated genomic DNA presided in the interior, rather than the exterior of the exosomes, the latter of which would represent the circulating cell free DNA (cfDNA) fraction. Additionally, as opposed to cfDNA, which exists in the form of fragmented DNA molecules of ~170bp, exoDNA consisted of high molecular weight DNA. Numerous groups have since reported the presence of exosomes enriched with long and/or fragmented genomic DNA of varying sizes from different sources, including plasma, urine, and pleural effusions, with whole-genome sequencing studies subsequently revealing that exoDNA covered the entire compendium of human chromosomes without a bias towards particular regions of the genome (69-72).

The shielding of the genomic DNA by the exosome exterior appears to attenuate DNA degradation by extracellular DNAses, and enhances the stability of the exoDNA, an observation that raises the possibility of using tumor-secreted exosomes paired with next generation sequencing (NGS) as a liquid biopsy platform for comprehensive interrogation of the cancer genome (73). Additionally, having the ability to profile DNA from different sources in circulation may allow for characterization of differing biological underpinnings that occur during tumor progression. In other words, it is generally believed that cfDNA is released in circulation from cells undergoing active apoptosis or necrosis, *versus* exoDNA that may be derived from cells that undergoing rapid proliferation and active biogenesis of exosomes. A recent study hypothesizes a potential mechanism of DNA packaging within exosomes involving the enrichment of Histone H2B proteins within exosomes (74). In other words, these proteins have a role in identification of foreign or aberrant cytosolic DNA molecules and have been shown to co-localize with exosomal proteins such as CD63, which is involved in exosome cargo trafficking.

It is thus thought that exosomes may provide a mechanism for exporting of mutated DNA molecules out of the cells as a means of self-defense.

Detection of Mutational Signatures in Genomic DNA-Enriched Exosomes

Mutation detection within exoDNA of pancreatic cancer patient plasma initially demonstrated utility using polymerase chain reaction (PCR) and Sanger sequencing to determine trademark *KRAS* and *TP53* mutations, known common genetic drivers of pancreatic cancer (70). Subsequent reports confirmed that Sanger sequencing detection of mutational signatures can also be performed in exosomes secreted by prostate cancer cells (75). For prostate cancer patients, this methodology can be applied not only in excreted urine, but also in circulation, as high molecular weight exosomal DNA fragments were also identified in the plasma of prostate cancer patients (75, 76). Interestingly, the presence of exosomes has been acknowledged in a range of biological fluids including blood, urine, milk, and saliva, creating several opportunities for applications that rely on the fluid context, such as the use of exosomes in the urine for urinary tract malignancies, exosomes in pleural fluids for lung/mesothelial cancers, or exosomes within the blood for visceral malignancies (77) .

Exosomes as Agents for Early Detection, Diagnosis, and Stratification

In recalcitrant cancers such as pancreatic ductal adenocarcinoma (PDAC), diagnosis often occurs at a late stage of the disease when the cancer becomes virtually uncurable. This is typically attributed to the late presentation of disease symptoms and an inability to discern low volume (early stage) disease. Currently, carbohydrate antigen 19-9 (CA 19-9) is the circulating tumor marker most commonly used for diagnosis in the clinic. Because CA 19-9 is not elevated in the early stages of PDAC, and is also present in many benign cases of pancreatitis and biliary obstruction, it has mostly been used as a prognostic tool to track tumor progression. As a result, new methodologies with the capacity to detect tumors at an early, treatable stage without the

direct, invasive sampling of the cancer, are desperately needed to address these types of aggressive cancers. Noninvasive liquid biopsy strategies involving the isolation of circulating tumor cells (CTCs) and ctDNA from patient blood to determine the presence of an asymptomatic cancer have shown promise, but the diagnostic and early detection potential of circulating exosomal DNA (exoDNA) is just beginning to be understood (42, 44, 78).

As the principal driver mutation, *KRAS* is near ubiquitous in PDAC, with an estimated ~95% of tumors exhibiting some *KRAS* mutations (79, 80). This near ubiquitous presence of *KRAS* in PDAC tumors, and the fact that it represents one of the first mutations that is acquired during carcinogenesis, suggests that a strategy for its detection in the context of liquid biopsies may provide an avenue for early detection and treatment monitoring (81). Using an ultrasensitive mutation detection methodology known as droplet digital polymerase chain reaction (ddPCR), Allenson et al demonstrated the feasibility of detecting *KRAS* mutations in exoDNA from PDAC patients, and determining the circulating mutant allele frequency (MAF) for the oncogenic allele amongst a sea of wild type DNA (82). This study demonstrated the ability to detect mutant alleles in exoDNA obtained from all stages of PDAC, as well as allowing for stratification of patient survival outcomes based on the *KRAS* MAF. Notably, mutation detection of exosomal *KRAS* (exo*KRAS*) was seen in 7.4% of age matched healthy controls, 66.7% of localized disease, 80% of locally advanced disease, and 85% of metastatic PDAC, representing 75.4% sensitivity and 92.6% specificity for exo*KRAS* as a tumor biomarker for evaluating PDAC. Furthermore, a patient that tested positive for exo*KRAS* was 8.17 times more likely to have an early stage cancer rather than be tumor-free. Interestingly, exo*KRAS* MAF levels correspond with disease-free survival in patients with localized disease, where patients with an exo*KRAS* of >1.0% experiencing poorer disease free survival, a relationship that the prognostic biomarker CA 19-9 did not illustrate. This suggests that there may be a subpopulation of patients that may require more aggressive intervention and follow-up.

In the aforementioned study, it was also notable that exoDNA outperformed ctDNA in the detection of PDAC, and generated significantly higher detection rates of positivity across all stages of the disease, but most important in the early stages (resectable stages) of cancer. The ddPCR analysis of cfDNA revealed mutant cf*KRAS* detection in 14.8% of healthy controls, 45.5% of localized disease, 30.8% of locally advanced disease, and 57.9% of metastatic PDAC. A possible explanation for this discordance is that ctDNA is theorized to be released extensively into circulation only at the later phases of PDAC, where dying cells becomes more pervasive, and as a result, may be less effective at pinpointing early stage disease manifestations (83). Thus, exoDNA, a product of normal biogenesis pathways, may be a promising alternative to ctDNA for the earlier detection of PDAC. As a cautionary note, mutant *KRAS* was also found in healthy individuals (including two independent cohorts from the US and Europe), a phenomenon that appears to increase with age-related clonal hematopoiesis and/or the likely presence of *KRAS*-mutant precursor lesions within the pancreas, GI tract or lung. This finding serves to add an important caveat to the utility of the current methodology as an early diagnostic tool, and prevent the phenomenon of "overdiagnosis". It is thus important to consider limiting such screens to high-risk populations using current assay technologies, or develop methodologies that may increase specificity, such as detection of a panel of mutations that represents a higher probability for an underlying cancer (as opposed to a clinically insignificant precursor lesion).

Genomic Molecular Profiling of Exosomal Cargo

A key component of a precision medicine approach to cancer is the ability to profile the molecular characteristics of a patient's underlying cancer. This is particularly difficult for visceral cancers such as PDAC where attempts at surgical sampling of tumor tissue are inherently invasive and frequently limited by the obscure tumor location and risk accompanied with surgical procedure (84). Minimally invasive liquid biopsies have been attractive alternatives to direct tissue sampling. Investigators have previously used plasma-derived, cfDNA to identify key

oncogenic "hotspot" drivers (ie. *BRAF, KRAS, EGFR*) via digital PCR, but the highly fragmented nature of cfDNA makes applications involving next-generation sequencing (NGS) platforms more challenging (85-87). Though attempts at using cfDNA for targeted genomic profiling have been published (and companies such as Foundation Medicine, GRAIL, and Guardant Health are heavily investing in such cfDA "liquid biopsy" assays), the feasibility of circulating exosomes as means for tumor profiling and disease monitoring has only just begun to be described.

A recent study sought to determine the efficacy of exosomes in visceral tumor genomic profiling (72). San Lucas et al isolated circulating exosomes from various bodily fluid sources including peripheral whole blood and pleural effusions of metastatic PDAC patients. The exoDNA extracted from these exosomes contained genomic DNA of high molecular weight, which was representative of the entire human genome (65%-91% genomic representation on whole-genome sequencing). The exoDNA isolates further revealed high representation of tumor fraction ranging from 56%-82%, suggesting that this liquid biopsy compartment may confer an enriched source of tumor derived material in circulation. This is further emphasized by the high cancer-derived DNA fraction found in exosomes obtained from a pleural effusion (82%) in the context of <1% malignant cells on cytospin in the same sample. Whole exome sequencing of exoDNA further revealed several potentially actionable mutations, including COSMIC (Catalogue of Somatic Mutations in Cancer) alterations that could be used to monitor tumor genomic evolution over time, and COSMIC genes that could be addressed through a particular clinical trial or chemotherapy. Sequencing data of exoDNA also illustrated amplified copy numbers of major mutational signatures such as *KRAS, EGFR,* and *ERBB2*. In a particularly interesting case demonstrating the potential utility of exoDNA for therapeutic selection, the investigators detected an unexpected somatic *BRCA2* mutation, known to impair homologous recombination, a critical DNA repair mechanism in actively dividing cells. This patient subsequently achieved a striking response to a regimen comprising of cisplatin, a crosslinking agent that generates widespread DNA damage. Although retrospective and correlative in nature, this data suggests that further

characterization of how mutation detection through exoDNA can impact therapeutic decision-making is further warranted.

In a separate study, Castillo et al describe an enrichment methodology to specifically capture cancer-specific exosomes (CSEs) from the circulation, allowing for the ability to perform high resolution genomic characterization through the captured cargo (74). The authors identified a panel of six proteins - CLDN4, EPCAM, CD151, LGALS3BP, HIST2H2BE and HIST2H2BF - that were specifically expressed on the surface of PDAC-derived CSEs ("surfaceome"), and could be exploited through an immunocapture approach for enriching CSEs. As opposed to ctDNA, which cannot be specifically captured from the total cfDNA compartment, exosomes have the added benefit of expressing tumor specific markers that can be used to separate tumor and normal tissue derived exosomes. This is particularly relevant in the context of those patients undergoing active therapy where circulating tumor burden can dramatically decrease to the point of making mutational events in circulation undetectable using current technologies, or in the context of early detection of an asymptomatic cancer where the volume of CSEs might be overwhelmed by the complement of normal exosomes. To overcome this limitation, Castillo et al applied an antibody cocktail through an immunocapture technique that allowed for positive selection of CSEs, which can be subsequently used for mutation detection. Using this assay, they achieved an increase in mutation detection from 44% to 73% in non-captured *versus* captured exosomes. The authors also demonstrated the utility of this technique in being able to perform NGS on CSE-derived exoDNA through a molecular barcoding targeted sequencing approach. In an index case of a patient who initially responded to PARP inhibitor therapy secondary to a somatic *BRCA2* stop-gain mutation, and subsequently progressed, the authors were able to identify a putative mechanism of resistance through a second splice site mutation of the same gene, which allowed for reversion of the initial stop-gain ("*BRCA2* reversion mutation"). This further demonstrates the ability of exosomes to not only detect genomic

vulnerabilities, but also to provide a means to identify mechanisms of resistance for real-time precision oncology decision making.

Transcriptomic Characterization of Tumors Through Liquid Biopsies

As a source a highly enriched tumor material, exosomes also contain a milieu of cargo that can be used for tumor characterization, such as mRNA. Whereas cfRNA is largely comprised of highly fragmented circulating RNA transcripts, limiting the molecular assays to those involved in microRNA detection, RNA within exosomes (exoRNA), provides a source of long mRNA transcripts that allow for more detailed characterization of tumors through liquid biopsies. In the study by San Lucas et al, exoRNA allowed for the orthogonal validation of gene amplifications, as in the case of overexpression of *ERBB2* (72). In addition, the benefits of this transcriptome-based approach may also extend towards the determination of novel cancer-specific fusion transcripts that may otherwise not be apparent from genomic sequencing only. Further, the identification of expressed cancer-derived neoantigens (both missense mutations and fusions) may facilitate emerging precision immunotherapies that rely on discovery of such neoantigens in a patient-specific manner. Ultimately, this may also allow for profiling of the dynamic changes in the neoantigen repertoire, which may occur from selective pressures and "antigen editing" that occurs during tumor progression. Through serial monitoring of tumor associated antigens and how these evolve over time, one can begin to suggest novel therapeutic approaches relating to ideal immunotherapeutic stratification. Specifically, quantitative estimates of neoantigen load through liquid biopsies may provide an early surrogate of response to immunotherapies such as vaccines or engineered T-cell receptors, of which there is currently no readily available biomarker.

Conclusions

Next-generation sequencing of circulating exosomes (including enriched CSEs) provides promising strategies for non-invasive tumor profiling and disease monitoring. Recent data from many laboratories suggests that exosomes are an important component of liquid biopsies, facilitating identification of actionable mutations critical to developing patient-tailored precision treatment regimens. In addition, the ability of exoRNA to profile the tumor transcriptome presents many new exciting opportunities, such as the discovery of novel neoantigens that may serve as the basis for emerging adoptive T-cell immunotherapies. This system also exhibits high clinical relevancy with abridged times from patient blood draw to exosome sequencing and data analysis. These promising data warrants the further development of exosomes as a complementary clinical tool in early disease detection, disease monitoring, and therapeutic stratification.

Chapter 2 – Materials and Methods

Chapter 2 – Materials and Methods

Cell lines and culturing

PATC43, PATC66, and PATC92 were established from patient derived tumor xenografts (88). These lines were maintained in RPMI-1640 medium with 10% FBS. MIAPaCa-2, Pa01C, Pa02C, Pa03C, Pa04C, Pa07C, Pa08C, Pa09C, Pa021C, and Pa028C are established pancreatic cancer cell lines from primary or metastatic tissue (10). These lines were maintained in DMEM medium with 10% FBS. Non-neoplastic cell lines used include HPNE, an hTERT-immortalized human pancreatic epithelial line; CAF19, an immortalized cancer-associated fibroblast line from a PDAC patient; and SC2, an immortalized fibroblast line established from non-neoplastic pancreas tissue (89, 90). CAF19 and SC2 were maintained in DMEM medium with 10% FBS. HPNE was grown in 75% DMEM without glucose, 25% Medium M3 Base (Incell Corp. Cat# M300F-500), 5% FBS, 10ng/ml human recombinant EGF, and 5.5mM D-glucose (1g/L).

Exosome isolation from cell lines

PDAC and non-neoplastic pancreas epithelial cell lines were cultured in HYPERflasks in respective medium (Corning). Upon reaching 70% confluency, cell lines were starved of 10% FBS for 48 hours and media supernatant was harvested. In summary, 4000mL of media was centrifuged serially at 1000 RPM for 10 minutes at 4°C, where cell pellets were discarded and then the supernatant centrifuged at 5000 RPM for 10 minutes at 4 °C to remove cellular debris (Figure 1). Resultant supernatant was filtered through a 0.22 µm pore filter, then ultracentrifuged at 154,000g at 4 °C overnight. The resulting pellet was resuspended in 66 ml of PBS with a subsequent ultracentrifugation step performed at 154,000g at 4 °C for 2 hours. The resulting exosome pellet was resuspended in 100ul of PBS and harvested for downstream analyses

Exosome isolation from patient samples

Three 8.5ml Acid Citrate Dextrose tubes (BD) of blood were collected from each patient. The red blood cells and plasma were separated by centrifuging blood samples at 2500 rpm for 10 minutes at room temperature. On average, a total of ~11.7ml of plasma was obtain and diluted in PBS to 50mls. The plasma was centrifuged at 1000 rpm for 5 minutes, then the supernatant was decanted and centrifuged at 5000 rpm for 10 minutes to remove the remaining cellular debris. The plasma solution was split between 3 ultracentrifuge tubes, diluted in PBS to a maximum volume of 66ml and spun overnight at 154,000xg. The plasma pellet was washed with PBS and spun in the ultracentrifuge for 2 more hours at 154,000xg. The supernatant was discarded and the exosome pellets were collected by resuspending in 600ul of PBS. Exosomes in the "total exosome control cohort" were processed immediately for DNA isolation using the QIAamp Circulating Nucleic Acid Kit (Qiagen, Cat# 55114) per the manufacturer's protocol. Exosomes samples within the "Captured exosomes" cohort were processed as described below.
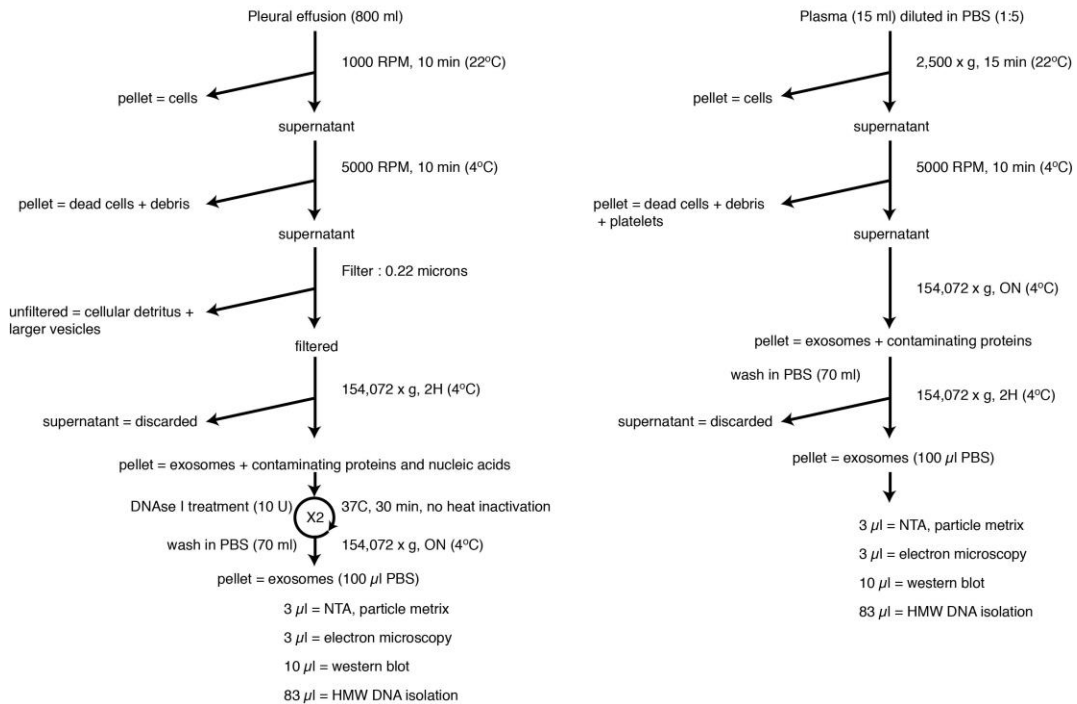
Figure 1: Exosome isolation scheme from cell culture media and human plasma for downstream analysis

DNA isolation and mutation detection

Cell-free DNA (cfDNA) was isolated using the QIAamp Circulating Nucleic Acid Kit (Qiagen) according to the manufacturer's protocol. In selected samples in which cfDNA was not initially detected, cfDNA was subsequently amplified using the RepliG Cell WGA kit (Qiagen) according to the manufacturer's protocol. ExoDNA was isolated using the MagAttract High Molecular Weight DNA kit (Qiagen) according to the manufacturer's protocol. DNAase I treatment of exosomes was performed as previously reported to confirm extraction of DNA from the exosome compartment and not cfDNA[1]. In select samples in which gene mutations were not initially detected in exoDNA, whole genome amplification was performed using the RepliG Cell WGA kit (Qiagen) according to the manufacturer's protocol.

Digital PCR

Droplet digital PCR (ddPCR) (QX200; BioRad, Hercules, Calif) was used for highly sensitive detection of genetic mutations with a multiplex KRAS assay containing G12V, G12D, G12R, G12C, G12S, G12A, G13D mutant codons. Estimation of false-positive rate (FPR) was first determined across multiple wells containing KRAS wild type DNA from a healthy individual as well as a non-template control (NTC). A cutoff of more than 2 droplets in the mutant channel was determined to be optimal for providing no FPR and classifying a sample as having mutant molecules. A lower limit of detection (LOD) was then determined of 0.01% MAF (Figure 2). Subsequently, for each experiment done on clinical samples, wells containing a positive control and two negative controls were included to determine the absence of contamination and PCR efficiency of the ddPCR probes in each plate. Positive controls consisted of one of either pancreatic cell line (Pa04C or Panc1), while the negative controls included a wild-type well of DNA from a healthy individual and a well with just water as a non-template control. Interpretation

Titration experiment
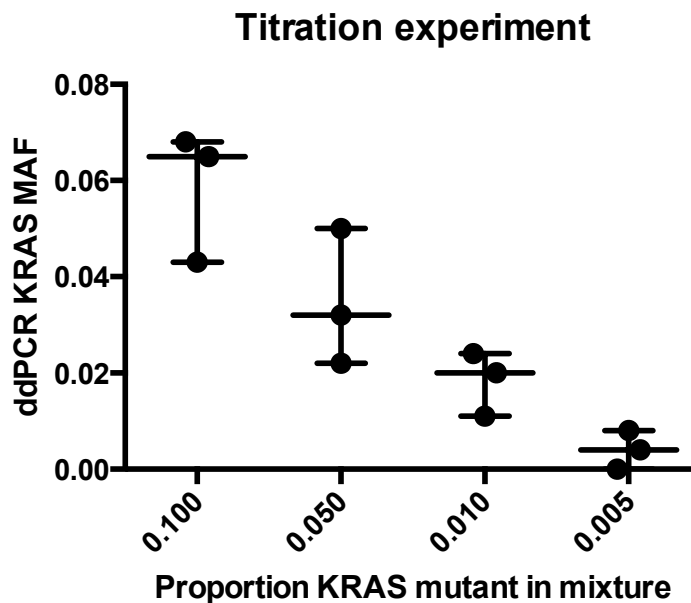
Figure 2 Low limit of detection of KRAS mutations through droplet digital PCR

and analysis of results was done in accordance with BioRad Rare Mutation Detection Best Practice Guidelines for Droplet Digital PCR. Data was processed using QuantaSoft v.1.6 (Bio-Rad).

Statistical analyses

Statistical analyses were performed using the R and SAS programming languages. Descriptive comparisons of study variables used the Fisher's exact test for categorical data and the Wilcoxon rank sum test for continuous data. Univariate analyses using Cox proportional hazard models were performed to examine potential clinical and molecular factors contributing to survival. Survival curves were generated using the Kaplan-Meier method, and log-rank tests were used to compare survival curves. Clinical outcomes were established as defined by the National Cancer Institute (91). *KRAS* sensitivity and specificity was determined as related to the patient's cancer status.

Exosome Protein Fractionation

Exosome surface and cargo proteins were isolated from the same sample (Figure 3). To isolate exosome surface from cargo proteins, the exosome pellet was biotinylated with 5 ml of 1 mg/ml of Sulfo-NHS-SS-BIOTIN (Pierce) in PBS for 30 min at 4 °C. The residual biotinylation reagent was quenched with 10mL of 100 mM lysine in cold PBS for 15 min at 4 °C. Biotinylated exosomes were recovered through ON ultracentrifugation at 100,000 g. Biotinylated exosomes were then sonicated in 2 ml of 4M Urea, 3% IsoPropanol, 20 mM Tris, 2% OG and protease inhibitors (complete protease inhibitor cocktail, Roche Diagnostics) followed by centrifugation at 20,000 g at 4 °C for 30 min. Biotinylated proteins were isolated by affinity chromatography using 2 ml of UltraLink Immobilized Neutravidin (Pierce) according to the manufacturer's instructions. Proteins bound to the column were recovered by reduction of the biotinylation reagent with 1 ml of a solution containing 65 µmol of DTT and 2% (w/v) OG detergent overnight at 4 ºC and referred to as exosome surface proteins. Proteins not bound to the column (flow through) were also collected and named cargo proteins. Exosome surface and cargo proteins were fractionated by reversed-phase chromatography, using the same amount of proteins across different samples for a given

exosome compartment. All three extracts were reduced by DTT and alkylated with iodoacetamide prior to chromatography. Separation were performed in an off-line 1100 series HPLC system (Shimadzu) with reversed phase column (4.6 mm ID × 150 mm length, Column Technology Inc) at 2.7 ml/min using a linear gradient of 10 to 80% of organic solvent over 30 min run. Solvent system used was: aqueous solvent – 5% acetonitrile / 95% water / 0.1% of trifluoroacetic acid; organic solvent – 75% acetonitrile / 15% isopropanol / 10% water / 0.095%
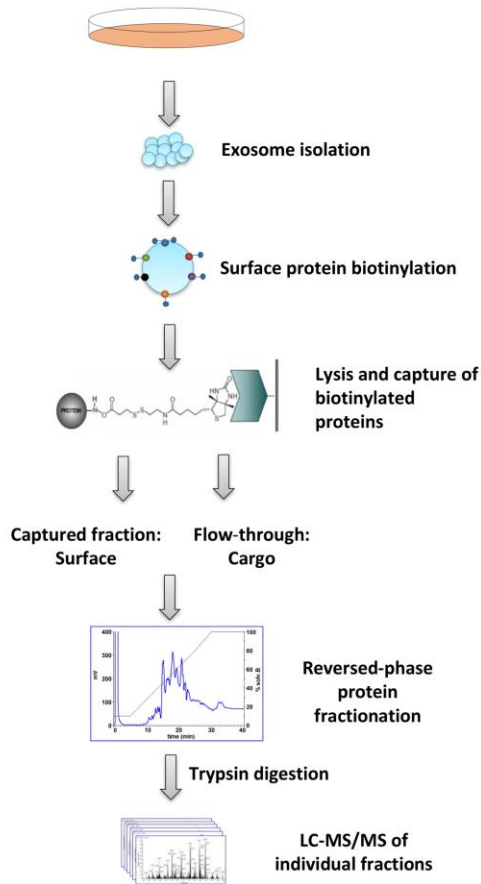
Figure 3: Schematic representation of surface exosome protein extraction

trifluoroacetic acid. Fractions were collected at a rate of 3 fractions per minute.

Mass Spectrometry Analysis

Each fraction from the reverse phase chromatography were in-solution digested overnight at 37 °C with 400 ng of trypsin. The resulting trypsinized fractions were pooled into 4 to 10 pools based on chromatographic features. Pools were individually analyzed by LC-MS/MS. LC-HDMSE data were acquired in resolution mode with SYNAPT G2-S using Waters Masslynx (version 4.1, SCN 851). The capillary voltage was set to 2.80 kV, sampling cone voltage to 30 V, source offset to 30 V, and source temperature to 100°C. Mobility utilized high-purity N2 as the drift gas in the IMS TriWave cell. Pressures in the helium cell, Trap cell, IMS TriWave cell, and Transfer cell were 4.50 mbar, 2.47e-2 mbar, 2.90 mbar, and 2.53e-3 mbar, respectively. IMS wave velocity was 600 m/s, helium cell DC 50 V, Trap DC bias 45 V, IMS TriWave DC bias V, and IMS wave delay 1000 µs. The mass spectrometer was operated in V-mode with a typical resolving power of at least 20,000. All analyses were performed using positive mode ESI using a NanoLockSpray source. The lock mass channel was sampled every 60s. The mass spectrometer was calibrated with a [Glu1] fibrinopeptide solution (300 fmol/µL) delivered through the reference sprayer of the NanoLockSpray source. Accurate mass LC-HDMSE data were collected in an alternating, low energy (MS) and high energy (MSE) mode of acquisition with mass scan range from m/z 50 to 1800. The spectral acquisition time in each mode was 1.0 s with a 0.1-s inter-scan delay. In low energy HDMS mode, data were collected at constant collision energy of 2 eV in both Trap cell and Transfer cell. In high energy HDMSE mode, the collision energy was ramped from 25 to 55 eV in the Transfer cell only. The RF applied to the quadrupole mass analyzer was adjusted such that ions from m/z 300 to 2000 was efficiently transmitted, ensuring that any ions observed in the LC-HDMSE data less than m/z 300 arised from dissociations in the Transfer collision cell. The acquired LC-HDMSE data were processed and searched against protein knowledge database (UniProt) through ProteinLynx Global Server (PLGS, Waters Company) with 4% False Discovery rate. Each dataset was normalized to the total number of spectral counts of the each compartment.

PDAC specific "surfaceome" profiling of exosomes

Proteins that were expressed at a higher prevalence in normal samples compared to tumor samples in ExoCarta were filtered out, resulting in 139 PDAC-specific exosomal surface protein markers (corresponding to 103 genes; Supplementary table 2). Subsequently, we identified three additional "borderline" proteins in our initial PDAC-specific exosomal marker list that did not meet these filtering criteria: CD151, UBA52 and HIST2H2BF, but have been previously described in the context of exosomes and tumorigenesis (CD151) (92), were found in a high proportion of cancer cell lines (11/13) even though being found in one non-neoplastic line (UBA52), or have biological and complementary relevance to other identified candidates HIST2H2BF (93). We then manually selected candidates for pull-down that were collectively represented across all of the PDAC cell lines and prioritized validation based on biological rationale and availability of targeting antibodies

Captured Exosomes/Pulldown

Antibody coating of beads was performed with 3ul of Aldehyde/Sulfate latex beads resuspended in 500ul PBS and incubated with 200ug of primary antibody anti-Histone H2B (Mouse monoclonal mAbcam 52484, Abcam), Anti-CD151 (Mouse monoclonal 11G5a, AB33315, Abcam), anti-LGALS3BP (Mouse monoclonal 3G8, AB123921, Abcam), anti Epcam, (Mouse monoclonal AUA1, AB20160, Abcam) or anti Claudin-4 (Mouse monoclonal 3E2C1, Thermo-Scientific) per 1ml of beads and incubated overnight at 4C on a Eppendorf ThermoMixer® C. The following day, 500ul of 1% BSA was added and incubated for 30 minutes. Coated beads were then pelleted down through centrifugation at 12,000RPM for 5 minutes. Pellet was resuspended in 1ml of 1%BSA 100mM Glycine solution for 30 minutes followed by centrifugation at 12,000 RPM for 5 minutes. Pellet was resuspended in 200ul of 1%BSA and incubated with samples of patient derived exosomes overnight at 4C. Exosome coated beads were centrifuged at 12,000 RPM for

5 minutes and washed 3 times with 800ul of 1% BSA. For flow cytometry analysis, resulting exosome attached beads were stained with PE conjugated Mouse Anti-Human CD63 (BD Bioscience, #556020). Isotype control was stained by Simultest IgG2a/IgG1 (BD Bioscience, #340394). Flow cytometry was performed on an Accuri C6 System (BD Bioscience) and analyzed on Flow Jo software. For DNA isolation, washed pellet was resuspended in appropriate lysis buffer for DNA isolation using the QIAamp Circulating Nucleic Acid Kit (Qiagen, Cat# 55114) per the manufacturer's protocol.

Electron microscopy

Microscopy imaging was performed in the High Resolution Electron Microscopy Facility at MD Anderson. In summary, exosome-diluted aliquots were fixed in Formaldehyde/Glutaraldehyde, 2.5% each in 0.1M Sodium Cacodylate Buffer, pH 7.4 for 15 minutes. For TEM imaging, samples were placed on 100 mesh carbon coated, formvar coated copper grids treated with poly-l-lysine for approximately 1 hour. Samples were then negatively stained with Millipore-filtered aqueous 1% uranyl acetate for 1 min. Stain was blotted dry from the grids with filter paper and samples were allowed to dry. Samples were then examined in a JEM 1010 transmission electron microscope (JEOL, USA, Inc., Peabody, MA) at an accelerating voltage of 80 Kv. Digital images were obtained using the AMT Imaging System (Advanced Microscopy Techniques Corp., Danvers, MA). For SEM images, fixed samples were placed on round coverslips treated with poly-l-lysine for approximately 1 hour, washed with 0.1 M cacodylate buffer, pH 7.3, post fixed with 1% cacodylate buffered osmium tetroxide, washed with 0.1M cacodylate buffer, then in distilled water. Afterwards, the samples were sequentially treated with Millipore-filtered 1% aqueous tannic acid, washed in distilled water, treated with Millipore-filtered 1% aqueous uranyl acetate, then rinsed thoroughly with distilled water. The samples were dehydrated with a graded series of increasing concentrations of ethanol, then transferred to graded series of increasing concentrations of hexamethyldisilazane (HMDS) and air dried overnight. Samples on coverslips

were mounted on to double-stick carbon tabs (Ted Pella. Inc., Redding, CA), which have been previously mounted on to aluminum specimen mounts (Electron Microscopy Sciences, Ft. Washington, PA). The samples were then coated under vacuum using a Balzer MED 010 evaporator (Technotrade International, Manchester, NH) with platinum alloy for a thickness of 25 nm., then immediately flash carbon coated under vacuum. The samples were transferred to a desiccator for examination at a later date. Samples were examined in a JSM-5910 scanning electron microscope (JEOL, USA, Inc., Peabody, MA) at an accelerating voltage of 5 kV.

Exosomes size distribution measurement

Exosomes were resuspended in PBS and serially diluted to the optimum dynamic range of the Zetaview nanoparticle analyzer (Particle Metrix, Diessen, Germany) for measurement of size and particle density. Observed and tracked particles were incorporated into size distribution calculations according to the particles' Brownian motion. The diffusion constant is then calculated and transferred into a size histogram via the Einstein Stokes relation between diffusion constant and particle size. For calculation of exosome concentrations, exosome yield was extracted by analyzing the Zetaview raw data and taking into account input plasma, dilution factor, and exosome volume.

Flow cytometry

Plasma exosomes were captured using the CD63+ Dynabead exosomes isolation kit according to manufacturer's instructions (Invitrogen, Life Technologies #10606D). Flow analysis of patient exosomes bound to Dynabeads conjugated with antibody was done according to the manufacturer's protocol. Briefly, 10 µl of exosomes were incubated with 90 µl of CD63+ Dynabeads overnight at 4°C. A Dynabead magnet was then used to positively select for bound exosomes, which were then stained with PE Mouse Anti-Human CD63 (BD Bioscience, #556020). Isotype control was stained by Simultest IgG2a/IgG1 (BD Bioscience, #340394). Flow

cytometry was performed on an Accuri C6 System (BD Bioscience) and analyzed on Flow Jo software (v.10.0.7).

Western Blot Analyses

Proteins extracted from the human cell lines SC2, CAF-19, PA01C, Pa03C and Pa04C and exosomes from the respective cell lines were used to examine different protein markers. Exosomes were lysed with RIPA buffer 1x (Sigma-Aldrich) and 1x Protease Inhibitor Cocktails (Sigma-Aldrich). Sample loading was normalized according to Bradford relative protein quantification. The proteins were mixed NuPAGE® LDS Sample Buffer (4X) and 10x NuPAGE® Sample Reducing Agent (Invitrogen) to a final concentration of 20ug(per sample), then heated at 70°C for 10 min and loaded onto a 1.0 mm × 10 well 4–12% Tris-Glycine gel (Novex) and thus the proteins were separated following an electrophoretic gradient across polyacrylamide gels. The gel was run under denaturing conditions at 180 V for 1h and then transferred nitrocellulose membrane (Bio-Rad) using the Trans-Blot® Turbo™ Transfer System with and 1x transfer buffer 10% with ethanol at 1.3Ampers - 25Volts – 8Minutes. The protein blot was blocked for 1 h at room temperature with 5% non-fat dry milk in PBS/0.05% Tween and incubated overnight at 4 °C with the following primary antibodies 1:1000 anti-Histone H2B (Mouse monoclonal mAbcam 52484, Abcam), 1:1000 Anti-CD151 (Mouse monoclonal 11G5a, AB33315, Abcam), 1:1000 anti-LGALS3BP (Mouse monoclonal 3G8, AB123921, Abcam), 1:1000 anti CD63 (Mouse monoclonal TS63, AB59479, Abcam), 1:1000 anti Epcam, (Mouse monoclonal AUA1, AB20160, Abcam), 1:1000 anti GPC1 (Rabbit polyclonal, PA5-24972 Thermo-Scientific), 1:1000 anti Claudin-4 (Mouse monoclonal 3E2C1, Thermo-Scientific), 1:1000 anti GAPDH (Rabbit monoclonal EPR16884, AB181603, Abcam), 1:1000 anti TSG-101 (Mouse monoclonal 4A10, AB83, Abcam). Afterwards, secondary antibody goat anti-rabbit IgG-HRP (sc-2004, Santa Cruz) or secondary antibody goat anti-mouse IgG-HRP (sc-2005, Santa Cruz) were used. The membranes were incubated for 1 h at room temperature. Membranes were cleared after antibody incubations in

an orbital shaker four times at 5-min intervals with PBS 0.05% Tween20. Clarity™ Western ECL substrate Chemiluminescence kit was utilized on the next step; Membranes were developed for 10 seconds to 1 min and the picture was analyzed.

Whole exome, genome, and transcriptomic sequencing

For each patient we performed whole genome, exome and transcriptome sequencing on their exoDNA and exosomal mRNA. We also performed exome sequencing of the peripheral blood mononuclear cells (PBMCs) for each patient for use as a reference in determining the somatic status of identified events. DNA was captured for exome sequencing using the Agilent SureSelect Clinical Exome Kit and subsequently sequenced on an Illumina HiSeq 2500 by the Avera Institute for Human Genetics to a mean sequencing depth of 490, 256 and 133 for LBx01-03 exoDNA and 60x for PBMC DNA using 100-base paired-end reads. Custom bioinformatics pipelines were applied to raw Illumina HiSeq reads for analyzing the patient exomes, including the metastatic lung tissue exome sequencing reads provided by Dr. Arul Chinnaiyan at the University of Michigan. Briefly, for DNA sequencing read alignment, the Burrows-Wheeler Aligner (BWA) (94) is used for initial alignment to the human genome reference build hg19, Picard is used for manipulating and preprocessing Sequence Alignment/Map (SAM) format files (95), and the Genome Analysis Toolkit (GATK) (96) is used to perform local realignment of sequencing reads. For the metastatic lung RNA-seq (reads provided by Dr. Arul Chinnaiyan) and the exoRNA, cDNA reads were aligned using RNA-Seq by Expectation-Maximization (RSEM) (97). LBx01 cDNA alignment resulted in 1101228222 mapped reads. LBx02 had 118429984 mapped reads, and LBx03 had 274391009 mapped reads.

Identification of somatic events

Given the aligned reads, MuTect was run on exosome and PBMC sample pairs for the sensitive detection of point mutations (98). In a similar analysis, the metastatic lung tissue exome from

LBx01 was compared with the corresponding PBMC exome. IndelLocator was used to identify small somatic insertions and deletions using similar "tumor/normal" paired analyses (96). Somatic mutation reports were generated and filtered using Variant Tools (99), which annotated our mutations with information from COSMIC (100), dbNSFP (101), the 1000 Genomes Project (102), the Exome Sequencing Project (103), ClinVar (104) and potentially actionable gene lists from Jones et al (105) and MD Anderson Cancer Center (unpublished). Gene fusion events were detected in RNA-sequencing data using ChimeraScan (106).

Filtering and annotation of somatic mutation calls

Using a probabilistic model that is dependent on read quality, sequence context and allele counts, MuTect provides a PASS or REJECT status for each putative mutation. We filtered out point mutations with non-PASS statuses. To help control for false-positives point mutations and indels, we required a minimum read depth of 20x in the germline and exoDNA to make a positive call. Any mutation that had at least 1 mutant read in the normal DNA was filtered out. We explicitly attempted to filter out exoDNA false-positive mutations that might be germline variants missed in the PBMC data (or common polymorphisms) by cross-checking candidate mutations against population variant annotations (including the 1000 Genomes project and the Exome Sequencing Project), where we removed mutation calls seen in 1% or more of the samples in these population-level projects. We visually verified nonsynonymous mutations using the Integrated Genomics Viewer (IGV) (107). For each patient, we performed visual verification on events by inspecting the sequencing reads at each candidate mutation site across all of that patient's samples. These QC filters were relaxed in cases where the mutation was seen with high frequency (at least 10 times) in the COSMIC database. The set of mutations used for estimation of mutation rates include those point mutations that passed this filtering step with the additional removal of mutations with less than a 5% mutant allele frequency to try to globally control for false positives.

Potentially clinical somatic events

Only nonsynonymous SNV, stopgain and frameshift insertions and deletions in exoDNA (called from exome sequencing) were considered for potential actionability. Mutations residing in a list of actionable genes, an aggregate list of actionable genes composed of those from Jones et al 2015 (105) and a list compiled from MD Anderson experts were annotated as potentially actionable. To help control for false positives, from the remaining mutations with a 5% mutation allele frequency or less, potential actionable mutations had to be seen in COSMIC or verified in the patient exosomal mRNA or exoDNA (through whole genome sequencing) to be considered as a candidate for potential actionability.

Identification of cancer-associated copy number events

Copy-number events were called using control-FREEC 7.2 on whole genome sequencing data with unpaired samples (108). A list of cancer-associated genes was downloaded from the Cancer Gene Census from the COSMIC database. Coordinates for each gene for the start and end of transcription were retrieved from the UCSC Genome Browser (hg19) (109). We intersected the coordinates of the copy-number events with the maia transcription coordinates of the cancer-associated genes and assigned the estimated copy-number (from control-FREEC) to each gene that had overlapping coordinates with the event. The data were subsequently visualized using a custom R script.

Estimation of tumor fraction and ploidy of exoDNA

We analyzed paired exome data from exoDNA and PBMC DNA using Sequenza 2.1.0 to estimate tumor fractions and ploidy (110). Sequenza is an implementation of a probabilistic model that incorporates average depth ratios between tumor and normal samples and allele

frequencies at germline heterozygous positions to segment DNA into copy number variant regions while estimating tumor cellularity and ploidy. The log posterior probability (LPP) of the observed copy number and allele frequencies are calculated by Sequenza for a range of candidate ploidy and cellularity values. The point estimate is given for the ploidy and cellularity with maximum LPP. The 95% confidence range is a region of point estimates with a total posterior probability of greater than 0.95. In the liquid biopsy context, exoDNA represents the tumor sample and PBMC DNA the normal sample in the Sequenza configuration, and for interpretation we use the *tumor cellularity* estimate as an estimate of the *tumor fraction* in the exoDNA. To run Sequenza, we first generated a GC content profile for the human genome hg19 using a window size of 50 base pairs. Then for each patient, we generated depth profiles for both the exoDNA and the PBMC DNA using the mpileup command of SamTools 0.1.19 (95) for subsequent processing using Sequenza.

Gene quantification and fusion detection

RNA-seq reads were aligned and quantified using RSEM (97). Expressed transcripts were checked for overrepresentation of GO terms and biological pathways using the DAVID Bioinformatics resource (111). The enrichment program is limited to 3000 genes as a maximum, thus, for the plasma exosomes samples, the expressed transcripts were limited to those expressed at larger than 10 TPM. For the pleural effusion sample, transcripts expressed at 50 TPM or more were included. This allowed for the approximately top 3000 expressed transcripts for each sample to be included in the enrichment analyses. The TPM threshold for the pleural effusion exosomes is higher because it was more deeply sequenced compared to the plasma samples. Gene fusions were called using ChimeraScan 0.4.6 on RNA-sequence data (106). The reference transcriptome (UCSC known genes) was downloaded from the chimerascan download site (http://chimerascan.googlecode.com/files). Only those events in the plasma samples with at least 10 read pairs (and 20 read pairs in the pleural effusion sample) were included as candidate

fusion events. Again, because of the deeper sequencing of the pleural effusion sample, the threshold used was higher.

Mutation signatures

We characterized mutational signatures using 6 base substitutions (i.e., C>A, C>G, C>T, T>A, T>C, and T>G) and their 5′ and 3′ bases adjacent to the mutation site, generating 96 combinations of substitutions. Coordinates and base substitutions for each sample for all mutations were fed into a custom R script that utilizes the SomaticSignatures package to retrieve adjacent bases from a genome reference for each mutation (112). Previous studies have identified existing mutational signatures across various types of cancers, which have since been included in the COSMIC database (100, 113). We downloaded 30 mutation signatures from the COSMIC database and visually assessed similarities of pancreatic and lung cancer signatures with our signatures.

Next generation sequencing with molecular barcodes

Illumina NGS libraries were prepared from enriched plasma derived exosomal DNA and genomic DNA. A total of 10-80ng of DNA was used for library construction through the QIAseq Targeted DNA Panel (Qiagen, Cat# DHS-3501Z) which employs a molecular barcoding approach. First, genomic DNA samples were fragmented, end repaired and A-tailed. The DNA fragments were then ligated at their 5' ends with Illumina adapters containing a 12-bp Unique Molecular Index (UMI) and sample index. These fragments underwent target enrichment PCR - with 11,311 gene-specific primers and one universal forward primer complementary to the adapter sequence. Afterwards, the library is further amplified through universal PCR.

Bioinformatics with molecular barcodes

The 12-bp barcode provides a possibility of 16,777,216 unique indexes. After mapping to the 275 genes in the QIAseq Targeted DNA panel there is sufficient entropy that the chances of overlap in of both barcode and template start/stop locations is negligible. Post-amplification, the reads are grouped according to loci and barcodes. The duplicates are then condensed into 'Super Reads' based on the consensus sequence of each barcode. The selection of this consensus sequence removes a majority of amplification and sequencing errors.

The Illumina sequencing data was analyzed through Qiagen's Biomedical Genomics Workbench. The raw output data was initially processed through the standalone workflow 'Prepare Raw Data' to trim any remnants of the Nextera Trim Adapters. Post-trimming, the reads were run through the 'QIAseq DNA V3 Panel Analysis' ready-to-use Workflow. This workflow employs the following steps: First, PCR adapters are trimmed before the sequences are annotated with their UMI's. The sequences are then mapped to a reference using BWA-MEM (114) before being grouped according to their UMI's. These groups are then used to create 'Super Reads' which are further processed to remove ligation artifacts and identify any structural variants. Then, these reads undergo local realignment using the Smith-Waterman algorithm before a primer trimming step. Finally, a low frequency variant detection workflow is utilized to identify variants using smCounter, a variant caller based on a posterior Bayesian probabilistic model (115).

Chapter 3 – Liquid biopsies for detection of early stage pancreatic cancer

Introduction

Pancreatic ductal adenocarcinoma (PDAC) composes 85% of all pancreatic malignancies and is associated with a dismal 5-year survival of 6% (116, 117). While cancer prevention initiatives and advances in targeted therapies have produced tangible survival improvements in breast, colon, and lung cancers, long-term PDAC survival remains poor and the nature of the disease does not readily present opportunities for screening and early detection (118-123). Under the best of circumstances, resection of early stage disease at experienced and high-volume centers improves 5-year survival to only 24-29% (117, 124-126).

Given the aggressive and recalcitrant clinical course of pancreatic cancer, many efforts have focused on identifying novel protein, DNA or RNA biomarkers to serve as a means for early detection or prognostic stratification (127). Blood-based liquid biopsy is particularly attractive in the context of PDAC, as the primary tumor itself is not routinely accessible in its retroperitoneal location, and sampling of the tissue is not without morbidity. Circulating tumor DNA and *KRAS* genetic mutations as a surrogate for PDAC-specific genetic material has been previously studied (128-136), and a study by Bettegowda et al, using a bead-based ultrasensitive PCR assay, demonstrated 48% and 77% detection rates for patients with early and late stage tumors, respectively (42).

Other reservoirs of proteins, DNA, and RNA have recently been identified in the form of microvesicles termed exosomes (72, 137, 138). Exosomes are 40-150nm lipid bilayer membrane bound particles derived from specific biogenesis pathways within cells and accessible within the plasma of the circulating peripheral blood (139). Biologically, exosomes have been shown to be capable of intercellular communication and modulation of the tumor microenvironment (67, 140). Perhaps more importantly, it is believed that the contents contained within these particles remains distinct from the remainder of the peripheral blood and thus, might represent an enrichment of tumor-specific genomic material (72, 137). While many have

commented on the utility of "circulating tumor" or "cell-free" DNA (cfDNA) in the context of liquid biopsy for cancer, here we tested the potential for exosome-derived DNA (exoDNA) to represent an additional blood-based compartment which may be complementary to cfDNA in the diagnosis and therapeutic stratification of patients with pancreatic cancer.

Study populations

Discovery cohort

Whole blood samples were collected at MD Anderson Cancer Center (MDACC) through informed consent following institutional review board (IRB) approval (PA14-0552). Patients with all stages of pancreatic cancer were included in the study. Healthy control samples were obtained from volunteers in the clinic waiting rooms, and for the most part, are relatives of the patients. Demographic information and personal medical history was collected from these volunteers, but samples were de-identified after collection, so follow-up of these volunteers was not possible. Individuals with diabetes, a history of pancreatitis, or a family history of pancreatic cancer were excluded from the discovery cohort. Whole blood was collected in green top (Sodium Heparin, BD Vacutainer) tubes. Blood samples were centrifuged at 2500xG for 10 minutes for plasma isolation and then stored at -80 degree until the time of exosome isolation. Samples were collected between 2003 and 2010, and between 0.9 and 1.5ml of plasma were available per patient for both cfDNA and exoDNA analysis. Medical records were queried for the American Joint Committee on Cancer staging, treatment status, and clinical outcomes. Staging considerations were supplemented with National Comprehensive Cancer Network guidelines with regard to borderline-resectable tumors. A total of 68 patients with PDAC of all clinical stages, an additional 20 PDAC patients initially staged with localized disease, with blood drawn *after* resection for curative intent, and 54 age-matched healthy controls were included in this cohort.

Validation cohort

A total of 39 early stage PDAC patients and 82 age-matched healthy controls were recruited through an International Agency for Research on Cancer (IARC) case-control study coordinated in the Czech Republic and Slovakia following informed consent. Researchers were blinded to the cancer-status of the clinical samples at the time of processing and data analysis. Peripheral blood was collected in EDTA tubes at the time of consent and processed as rapidly as possible. Blood samples were centrifuged at 2000xG for 10 minutes for plasma isolation and then stored

at -80 degree until the time of exosome isolation, where 200ul of plasma were available for exoDNA analysis.

Results

Exosome size and concentration

The presence of extracellular vesicles in exosome isolations was confirmed by means of Zetaview nanoparticle tracking analysis, western blot for exosomal markers, and scanning and transmission electron microscopy, with the latter in selected samples (**Figure 4).** Average particle size was greater among patients with PDAC compared to healthy controls. Further, average particle size was observed to be greater with more advanced disease (**Figure 4B),** particularly, those particles that were between 141 to 220 nm **(Figure 4C).** Exosome concentration was defined as number of exosomes per mL plasma. A cutoff value of 5.0 x 10^9 exosomes was identified through this discovery cohort and found to be associated with overall survival for both localized and metastatic patients, with a higher exosome concentration predicting worse survival (**Figures 5B and 5C).** Localized pre-surgical patients with less than 5.0 x 10^9 exosomes per mL plasma had a median survival of 1040 days compared to 421 days for those with higher exosome concentrations (P=0.047). Similarly, metastatic patients with less than 5.0 x 10^9 exosomes per mL plasma had a median survival of 479 days compared to 97

days   for   those   with   higher   exosome   concentrations   (*P*=0.015).
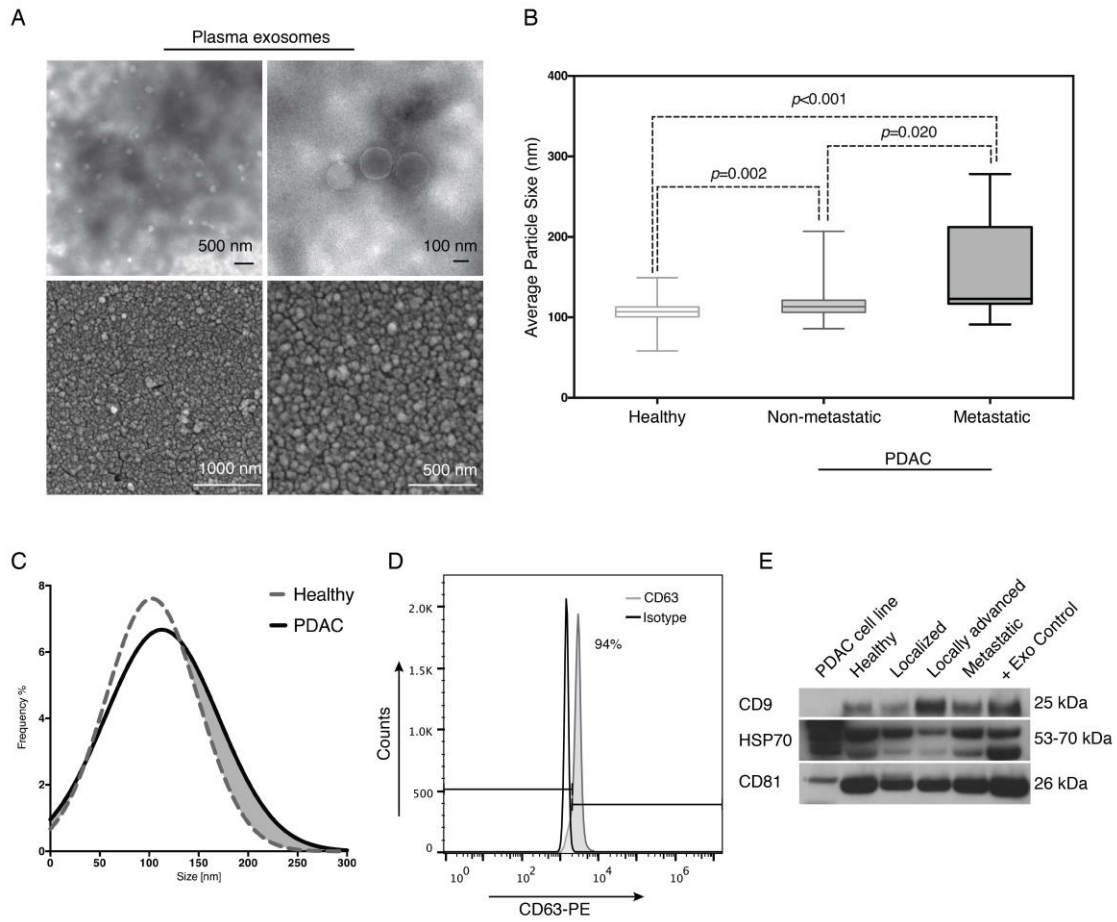
Figure 4: Profiling of exosomal physical characteristics

A. Transmisison and scanning electron microscopy of exosomes demonstrates a bilipid membrane falling within the size range of a define exosome. B, C. Average particle size oserved based on Zetaview nanoparticle tracking analysis. D. Flow cytrometry demonstrating presence of known surface exosome marker, CD63, compared to isotype control. E. Western blot analysis demonstrates expression of known exosomal markers in exosomes isolated from all patient populations.
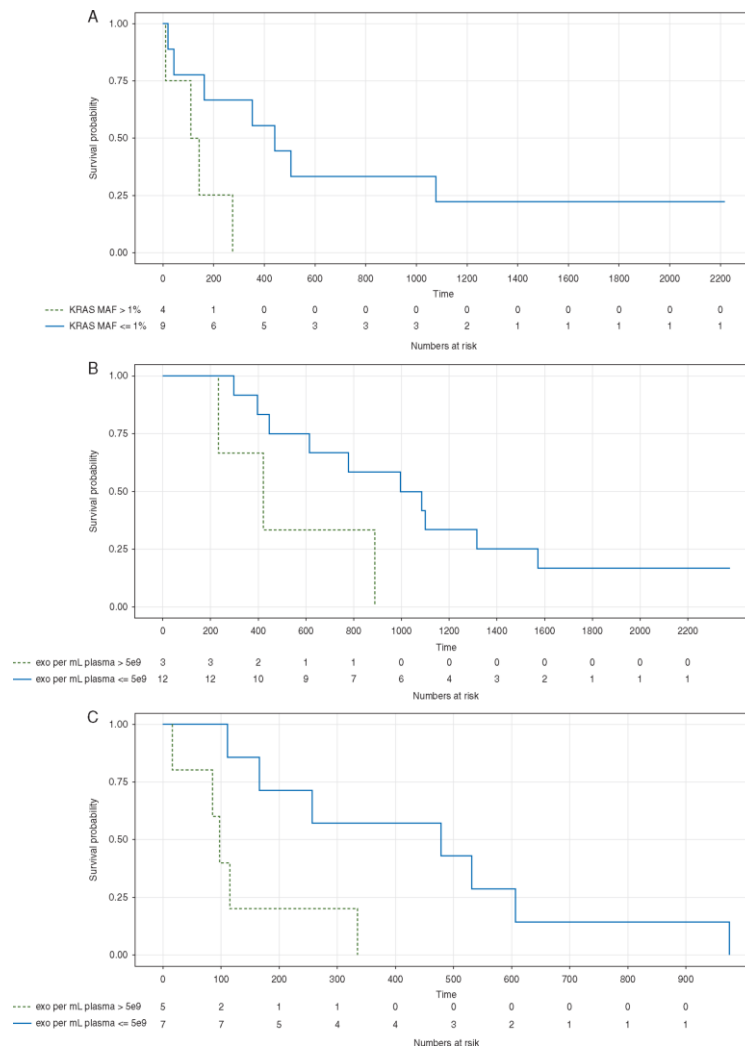
Figure 5: Liquid biopsy Kaplan-Meier curves

(A) Stratification of exo*KRAS* at a mutant allele frequency of 1% was associated with disease free survival in patients with localized disease who were treatment naïve at the time of blood draw ($n = 13$) with a median survival of 441 days compared to 127 days ($P = 0.031$). Two treatment naïve patients with no *KRAS* mutant droplets were excluded from this survival analysis to account for the possibility that they have a *KRAS* mutation that is not a target of the *KRAS* multiplex ddPCR kit used. (B and C) Exosome concentration of 5×10^9 per ml of plasma was associated with overall survival in treatment naïve blood draws in patients with (B) localized disease ($n = 15$, median survival 616 versus 233 days, $P = 0.048$) and (C) metastatic disease ($n = 12$, median survival 479 versus 97 days, $P = 0.015$).

Liquid biopsy detects exoDNA *KRAS* mutants by digital PCR

In the discovery cohort, ddPCR analysis of exoDNA detected *KRAS* mutations in 66.7% (22/33), 80% (12/15) and 85% (17/20) of localized, locally advanced, and metastatic PDAC patients, respectively, and in 7.4% (4/54) of controls (Table 1). For predicting PDAC status, the resultant sensitivity and specificity are 75.4% and 92.6% respectively. Positive mutant *KRAS* status from exoDNA was significantly associated with early stage PDAC when comparing patients with localized disease to healthy individuals (Fisher's exact test $P<0.001$), where an individual with positive *KRAS* status is 8.17 times (95% CI: 2.46 to 35.58) more likely to have early stage pancreatic cancer than to be cancer free. Further, compared to localized pre-resected patients with a mutant *KRAS* detection rate of 66.7%, in a similar cohort of 20 localized PDAC patients with blood sampled *after* resection, mutant detection rate was much lower at 5%. Mutant *KRAS* status was significantly associated with pre-resection blood sampling (Fisher's exact test, $P<0.001$). Of note, healthy controls had a mutant detection rate of 7.4% (4/54). *KRAS* mutant status in the healthy controls was associated with increased age (mean age of 75 years in mutant *KRAS* individuals versus 64 years in wild-type *KRAS* individuals; Wilcoxon rank sum test $P=0.004$).

Table 3: Liquid biopsy mutant call rates among patient populations

Stage of disease	cf*KRAS* mutant call rate (%)	exo*KRAS* mutant call rate (%)
Discovery cohort		
Healthy	8/54 (14.8)	4/54 (7.4)
Localized	15/33 (45.5)	22/33 (66.7)
Localized postsurgical	0/20 (0)	1/20 (5)
Locally advanced	4/13 (30.8)	12/15 (80)

Stage of disease	cf*KRAS* mutant call rate (%)	exo*KRAS* mutant call rate (%)
Metastatic	11/19 (57.9)	17/20 (85)
Validation cohort		
Healthy	–	17/82 (20.7)
Localized	–	17/39 (43.6)

In the validation cohort, 44% (17/39) of early stage pancreatic cancer patients tested positive for *KRAS* compared to 20% (17/82) of healthy individuals, confirming that *KRAS* positivity is associated with pancreatic cancer (Fisher's exact test, P=0.0163). An individual with *KRAS* positivity was 2.96 times (95% CI: 1.29 to 6.76) more likely to have pancreatic cancer than to be healthy. Unlike with the discovery cohort, no association of age with mutant exo*KRAS* status was found in the healthy controls.

Mean *KRAS* mutation allele frequencies were higher in metastatic compared to localized samples (mean of 10.09% versus 2.7% respectively; Wilcoxon rank sum test P=0.0109).

Stratification of localized patients based on a pre-surgery exo*KRAS* MAF threshold of 1% was associated with disease-free survival following resection, (Figure 2A), with a median disease-free time of 441 vs 127 days for patients with less than 1% MAF compared to those with more than 1% MAF (P=0.031; Figure 2A). In addition, greater than a 1% MAF was a significant risk factor impacting disease-free survival (RR, 4.68; 95% CI, 1.014-21.61). While a slight, yet statistically significant positive correlation existed between *KRAS* MAF and CA19-9 levels (P=0.019, r=0.303), only *KRAS* MAF was associated with disease-free survival. Cox proportional hazard analyses were also performed on locally advanced and metastatic patients but no clinical factors were found to be significantly associated with overall or progression-free survival.

Performance of cfDNA in liquid biopsy

In the discovery cohort, mutant cf*KRAS* was detected in 14.8% (8/54), 45.5% (15/33), 30.8% (4/13), and 57.9% (11/19) of healthy controls, localized, locally advanced, and metastatic patients. Of these positive cfDNA calls respectively, 12.5% (1/8), 73.3% (11/15), 100% (4/4) and 100% (11/11) were also called positive through exoDNA. As opposed to the exoDNA results, *KRAS* positive status in healthy control cfDNA was not associated with increasing age (data not shown). In the metastatic group, the presence of mutant *KRAS* cfDNA suggested worse overall survival (median survival of 115 days compared to 506 days for mutant *KRAS* negative patients), but this was not statistically significant (P=0.107).

Discussion:

Exosomes, which have been shown to harbor DNA (70, 72), are the product of specific biogenesis pathways and are shed from viable cells by the tens of millions into circulation. Conversely, traditional cfDNA is derived from apoptosis and necrosis of tumor cells, which are characteristic of later stage disease (141). It may thus be possible that exoDNA is a significant contributor of the DNA in circulation in patients of earlier clinical stage, before cell death and tumor necrosis begin to occur. In this context, the origin of the circulating DNAs may explain why the detection rate for early stage patients in this study was slightly higher with exoDNA than that previously described for cfDNA, but also why the identification of late stage patients was concordant (42).

Most encouraging is the observation of a precipitously lower detection rate in the localized pre and post-resection cohorts, from 66% to 5%. With mutant *KRAS* being a surrogate for tumor-specific DNA, and resection for curative intent aimed at removing the entirety of the localized disease, pre- and post- procedure liquid biopsies may have utility in determining the early

success of resection. It is important to mention though, that the lower *KRAS* detection may be an overall marker of response to any therapy, and not just surgery alone. We are unable to draw such conclusions from this data set as time points before and after other treatment modalities are not available for our cohorts.

In this study, exo*KRAS* mutant allele frequency, but not CA19-9, was associated with disease free survival in localized disease. Whereas presence or absence of cfDNA and overall amount of DNA has previously been used for stratification, we did not identify such a clinical correlation. In a tumor where oncogenic *KRAS* gene mutations are believed to be near ubiquitous, to the best of our knowledge, this is the first time *KRAS* mutant allele frequency in exoDNA has been used for prognostic stratification. While a 1% mutant *KRAS* fractional abundance was identified in our discovery cohort as being informative towards disease-free survival, further validation is warranted for any such proposed cancer biomarker (142).

CfDNA was detected between 30.8-57.9% across stages, which is concordant with the findings of earlier studies (42). No studies to date have described the detection rate of *KRAS* mutant alleles within exosomes across a series of PDAC patients across all stages, nor compared these directly with cfDNA. For this reason, we performed a parallel analysis of liquid biopsy for cfDNA *KRAS* mutations from plasma samples from the same patients to serve as a comparison, in addition to historical cfDNA detection rates in the literature. In our study, rates of detection of *KRAS* mutants in exosomes were superior to cfDNA across all stages. Of particular interest is our finding that exoDNA revealed a greater detection of patients with localized disease than previously observed using a highly sensitive method of detection (42). Validation is warranted, but this finding has potential ramifications for liquid biopsy based diagnostics, especially in tumors where specific mutant detection yields the opportunity for treatment with targeted therapy.

Identification of *KRAS* mutations in 7.4% of exoDNA and 14.8% of cfDNA healthy controls in the discovery cohort and in 20.7% in the exoDNA of the validation cohort was an unexpected finding with potential implications for using liquid biopsies as a screening tool. Indeed a survey of the literature shows that *KRAS* mutations in apparently healthy samples have been previously described (See Supplemental table 1) both in a liquid biopsy setting, and in autopsy series (in non-cancerous pancreata). It is important to mention that in an era where highly sensitive detection techniques are now available, detection rates for "background" oncogenic mutations are likely to increase. It is possible that the finding of such mutations describe a pre-malignant process within the pancreas or a *KRAS*-mediated malignancy outside the pancreas. Perhaps, these mutations accumulate in organs with increasing age but the rate at which these mutations progress to invasive cancer is unknown. Mutant *KRAS* findings in the normal controls of the discovery cohort suggests that accumulation of driver mutations may be an age-related phenomena as recently described by Krimmel and colleagues for *TP53* mutations in control patients (143). However, no association of age and mutant *KRAS* status in healthy controls was found in our validation cohort. For purposes as an early cancer-screening diagnostic, the specificity of our approach would need to be improved possibly by requiring a minimum *KRAS* mutation allele frequency to make a positive mutant status call, which is the focus of continued work. Additional biomarkers, such as other cancer DNA mutations or protein biomarkers could also be added into the screening model to increase the sensitivity to make it clinically useful.

In the setting where the patient's cancer status is known a priori, then the utility of a liquid biopsy lies in the ability to observe serially the response of genetic mutations as a form of personalized biomarkers to therapy. It is necessary to consider that *KRAS* mutations as a PDAC biomarker may be of particular value in terms of assessing response to therapy in those 5-20% of patients who do not express the Sialyl Lewis-A, or CA 19-9 antigen (144), and furthermore in those patients in whom CA-19-9 becomes unreliable in the frequent setting of obstructive jaundice. Additionally, the radiologic appearance and response of PDAC to therapy on cross-sectional

imaging is negligible to the point that non-progression on therapy has become a qualifier to proceed to surgery in borderline-resectable patients (145).

Conclusion

In this study, exoDNA outperformed cfDNA for the detection of mutant *KRAS* in PDAC patients. Further, the exoDNA detection rate of patients with early stage tumors is greater than that previously reported. However, a substantial portion of healthy control patients also exhibited *KRAS* mutations**.** This suggests that follow-up studies more generally focused on uncovering the prevalence of known cancer mutations (in addition to *KRAS* mutations) in healthy individuals are needed to try to put these mutations into biological context and to ultimately understand their clinical repercussions.   In the context of liquid biopsy, the application for ultrasensitive identification of a single genetic mutation as a predictor for PDAC may be limited.

Chapter 4 – Predictive and prognostic utility of liquid biopsies in pancreatic cancer

Abstract

Background and Aims: We aim to investigate the clinical utility of liquid biopsies, specifically circulating tumor DNA (ctDNA) and exosomal DNA (exoDNA) in localized and metastatic pancreatic cancer.

Methods: We have utilized liquid biopsies to measure *KRAS* mutant allele frequency (MAF) by droplet digital PCR (ddPCR) in paired exoDNA and ctDNA in a prospective cohort of 194 localized and metastatic pancreatic cancer patients, comprising 425 blood samples.

Results: Concordance rates of KRAS mutations present in tissue and detected in liquid biopsies was 95.5% in 34 patients. Among 34 potentially resectable patients, an increase in exoDNA following neoadjuvant therapy was significantly associated with progressive disease (p=0.003), while profiling of ctDNA in this cohort did not reveal significant correlations to outcomes. Metastatic patients (n=104) with detectable ctDNA at baseline status experienced shorter progression free (PFS) (HR 1.8, 95% CI 1.1 – 3.0, p=0.019), and overall survival (OS) (HR 2.8, 95% CI 1.4-5.7, p=0.0045) on univariate analysis. On multivariate analysis, exoDNA MAF ≥5% emerged as a significant predictor of shorter PFS (HR 2.28, 95% CI 1.18-4.40, p=0.014) and OS (HR 3.46, 95% CI 1.40-8.50, p=0.007). A multi-analyte approach revealed detection of both ctDNA and exoDNA MAF ≥5% at baseline treatment naïve status as a significant predictor of OS (HR 7.73, 95% CI 2.61-22.91, P=0.00002) on multivariate analysis. Further, on longitudinal monitoring in 34 metastatic patients, an exoDNA *KRAS* MAF peak ≥1% was significantly associated with radiological progression (p=0.0003).

Conclusions: In a large clinical evaluation of pancreatic cancer, we demonstrate how the use of exoDNA and ctDNA provide complementary strategies for prognostication and therapeutic.

Introduction

Although rare, pancreatic ductal adenocarcinoma (PDAC) has recently become the third leading cause of cancer related deaths with projections of it rising to the second leading cause of cancer deaths within the next decade (1). While surgical resection provides a potential curative option in PDAC, only a minority of patients (<15%) will be diagnosed with disease that is amenable to surgery, and even in this subset of patients, 5 year overall survival (OS) rates remain below 30%. Neoadjuvant therapies are increasingly being adopted to enhance local disease control in resectable patients. As most PDAC patients present with surgically unresectable tumors, current therapeutic options in this patient population has resulted in modest benefits in OS with no means to personalize therapy currently. Among both localized and metastatic patient populations, there still remains a significant unmet need in developing more effective strategies for therapeutic stratification and management.

The use of blood based biomarkers for cancer diagnosis and therapeutic stratification has gained significant traction in cancer in the form of circulating proteins, RNA, and DNA. Specifically, circulating tumor DNA (ctDNA) detection in the blood of breast, colorectal, and lung cancer patients, amongst others, has shown clinical relevance in identifying patient relapses (146-150). In the context of PDAC, the use of ctDNA as a clinically significant biomarker has been inconsistent in regards to its prognostic and predictive potential (42, 82, 151-153). Additional sources of DNA and RNA in circulation have been recently identified in the form of microvesicles known as exosomes (154). Previous studies have shown the utility of profiling the genomic content of exosomes (exoDNA) as a surrogate for the mutational landscapes of established cancers, and for early detection (70, 74, 82). These 40-150nm lipid bilayer membrane bound vesicles are believed to form protective barriers of nucleic acid material from nuclease induced degradation in the plasma, thus allowing for the native material to exist in a high molecular weight format compared to ctDNA which is mostly found at 170bp size. Importantly, this could allow for greater resolution and sensitivity of molecular profiling of high quality DNA material.

In this study, we aimed to compare the utility of tumor monitoring in localized and metastatic PDAC patients using paired exoDNA and ctDNA, to determine how they may be used in a complementary manner for prognostication and therapeutic stratification. We performed longitudinal collection in a large prospective cohort of PDAC patients with localized and metastatic cancer, such that the dynamics of *KRAS* mutation detection in circulation could be correlated with disease progression and compared with standard readouts, such as imaging and CA19-9. To our knowledge, this study represents the first comprehensive comparison of these liquid biopsy compartments in the context of clinical utility. Additionally, we believe the longitudinal aspects of this study have implications for potential real-time therapeutic stratification of PDAC patients.

Study Design

Patients who were clinically and histologically confirmed as localized or metastatic pancreatic adenocarcinoma, defined by American Joint Committee on Cancer guidelines, were enrolled in this longitudinal cohort study. Metastatic disease was based on surgical or radiologic confirmation. A total of 194 patients were recruited at MD Anderson Cancer Center through informed consent following institutional review board (IRB) approval (PA14-0552 and PA11-0670) and treated between 04/07/2015 to 10/13/2017 (Figure 6). Of these, 104 patients presented at baseline treatment naïve status with metastatic PDAC. If receiving first-line therapy, treatment naïve patients underwent pre-treatment CT imaging and followed every 2-3 months with restaging imaging after initiation of chemotherapy. Progression in all patients was determined based on routine clinical evaluation by a blinded board certified radiologist based on RECIST 1.1 criteria of CT imaging. Progression free survival was defined by the time from start of first line therapy to progression based on CT restaging imaging.
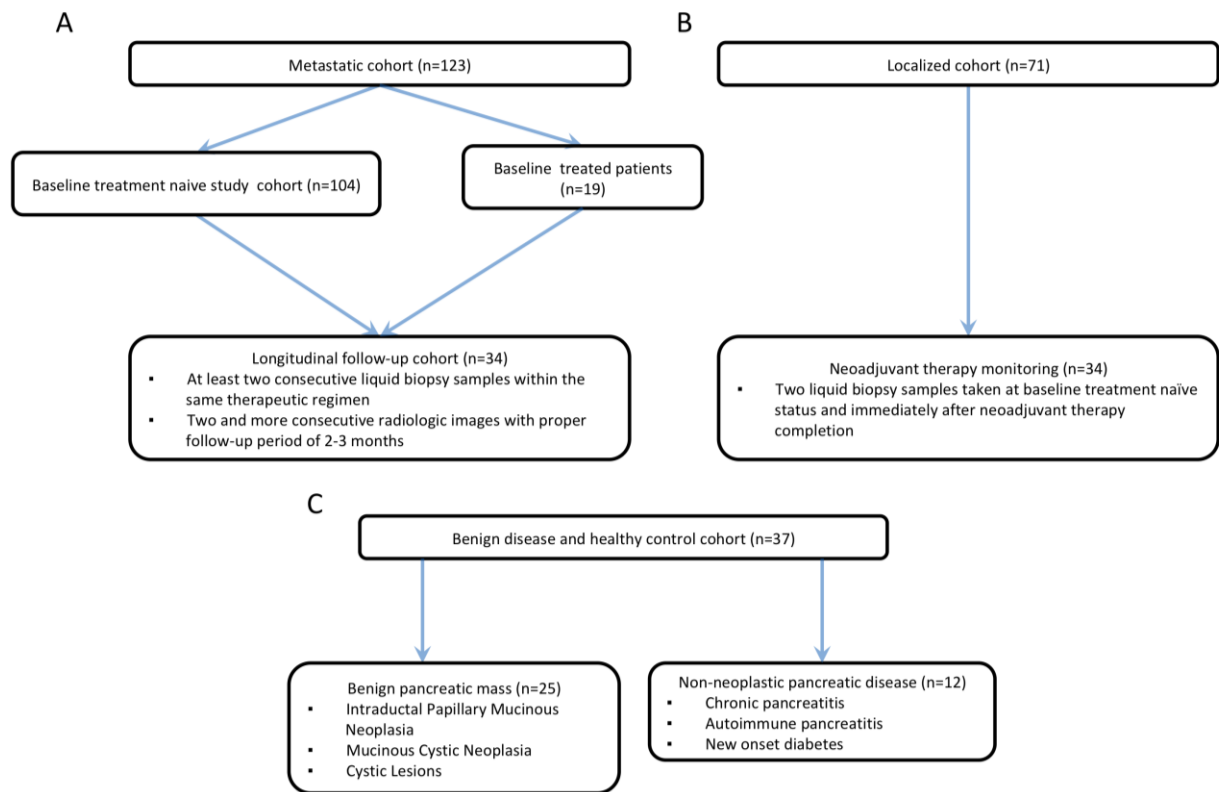
Figure 6: Patient population cohorts for baseline prognostication and longitudinal follow-up

Results

Characteristics of patients undergoing liquid biopsies

Study overview and patient stratification are presented in, Table 4. A total of 318 blood samples from 123 metastatic and 107 blood samples from 71 localized resectable patients were profiled using ddPCR. Median follow-up time for all patients was 187 days. ExoDNA and ctDNA profiled at baseline treatment naïve status revealed KRAS mutation detection rates of 61% and 53%, respectively in metastatic patients and 38% and 34%, respectively in localized disease patients (Figure 7A, B). To determine prevalence of circulating mutational events in other pancreatic diseases, an additional 37 patients with pancreatic lesions were evaluated for KRAS mutations in exoDNA and ctDNA. Mutation detection rates were 12% (3/25) and 16% (4/25) for pancreatic cysts, 25% (3/12) and 17% (2/12) for non-neoplastic pancreatic disease, within exoDNA and ctDNA respectively.

Table 4: Patient characteristics and stratification

Characteristics	Total Patients	exoDNA		ctDNA		Fisher Test	exoDNA		ctDNA	
		KRAS ≥ 5	KRAS < 5	KRAS > 0	KRAS = 0		exoDNA		ctDNA	
Age (years)										
Average		64.4	63.2	65	63.1	67.1				
Median		65	60	65	62	67				
Range	(39-86)	(45-86)	(39-84)	(39-86)	(46-84)					
Sex/Gender						P-value	0.135		0.8345	
Male	60 (57.7)	23 (22.1)	37 (35.6)	41 (39.4)	19 (18.3)	CI	0.817	5.7	0.447	2.758
Female	44 (42.3)	10 (9.6)	34 (32.7)	29 (27.9)	15 (14.4)	Odds Ratio	2.1		1.11	
Ethnicity						P-value	1		0.7144	
Hispanic or Latino	9 (8.7)	3 (2.9)	6 (5.8)	7 (6.7)	2 (1.9)	CI	0.164	5.49	0.312	18.422
Not Hispanic or Latino	95 (91.3)	30 (28.8)	65 (62.5)	63 (60.6)	32 (30.8)	Odds Ratio	1.092		1.769	
Race						P-value	0.8814		0.795	
Asian	3 (2.9)	1 (1)	2 (1.9)	2 (1.9)	1 (1)					
Black or African-American	11 (10.6)	4 (3.8)	7 (6.7)	9 (8.7)	2 (1.9)					
Caucasian (White)	85 (81.7)	26 (25)	59 (56.7)	56 (53.8)	29 (27.9)					
Native and Other	5 (4.8)	2 (1.9)	3 (2.9)	3 (2.9)	2 (1.9)					
Tumor Location						P-value	0.4439		0.2999	
Head of Pancreas	47 (45.2)	12 (11.5)	35 (33.7)	31 (29.8)	16 (15.4)					
Tail of Pancreas	25 (24)	10 (9.6)	15 (14.4)	18 (17.3)	7 (6.7)					
Body of Pancreas	30 (28.8)	11 (10.6)	19 (18.3)	20 (19.2)	10 (9.6)					
Neck of Pancreas	2 (1.9)	1 (1)	1 (1)	0 (0)	2 (1.9)					
Tumor Metastasis						P-value	0.02515		0.04322	
Liver	82 (78.8)	31 (29.8)	51 (49)	60 (57.7)	22 (21.2)					
Lung	11 (10.6)	0 (0)	11 (10.6)	6 (5.8)	5 (4.8)					
Peritoneal	10 (9.6)	2 (1.9)	8 (7.7)	4 (3.8)	6 (5.8)					
Ovarian	1 (1)	0 (0)	1 (1)	0 (0)	1 (1)					
Outcome						P-value	0.00312		0.0004775	
Death PC	32 (30.8)	16 (15.4)	16 (15.4)	24 (23.1)	8 (7.7)					
Death other	2 (1.9)	18 (17.3)	18 (17.3)	10 (9.6)	26 (25)					
Alive	58 (55.8)	11 (10.6)	47 (45.2)	36 (34.6)	22 (21.2)					
Lost to Follow-up	11 (10.6)	4 (3.8)	7 (6.7)	7 (6.7)	4 (3.8)					
Smoking History						P-value	0.5543		0.5641	
Lifelong Non-smoker	53 (51)	14 (13.5)	39 (37.5)	33 (31.7)	20 (19.2)					
Current reformed smoker	29 (27.9)	10 (9.6)	19 (18.3)	20 (19.2)	9 (8.7)					
Current smoker	6 (5.8)	2 (1.9)	4 (3.8)	4 (3.8)	2 (1.9)					
Not Available, EMR	16 (15.4)	7 (6.7)	9 (8.7)	13 (12.5)	3 (2.9)					
Alcohol History						P-value	0.5591		0.3651	
No	46 (44.2)	14 (13.5)	32 (30.8)	32 (30.8)	14 (13.5)					
Yes	43 (41.3)	14 (13.5)	29 (27.9)	28 (26.9)	15 (14.4)					
Denied	8 (7.7)	4 (3.8)	4 (3.8)	7 (6.7)	1 (1)					
Not Available-EMR	7 (6.7)	1 (1)	6 (5.8)	3 (2.9)	4 (3.8)					
Diabetes History						P-value	0.4924		0.4331	
No	64 (61.5)	21 (20.2)	43 (41.3)	44 (42.3)	20 (19.2)					
Long-standing type 2 diabetes	25 (24.0)	7 (6.7)	18 (17.3)	14 (13.5)	11 (10.6)					
Newly-diagnosed diabetes-within 1	7 (6.7)	4 (3.8)	3 (2.9)	6 (5.8)	1 (1)					
Long-standing type 1 diabetes	1 (1)	0 (0)	1 (1)	1 (1)	0 (0)					
Not Available, EMR	7 (6.7)	1 (1)	6 (5.8)	5 (4.8)	2 (1.9)					
Chronic Pancreatitis History						P-value	0.5506		0.5492	
No	92 (88.5)	29 (27.9)	63 (60.6)	59 (56.7)	33 (31.7)					
Not Available-EMR	9 (8.7)	4 (3.8)	5 (4.8)	8 (7.7)	1 (1)					
Yes	3 (2.9)	0 (0)	3 (2.9)	3 (2.9)	0 (0)					
Family history of Cancer										
Family history of cancer	71 (68.3)	21 (20.2)	50 (48.1)	45 (43.3)	26 (25)					
Familial PC	6 (5.8)	2 (1.9)	4 (3.8)	4 (3.8)	2 (1.9)					
Progression						P-value	0.03888		0.2846	
Progressed	66 (63.5)	53 (51)	13 (12.5)	47 (45.2)	19 (18.3)	CI	0.993		0.635	4.048
No Progression	38 (36.5)	23 (22.1)	15 (14.4)	23 (22.1)	15 (14.4)	Odds Ratio	2.632		1.606	

When comparing all patient populations, those with metastatic disease had significantly greater circulating mutant allelic fraction (MAF) of *KRAS* compared to localized disease and panceatic cyst patients (Figure 7C). Patients with localized disease had significantly greater MAF compared to panceatic cyst patients. We also determined gold standard validation of concordance rates between exoDNA and ctDNA with tumor tissue for *KRAS* mutation detection using ddPCR (Table 5). Concordance among 22 surgically resected primary pancreatic tumors was 95.5% and 68.2% for exoDNA and ctDNA respectively, while concordance from 12 samples derived by fine needle aspirates was 83.3% and 66.8% for exoDNA and ctDNA respectively.
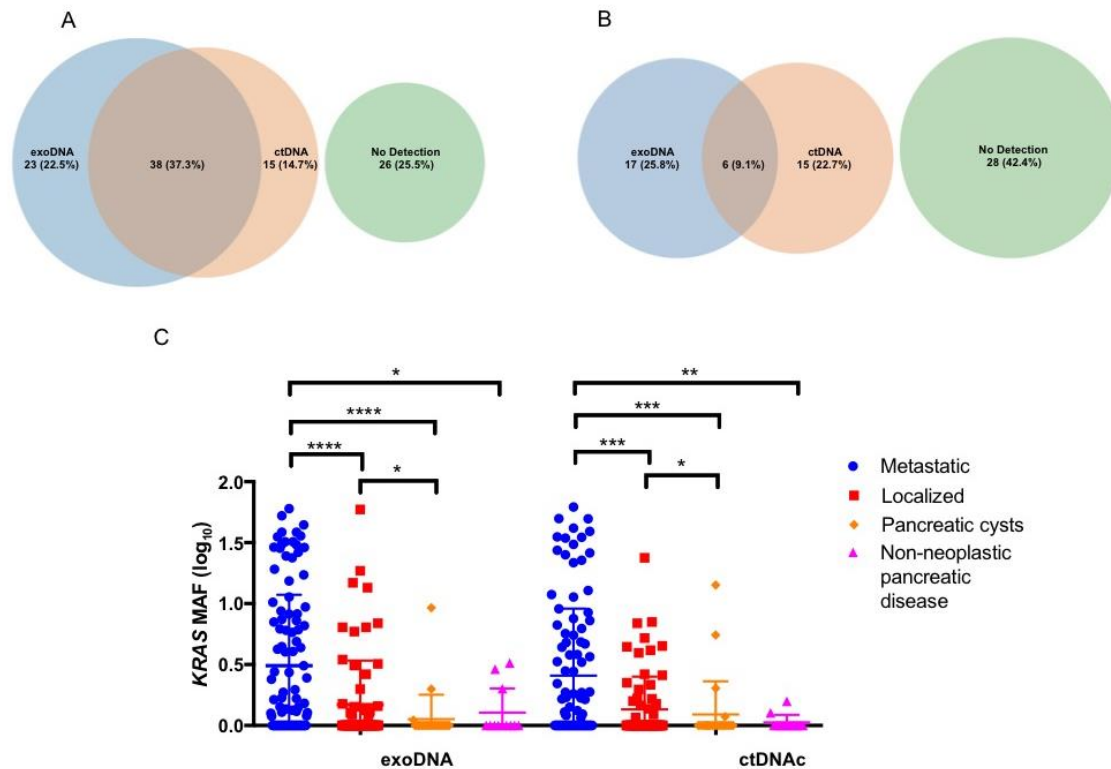
Figure 7 Mutant KRAS detection characteristics in a prospective cohort of tumor and benign pancreatic disease

Venn diagram of detection rates of codon 12/13 mutant *KRAS* by ddPCR among (A) 102 metastatic and (B) 66 localized PDAC patients with matched exoDNA and ctDNA analysis. (C) MAF of *KRAS* mutations detected through ddPCR in exoDNA and ctDNA among baseline treatment naïve localized and metastatic patients, and patients with benign pancreatic cysts and non-neoplastic pancreatic disease. Greater median MAF in exoDNA compared ctDNA in metastatic patients trended towards significance (p = 0.05), paired analysis performed by Wilcoxon test. Those patients with metastatic disease had higher *KRAS* MAF in both exoDNA (p<0.0001) and ctDNA (p=0.0004) when compared to patients with localized disease, by Mann-Whitney test. (p<0.05*, p<0.01**, p <0.001***, p<0.0001****)

Table 5 Concordance rates of tumor tissue and liquid biopsy mutant *KRAS* detection

Surgical Tissue Samples	Total Samples		22	Concordance (%)
	Liquid Biopsy match Tissue	20		95.45
	exoDNA match Tissue	21		95.45
	cfDNA match Tissue	14		68.18
Sample	**exoDNA**	**cfDNA**	**Tissue KRAS**	
MK238	-	-	-	
MK240	-	-	-	
MK248	+	-	+	
MK257	+	+	+	
MK259	+	+	+	
MK272	+	-	+	
AM62	+	+	+	
AM88	-	-	-	
MK44	+	-	+	
MK99	-	-	-	
MK116	-	-	+	
MK127	-	-	-	
MK160	-	-	-	
MK191	+	-	+	
MK212	-	-	-	
MK217	+	+	+	
MK230	+	-	+	
MK152	-	-	-	
MK227	+	-	+	
AM95	-	-	-	
MK307	-	-	-	
DH14	+	+	+	

ExoDNA		**ctDNA**	
Sensitivity	91.67%	Sensitivity	50%
Specificity	100%	Specificity	100%
PPV	100	PPV	100
NPV	90.91 (CI 60.49 - 98.49)	NPV	62.50 (48.63 - 74.59)

FNA Samples	Total Samples		12	Concordance (%)
	Liquid Biopsy match Tissue	11		91.67
	exoDNA match Tissue	10		83.33
	cfDNA match Tissue	8		66.67
Sample	**exoDNA**	**cfDNA**	**Tissue KRAS**	
WB02	-	+	+	
MK151	+	+	+	
MK229	-	-	-	
MK10	+	-	+	
MK17	+	+	-	
MK27	+	+	+	
GV79	+	+	+	
BW13	+	+	+	
WB27	+	-	+	
AM74	+	+	+	
MK12	+	-	+	
MK42	+	+	+	

ExoDNA		**ctDNA**	
Sensitivity	90.00%	Sensitivity	50%
Specificity	50%	Specificity	90%
PPV	90 (CI 68.91 - 97.34)	PPV	85.71 (CI 46.21 - 97.67)
NPV	50 (CI 8.96 - 91.04)	NPV	60.00 (45.09 - 73.26)

Serial liquid biopsies in localized PDAC patients receiving neoadjuvant therapy are predictive of eventual surgical resection

A total of 34 PDAC patients with localized disease were serially monitored during neoadjuvant therapy, comprising 68 cumulative blood draws taken at baseline and after the completion of neoadjuvant therapy (Table 6). Kinetics of circulating *KRAS* mutational burden were then measured in exoDNA and ctDNA using ddPCR. Mutant *KRAS* was detected in 41% (14/34) and 32% (11/34) of patients in exoDNA and ctDNA, respectively at baseline. Among the patients monitored, 50% (17/34) underwent subsequent surgical resection given an absence of

Table 6: Clinical characteristics of patients receiving neoadjuvant chemotherapy

Characteristics	Total (N=34)	Progression (n=17)	Non-progression (n=17)	χ^2/t	p
	M±SD	M±SD	M±SD		
Age (year)	64.9±9.1	65.8±11.1	64.4±8.3	0.332	0.743
Primary tumor size	30.2±9.1	30.5±11.6	30.0±8.0	0.122	0.904
	N (%)	N (%)	N (%)		
Gender					
Male	20	11	9		0.73[a]
Female	14	6	8		
Tumor location					
Head	27	13	14		1.000[a]
Body or Tail	7	4	3		
Neoadjuvant Chemotherapy					
GEM + ABR	18	10	8		0.49[a]
FOLFIRINOX	16	7	9		
Neoadjuvant XRT					
30Gy	11	5	6		1.000[a]
50.4Gy	15	6	9		
N/A	8	6	2		
Radiosensitizing Agent					
Capecitabine	22	10	12		0.61[a]
Gemcitabine	4	1	3		
N/A	8	6	2		
Change of ExoDNA KRAS					
No decrease	21	16	5		0.0002[a]
Decrease	13	1	12		
Change of cfDNA KRAS					
No decrease	25	11	14		0.44[a]
Decrease	9	6	3		
Change of CA 19-9					
Increase	9	8	1		0.003[a]
Non-increase	18	4	14		

disease progression, compared to 50% who experienced disease progression, primarily manifesting as the emergence of new metastatic lesions. In this cohort, reduction in exo*KRAS*

MAF from baseline at the completion of neoadjuvant therapy was significantly correlated with surgical resection, while the reverse was true for patients who did not emerge as surgical candidates (OR 38.4, CI 3.95-373.3, p=0.0002) (Figure 8A, B). Specifically, among patients who underwent resection, 71% (12/17) experienced a decrease in exo*KRAS* MAF from baseline treatment naïve values, while in those patients who did not, 16/17 (94%) saw an increase or no change in *KRAS* MAF in exoDNA from baseline status. As one example, in an index case, a rise in *KRAS* MAF in exoDNA suggested progressive disease, though that was initially not detectable by CA19-9 or CT imaging. On laparotomy, CT-occult omental metastasis was found resulting in an aborted resection. This correlation between changes in *KRAS* MAF and resectability was, however, not seen with ctDNA. After eliminating those patients who were considered as non-expressors of CA19-9 (values below 37 U/ml), changes in CA19-9 were also significantly correlated to those patients likely to undergo surgery (OR 28.0, CI 2.65-295.9, p=0.003). Among three patients where no detectable exo*KRAS* mutant was found, CA19-9 was able to predict progressive disease, underlining the complementary nature of how these biomarkers can be utilized.
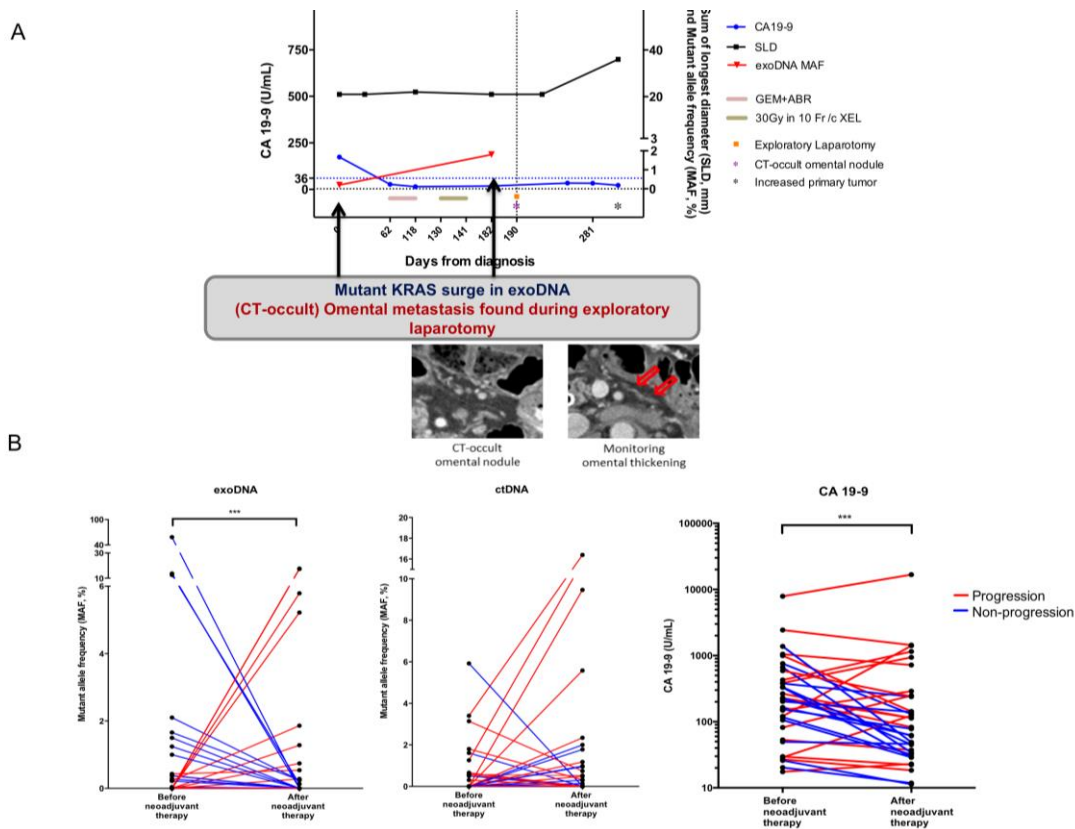
Figure 8 Liquid biopsy tumor monitoring of patients receiving neoadjuvant therapy

(A) Tumor monitoring before and after neoadjuvant chemoradiation in a patient experiencing progression undetectable by CA19-9 (blue line) or radiological based RECIST 1.1 (black line). (B) MAF kinetics of exoDNA and ctDNA before and after neoadjuvant therapy shows a significant correlation between a rise or no change in exoDNA MAF and progression (OR 38.4, CI 3.95-373.3, p=0.0002). No significant correlation was detectable by ctDNA. Changes in CA19-9 from baseline were also significantly associated to progressive disease (OR 28.0, CI 2.65-295.9, p=0.003).

Clinical correlates of liquid biopsies at presentation in metastatic PDAC patients

Among metastatic PDAC patients, clinical characteristics at the time of presentation were grouped according to exoDNA and ctDNA status are shown in **Table 4.** There was no significant association between *KRAS* MAF in exoDNA and ctDNA, and presenting characteristics. Overall, 66 (63%) had experienced radiologic progression and 69 (67%) were still alive at mila last follow-up date. Patients who experienced progression during serial monitoring or succumbed to disease had higher *KRAS* MAF in exoDNA at presentation (Wilcoxon signed-rank tests, p=0.03 and p=0.01, respectively) when compared to those that had not progressed **(Figure 9).** CtDNA tumor burden, as measured by *KRAS* MAF at presentation, was also significantly associated with survival (p=0.03) **(Figure 9B).** Patients with liver metastatic lesions had a significantly greater *KRAS* MAF in exoDNA and ctDNA, compared to patients with isolated lung and peritoneal lesions (p=0.04) **(Figure 10A-B)**. This correlation was likely impacted by the fact that patients with metastasis to the liver have larger volume of lesions compared to those with isolated lung and peritoneal metastases (**Figure 10C).** In fact, on linear regression analysis, exoDNA and ctDNA *KRAS* MAF at presentation was significantly correlated with tumor size as measured by total sum of lesion diameters (p=0.035 and p=0.0008, respectively) (**Figure 11).** Additionally, patients with progressively worse ECOG performance status harbored significantly greater *KRAS* MAF **(Figure 12) .**
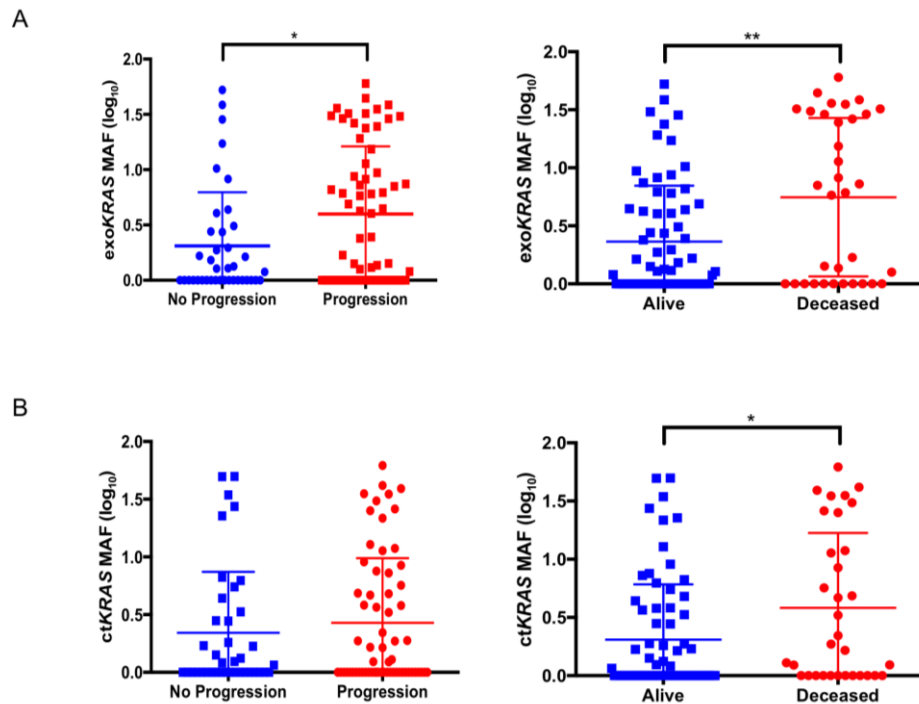
Figure 9 Correlates of survival and KRAS MAF at baseline treatment naïve status.

A. Median MAF of exo*KRAS* in metastatic patients is significantly greater in those patients that have progressed (p = 0.03) and are deceased compared (p=0.01) to those that are not. B. Median MAF of ct*KRAS* is significantly greater in those patients that are deceased compared (p=0.03) to those that are not, by Mann-Whitney test. All axis have been scaled to log10 for visual representation.
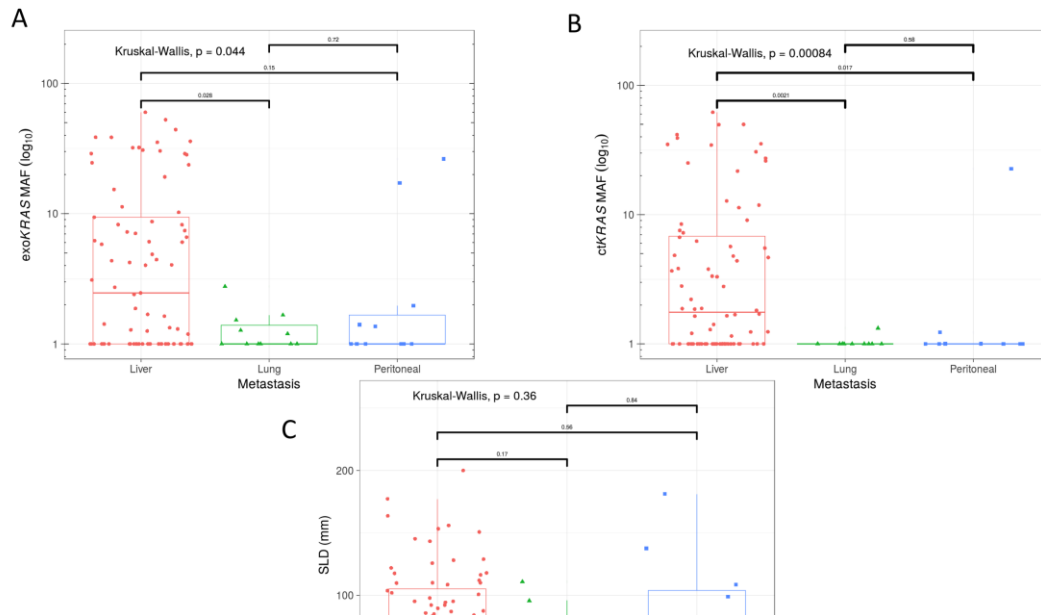
Figure 10 Distribution of exoKRAS, ctKRAS, and SLD stratified against type of metastasis

Boxplots of the distributions. $Log_{10}(x + 1)$ was used to transform the *KRAS* results. X + 1 was used to keep *KRAS* MAF values at 0. The Wilcoxon test was used to compare between two subsets and the Kruskal-Wallis was used to compare between all three. A. exo*KRAS* MAF (N = 103) plotted against metastasis type. Median and range for Liver, Lung and Peritoneal Metastasis were 1.463 (0-59.091), 0 (0-1.763), 0 (0-25.358) respectively. *P*-value between pairs of Liver and Lung, Liver and Peritoneal, and Lung and Peritoneal were 0.028, 0.15, 0.72 respectively. *P*-value for all three was 0.044. B. exo*KRAS* MAF (N = 100) plotted against metastasis type. Median and range for Liver, Lung and Peritoneal Metastasis were 0.760 (0-60.969), 0 (0-0.327, 0 (0-21.664) respectively. *P*-value between pairs of Liver and Lung, Liver and Peritoneal, and Lung and Peritoneal were 0.0021, 0.017, 0.58 respectively. *P*-value for all three was 0.00084. C. SLD (Sum of Longest Diameters) (N = 102) plotted against metastasis type. Median and range for Liver, Lung and Peritoneal Metastasis were 77.5 (21-200), 61 (43-111, 61 (40-181) respectively. *P*-value between pairs of Liver and Lung, Liver and Peritoneal, and Lung and Peritoneal were 0.17, 0.56, 0.84 respectively. *P*-value for all three was 0.36.
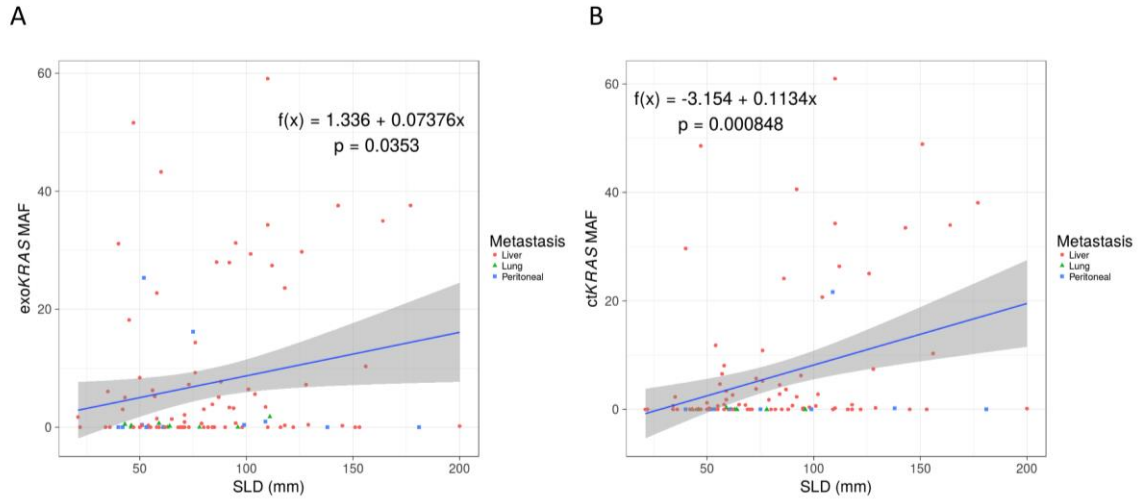
Figure 11 Trend between KRAS MAD and SLD

Linear regressions on between both exo*KRAS* and ct*KRAS* and SLD. (A) Exo*KRAS* modeled by f(x) = 1.336 + 0.07376x. *P*-value = 0.0353. R^2 = 0.04353, (B) ct*KRAS* modeled by f(x) = -3.154 + 0.1145x. *P*-value = 0.000848. R^2 = 0.1089

Figure 12 Distribtion of exoKRAS and cfKRAS stratified for ECOG performance status.

Boxplots of the distributions. $Log_{10}(x + 1)$ was used to transform the *KRAS* results. X + 1 was used to keep *KRAS* MAF values at 0. The Wilcoxon test was used to compare between two subsets and the Kruskal-Wallis was used to compare between all categories.

Prognostic impact of liquid biopsy parameters at presentation in metastatic PDAC patients

To avoid confounding effects of chemotherapy on exoDNA and ctDNA kinetics, we performed subset analysis on 104 metastatic patients who were treatment naïve at the time of presentation. An optimal threshold for ctDNA was assessed by receiver operating curve (ROC) analysis with the optimal cutoff achieving a sensitivity and specificity of 60% and 54% for OS, and 53% and 50% PFS, respectively. As previously described in other tumor types, the presence and absence of detectable ctDNA (i.e., any mutant *KRAS* on ddPCR) was significantly associated with patient outcomes (146, 149). For example, any detectable ctDNA was associated with significantly shorter PFS (log-rank test; HR 1.93, 95% CI 1.15-3.22, p=0.012) with a median PFS of 118 *versus* 321 days (for detection *versus* no detection, respectively, **(Figure 13B).** Detectable ctDNA also showed shorter OS (HR 2.36, 95% CI 1.16-4.79, p=0.018) with a median OS of 258 vs 440 days (detection and no detection, respectively, (**Figure 13B**). In the context of exoDNA, an optimal exo*KRAS* MAF was determined to be 5%, achieving the optimal cutoff by ROC analysis with a sensitivity and specificity of 51% and 85% for OS, and 89% and 36% for PFS respectively. Using this threshold of 5% *KRAS* MAF, patients with higher than 5% *KRAS* MAF were significantly associated with reduced PFS (HR 4.78, 95% CI 2.47-9.26, p<0.0001) and OS (HR 7.31, 95% CI 3.15-17.00, p<0.0001) on Kaplan-Meier analysis **(Figure 13A).** Similarly, survival analyses of the standard clinical biomarker CA19-9 **(Figure 14)** demonstrated that patients with a CA19-9 ≥ 300 at treatment naive presentation had worse OS (p=0.023), with PFS trending towards significance (p=0.06).

Using a Cox regression model **(Table 7),** univariate analysis revealed *KRAS* MAF ≥5% in exoDNA (HR 3.5, 95% CI 2.1 – 5.9, *p*<0.0001) and any ctDNA detection (HR 1.8, 95% CI 1.1 – 3.0, *p*=0.019), were significantly associated with shorter PFS. On multivariate analysis, exo*KRAS* ≥5% remained the only significant predictor of PFS (HR 2.28, 95% CI 1.18-4.40, P=0.014). Combining *KRAS* MAF ≥5% in exoDNA or ctDNA detection with a CA19-9 ≥300 did not reveal an increase in predictive significance of these biomarkers for poorer PFS.
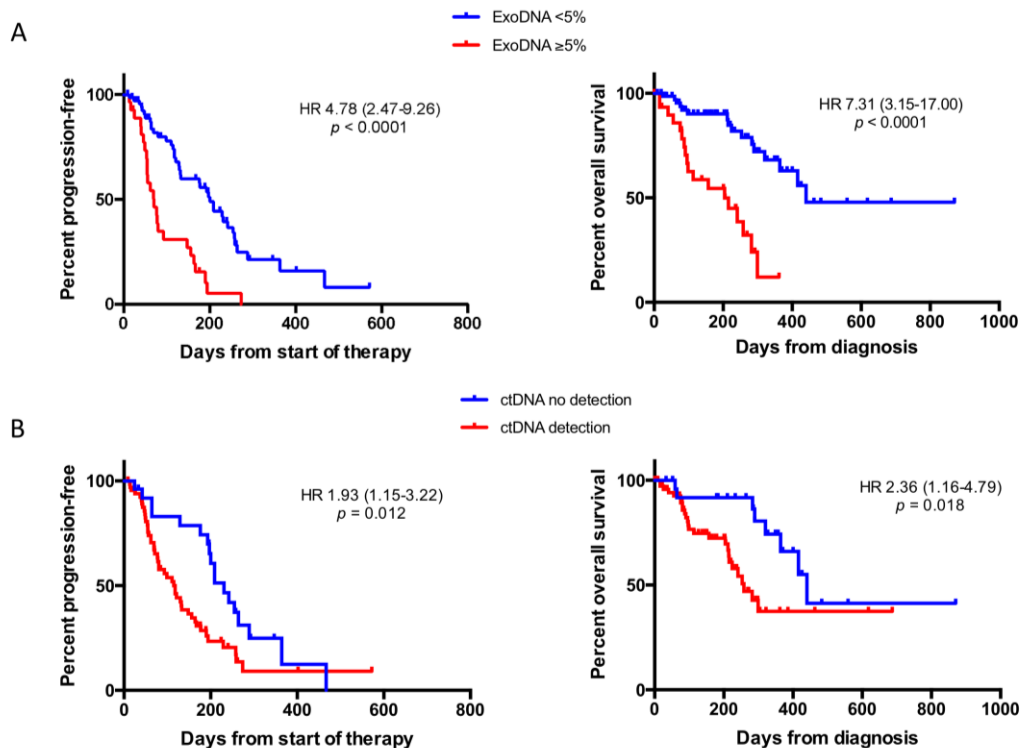
Figure 13 Kaplan-Meier curve stratification of baseline treatment naïve metastatic patients.

(A) Patients with exo*KRAS* ≥5% experienced worse PFS (median 71 vs 200 days) and OS (median 204 vs 440 days). Detection of ctDNA was significantly associated with worse PFS (median 118 vs 231 days) and OS (258 days vs 440 days).

Figure 14 Kaplan Meier curve stratification of baseline treatment naïve patients based on CA19-9.

(**Top)** Patients with CA19-9 ≥300 experienced worse OS (median 204 vs 264 days, p = 0.023), (**Bottom)** but not significantly worse PFS (p=0.06).

Table 7 Univariate and multivariate analysis of clinical characteristics with exoKRAS and cfKRAS

Univariate Cox Regression (PFS)

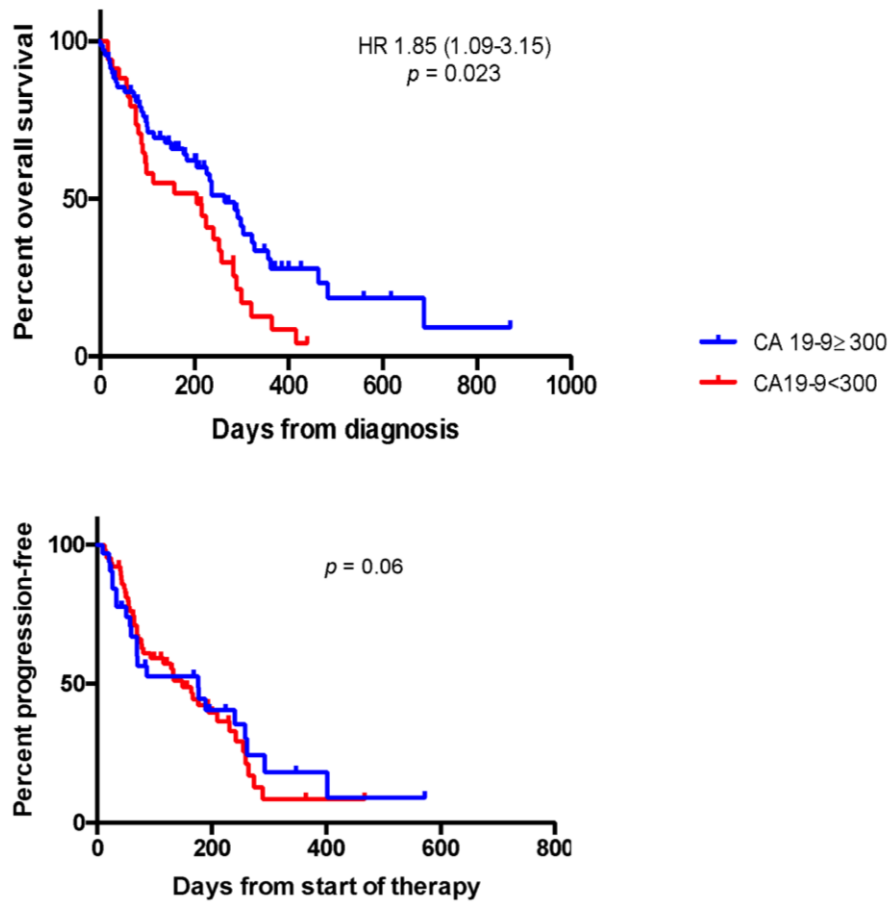|	beta	HR (95% CI for HR)	wald.test	p.value
exo*KRAS >5%*	1.2	3.5 (2.1-5.9)	22	3.5E-06
ctDNA Detection	0.59	1.8 (1.1-3)	5.5	0.019
Age	-0.0027	1 (0.97-1)	0.04	0.83
Gender (Male v Female)	0.45	1.6 (0.94-2.6)	3	0.084
ECOG (0 v 1)	0.6766	1.5 (0.72-3.04)	2.79	0.289
ECOG (0 v 2)	0.502	2.0(0.79-5.03)	2.79	0.145
ECOG (0 v 3)	0.442	1.51(0.40-5.68)	2.79	0.541
Regimen: GEM v FOLFIRINOX	0.53	1.7 (0.99-2.9)	3.7	0.054
Metastatic site: Liver v Lung	-0.775	0.4605 (0.2040-1.039)	5.29	0.0619
Metastatic site: Liver v Peritoneal	-0.719	0.4873 (0.2043-1.162)	5.29	0.1051
CA19-9 > 300	0.41	1.5 (0.89-2.6)	2.4	0.12

Multi-Analyte Analysis

	beta	HR (95% CI for HR)	wald.test	p.value
exoKRAS >5% and CA19-9 > 300	1.2	3.2 (1.9-5.5)	18	2.00E-05
exoKRAS >5% or CA19-9 > 300	0.64	1.9 (1.1-3.3)	4.7	0.03
ctDNA Detection and CA19-9 > 300	0.75	2.1 (1.3-3.5)	8	0.0048
ctDNA Detection or CA19-9 > 300	0.52	1.7 (0.89-3.2)	2.6	0.11
exoKRAS >5% + ctDNA Detection + CA19-9 > 300	1.4	3.9 (2.2-7.1)	21	5.20E-06

Multivariate Cox Regresssion Analysis (PFS)

	exp(coef)	exp(-coef)	lower .95	upper .95	Pr(>|z|)
exo*KRAS >5%*	2.2808	0.4384	1.1827	4.398	0.0139 *
ctDNA Detection	1.3236	0.7555	0.7568	2.315	0.3257
Gender (Male v Female)	1.3433	0.7444	0.7396	2.44	0.3324
ECOG (0 v 1)	1.2631	0.7917	0.5785	2.758	0.5577
ECOG (0 v 2)	2.8138	0.3554	0.9723	8.143	0.0564 .
ECOG (0 v 3)	1.1913	0.8394	0.2942	4.825	0.8062
Metastatic site: Liver v Lung	0.5615	1.7809	0.2193	1.438	0.2289
Metastatic site: Liver v Peritoneal	0.5103	1.9594	0.2083	1.25	0.1413
CA19-9 > 300	1.07	0.9346	0.6041	1.895	0.8166
Regimen: GEM v FOLFIRINOX	0.577298	1.78122	0.9987	3.177	0.0505

Likelihood ratio test= 26.36 on 9 df, p=0.001782
Wald test = 26.03 on 9 df, p=0.00202
Score (logrank) test = 29.31 on 9 df, p=0.0005753

Univariate Cox Regression (OS)

	beta	HR (95% CI for HR)	wald.test	p.value
exo*KRAS >5%*	1.5	4.6 (2.2-9.7)	17	0.000041
ctDNA Detection	1	2.8 (1.4-5.7)	8	0.0045
Age	0.017	1 (0.98-1.1)	0.84	0.36
Gender (Male v Female)	0.33	1.4 (0.7-2.8)	0.91	0.34
ECOG (0 v 1)	0.2677	1.307(0.45-3.81)	6.35	0.624
ECOG (0 v 2)	1.2708	3.564(1.04-12.3)	6.35	0.0439
ECOG (0 v 3)	0.8247	2.281(0.41-12.8)	6.35	0.3477
Regimen: GEM v FOLFIRINOX	0.85	2.3 (1.1-5.2)	4.4	0.036
Metastatic site: Liver v Lung	-1.2193	0.2954 (0.06948-1.256)	2.76	0.0987
Metastatic site: Liver v Peritoneal	-0.2011	0.8178 (0.28198-2.372)	2.76	0.7113
CA19-9 > 300	1.2	3.2 (1.3-7.7)	6.5	0.011

Multi-Analyte Analysis

	beta	HR (95% CI for HR)	wald.test	p.value
exoKRAS >5% and CA19-9 > 300	1.7	5.4 (2.6-11)	21	4.90E-06
exoKRAS >5% or CA19-9 > 300	1.2	3.3 (1.3-8.6)	6	0.015
ctDNA Detection and CA19-9 > 300	1.2	3.4 (1.7-6.7)	12	0.00052
ctDNA Detection or CA19-9 > 300	1.8	5.8 (1.4-25)	5.8	0.016
exoKRAS >5% + ctDNA Detection + CA19-9 > 300	1.9	6.6 (3.1-14)	24	9.30E-07

Multivariate Cox Regresssion Analysis (OS)

	exp(coef)	exp(-coef)	lower .95	upper .95	
exo*KRAS >5%*	3.4553	0.2894	1.4044	8.501	0.00695 **
ctDNA Detection	1.6662	0.6002	0.7416	3.744	0.21638
ECOG (0 v 1)	1.2134	0.8242	0.3945	3.732	0.73586
ECOG (0 v 2)	3.1891	0.3136	0.8828	11.52	0.07676 .
ECOG (0 v 3)	1.703	0.5872	0.2692	10.772	0.57162
Metastatic site: Liver v Lung	0.5372	1.8614	0.1102	2.62	0.44215
Metastatic site: Liver v Peritoneal	1.4894	0.6714	0.4822	4.6	0.48868
CA19-9 > 300	2.1451	0.4662	0.8415	5.468	0.10994
Regimen: GEM v FOLFIRINOX	0.612157	1.844406	0.7615	4.468	0.175

Likelihood ratio test= 29.01 on 8 df, p=0.0003163
Wald test = 25.22 on 8 df, p=0.001426
Score (logrank) test = 30.93 on 8 df, p=0.0001446

For OS, *KRAS* MAF ≥5% in exoDNA (HR 4.6, 95% CI 2.2-9.7, *p<0.0001*), any ctDNA detection (HR 2.8, 95% CI 1.4-5.7, *p=0.0045*), CA19-9 ≥300 (HR 3.2, 95% CI 1.3-7.7, *p=0.011*), and an ECOG performance status score of 2 (HR 3.56, 95% CI 1.04-12.3, *p=0.044*) were significant predictors of poorer outcomes on univariate analysis. On multivariate analysis, exo*KRAS* ≥5% (HR 3.46, 95% CI 1.40-8.50, P=0.007) remained as a significant predictor of poorer OS. An exo*KRAS* MAF ≥5% together with a CA19-9 ≥300 (HR 6.41, 95% CI 2.31-17.80, P=0.0004) at baseline treatment naïve status resulted as a significant predictor of poorer OS. Although on its own, ctDNA did not emerge as a significant predictor on multivariate analysis, detection of ctDNA emerged as a significant predictor of poorer OS when occurring with a CA19-9 ≥300 at baseline treatment naïve status (HR 6.37, 95% CI 2.36-17.24, P=0.0003). Additionally exo*KRAS* MAF ≥5% and ctDNA detection was correlated to poorer OS (HR 7.73, 95% CI 2.61-22.91, P=0.00002) on multivariate analysis when both occurring at baseline treatment naïve status in the same patient, underlining the potential complementary nature of these biomarkers).

Longitudinal monitoring of metastatic PDAC using serial liquid biopsies anticipates on-treatment progression

To fully evaluate the utility of liquid biopsies in monitoring the natural history of metastatic PDAC, we profiled exoDNA and ctDNA through 123 serial blood draws among 34 patients with a median follow-up time of 202 days. Specifically, we selected patients who had at least 2 blood draws taken during a concurrent therapeutic regimen, with two or more restaging imagings taken at standard 2-3 month intervals. Among the monitored patients, 20/34 (59%) progressed on therapy, with a median time to progression of 176 days. Patients who did not progress had a median follow-up time of 300 days. Analysis of plasma samples revealed that a *KRAS* MAF peak of ≥1% in any on-treatment serial exoDNA sample was significantly associated with eventual disease progression, as determined by RECIST 1.1 (p < 0.0001) **(Figure 15).** The

optimal MAF of ctDNA *KRAS* and exoDNA *KRAS* in predicting progression was assessed by ROC analysis with only exo*KRAS* achieving predictive significance with a sensitivity and specificity of 79% and 100%, respectively. Among the 20 patients who progressed, 16 (80%) saw an exoDNA *KRAS* MAF peak of ≥1% compared to none in those patients without progression 14/14 (100%). In contrast, serial ctDNA MAF did not correlate significantly with presence or absence of progression. Using a threshold of 20% or greater increase of CA19-9 during therapy, the sensitivity and specificity of CA19-9 in predicting progression was 70% and 89%, respectively. Importantly, when assessing for the length of time when *KRAS* MAF in serial exoDNA exceeded ≥1% and the subsequent onset of radiological progression, exo*KRAS* had a significantly longer lead time (median of 50 days, *p*=0.03) compared to lead times obtained by using 20% or greater increase in serial CA19-9 (which essentially coincided with the onset of radiological progression) **(Figure 15C).** Additional application of Bayesian inference provided us with posterior probabilities of 100% chance of progression given an exo*KRAS* peak ≥1% (P(Progression | exo*KRAS* ≥1%)) and 90% chance of prolonged response to therapy (No progression recorded before censor) given that exo*KRAS* remains <1% (P(No Progression | exo*KRAS* <1%)).
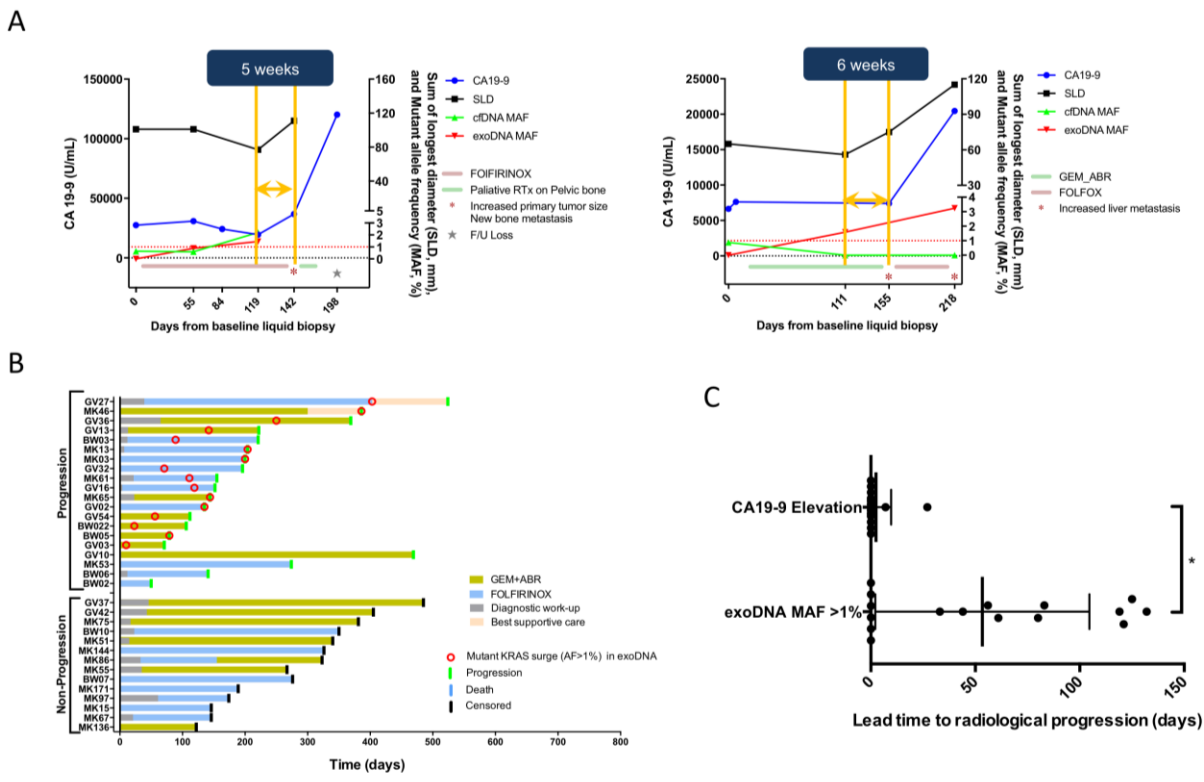
Figure 15 Tumor monitoring of metastatic PDAC using liquid biopsies

(A) Tumor monitoring using serial liquid biopsies demonstrating correlation between a exo*KRAS* peak ≥1% (red line) and radiological progression based on RECIST 1.1 (black line). The standard pancreatic cancer biomarker is plotted (blue) as well as ct*KRAS* (green) for comparison. (B) Tumor monitoring among 34 patients demonstrates the ability of exo*KRAS* peaks ≥1% (red circle) to predict radiological progression (green bar). Peaks are identified in 11/14 patients that progressed compared to in no patients that did not progress, 9/9. exo*KRAS* peak is significantly associated to progression (p =0.0003) on Fisher's exact test with an Odds ratio of 62.4 (95% CI 2.852 - 1367). (C) MAF *KRAS* peak demonstrates a significantly greater median lead time in predicting progression of 50 days (p=0.03) from the time clinically detectable progression was evident on CT imaging compared to CA19-9 (median lead time = 0 days).

Discussion

Nucleic acids derived from exosomes have been reported as a novel compartment of high quality DNA material which is protected from degradation in circulation (70-72). As opposed to ctDNA, which exists in the 150-170bp range, protected exoDNA is found in a high molecular weight format that readily lends itself to next generation sequencing (NGS) for molecular profiling. In our study, we profile matched exoDNA and ctDNA for mutant *KRAS* alleles by quantitative ddPCR in a large series of prospectively collected plasma samples from PDAC patients (N=194), and identify baseline detection rates of 61% and 53% in metastatic disease, and 38% and 34% in localized disease, for exoDNA and ctDNA, respectively. A substantial minority of patients (between 12-25%) with pre-neoplastic pancreatic cysts or non-neoplastic pancreatic diseases (such as chronic pancreatitis) harbored detectable circulating mutant. *KRAS* mutations are present in up to 80% of pre-neoplastic pancreatic cysts (including low-grade mucinous cysts) (155, 156), and thus their detection on ddPCR in the circulation is not surprising. Mutations in *KRAS* are also detectable in the pancreas as a consequence of non-neoplastic inflammatory processes such as chronic pancreatitis, although tissue based studies have confirmed a lower frequency of mutations than in either cancer or in pre-neoplastic cysts (131, 157, 158). In line with these observations, and as an indirect derivation of "tissue mutation load", quantitative ddPCR found average *KRAS* MAF to be highest in baseline metastatic samples, followed by localized disease, cystic lesions and finally, non-neoplastic panceatic diseases, in that order.

Beyond detection of tumor-derived DNA *per se* in liquid biopsies as a biomarker of an underlying neoplasm, recent studies have also focused on the potential prognostic value imparted by ctDNA or exoDNA measurement in cancer patients at the time of presentation. For example, Mohrmann et al reported that among 41 patients with advanced solid cancers, driver mutation detection by ddPCR in either exoDNA or ctDNA was associated with overall survival on Kaplan-Meier analysis, although only exoDNA at the time of presentation was an independent prognostic factor for OS on multivariate analysis (HR 0.15, 0.03-0.80, *p*= 0.026) (159). On these lines, several

studies have evaluated the prognostic potential of liquid biopsies in PDAC, most focusing on ctDNA measured using digital PCR. In a relatively small study, Earl et al, report *KRAS* mutant ctDNA detection in 8/31 (26%) patients across various PDAC stages, with detection being significantly correlated to OS (HR12.2, p =0.0002) (160). In a larger study of 105 patients, Hadano et al. report a cumulative rate of 31% ctDNA detection across stages, with median survival of 13.6 months vs 27.6 months in those patients with detectable *versus* no detectable ctDNA, respectively, and a significant association with OS (p<0.0001) (161). In our own series, detection of ctDNA and exoDNA at presentation were both associated with significant deleterious impact on OS and PFS on univariate analysis, although only an exoDNA *KRAS* MAF ≥ 5% was an independent negative predictor of poor survival on multivariate analysis (HR 2.28, 95% CI 1.18-4.40, p=0.014 for PFS and HR 3.46, 95% CI 1.40-8.50, p=0.007 for OS, respectively) when used independently. As previous work had demonstrated the utility of using a combination of biomarkers for early detection, particularly ctDNA and CA19-9 in the context of surgically resectable pancreatic cancer, we aimed to determine the prognostic significance of combining ctDNA detection or exoDNA MAF with CA19-9 (162, 163). Although ctDNA detection alone was not a significant predictor of outcomes, we did observe a combination of ctDNA detection and a CA19-9 ≥300 at baseline treatment naïve status to be a significant predictor of poorer OS (HR 6.37, 95% CI 2.36-17.24, P=0.0003), demonstrating the utility of a multi-analyte approach. We also saw this same phenomenon when combining ctDNA detection and exo*KRAS* MAF ≥5% as a significant predictor of OS (HR 7.73, 95% CI 2.61-22.91, P=0.00002). Ultimately, these blood based biomarkers demonstrate complementary utility in prognostic value where the presence of these thresholds suggests that those patients may require more intense followup to capture earlier progression, or more aggressive therapy than standard of care to influence outcomes. This helps underline how each may represent distinct biologies, despite sharing the moniker of "liquid biopsy", whereby ctDNA is released from apoptotic or necrotic cells, while exosomes may represent material released into circulation from rapidly dividing viable cells.

One major advantage of liquid biopsies is the ability to conduct longitudinal monitoring of on-treatment patients as a readout of therapeutic efficacy. While this is typically conducted in PDAC with serial imaging scans or with CA19-9, liquid biopsies might provide adjunctive, and potentially superior, predictive data on treatment response, with an opportunity for anticipating treatment intervention. In an earlier study, Tjensvoll et al reported pilot data from a cohort of 14 PDAC patients, using Peptide–nucleic acid–clamp PCR *KRAS* mutation detection (164). Monitoring ctDNA levels during chemotherapy demonstrated a correlation with CA19-9 and radiological progression among 3 patients. In a separate series, Sausen et al., used digital PCR for ctDNA detection following tumor resection in localized PDAC (36). Among nine patients with detectable ctDNA and radiological recurrence, the authors report ctDNA detection an average of 3.1 months after resection compared to 9.6 months when it becomes clinically detectable on CT imaging. These data suggest a potential role for using liquid biopsies to facilitate earlier detection of progression than radiological scans. In our cohort, we examined 34 metastatic patients who had sufficient longitudinal on-treatment follow-up and serial liquid biopsies to report tumor monitoring outcomes. Although we did not find significant association between progression outcomes with changes in ctDNA, we did find a significant correlation between exoDNA *KRAS* MAF and eventual radiological progression. Specifically, those patients with an exoDNA *KRAS* MAF ≥1% on any on-treatment serial biopsy have a 100% probability of progressing, with a median lead time to radiological progression of 50 days from the first sample with exoDNA *KRAS* MAF ≥ 1%. In contrast, patients who maintained exoDNA *KRAS* MAF <1% on serial monitoring had a 90% probability of not progressing on therapy in the ~1 year median follow up duration of our study. We believe this mutant exoDNA "spike" ≥1%, albeit transient, represents a growth spurt of the underlying cancer, likely coinciding with the incipient onset of resistance to ongoing therapy. The ability of serial liquid biopsies to predict which PDAC patients are most likely to fail first or second line chemotherapy is of clinical utility, since it provides an earlier opportunity than radiological imaging for changing course. It is also important to note, that continued exposure of patients to ineffective first or second line regimens may result in unnecessary toxicities and deterioration of

performance status, which might make patients no longer candidates for subsequent line therapies.

In addition to metastatic patients, our prospective series also examined the utility of serial liquid biopsies in patients with localized PDAC. At MD Anderson, and increasingly at other centers in the US, patients with localized disease receive preoperative (neoadjuvant) chemo-radiation therapy. The main objective of neoadjuvant therapy is to prolong the survival of patients undergoing surgery and minimize the use of surgery for patients unlikely to benefit from it (165). However, indicators of the effectiveness of neoadjuvant therapy and subsequent surgical resection remain a significant unment need. We postulated that liquid biopsy kinetics between initiation and culmination of neoadjuvant treatment may predict for response to neoadjuvant therapy and lack of progression, thus enabling surgery. In fact, a decrease in exoDNA *KRAS* MAF (but not ctDNA) between the beginning and the end of neoadjuvant therapy was significantly correlated with eventual surgical resection, when compared to those patients experiencing a rise in exoDNA *KRAS* MAF (OR 38.4, CI 3.95-373.3, p=0.0002). Although this same correlation held true for CA19-9 (OR 28.0, CI 2.65-295.9, p=0.003) which is not significantly different from exoDNA, it's worth noting how liquid biopsies may be used as complementary biomarkers in those patients that are deemed CA19-9 non-expressors or those patients with obstructive jaundice, where CA19-9 shows no correlation to progressive disease, as in 33% of patients in our series. Notably, even in one case where CT imaging did not detect overt progression despite a rise in exoDNA *KRAS* MAF, laparotomy confirmed the discovery of CT-occult omental metastasis. This data suggests a role for serial liquid biopsies, and specifically exoDNA, as a putative predictive biomarker for disease status following neoadjuvant therapy.

It is important to note several weaknesses of the current study. Although the strategy of using mutant *KRAS* molecules as a tumor marker may be theoretically optimal in a disease like PDAC where *KRAS* mutation rates exceed 90%, the stochastic nature of circulating nucleic acids released in circulation may underestimate the true circulating tumor burden if detection is limited

to a single mutation. This may likely be a contributing factor to the poor predictive potential of ctDNA in the context of metastatic disease as well as those patients undergoing neoadjuvant therapy. Of note, we do find notable differences in our previously published exo*KRAS* and ctDNA detection rates in metastatic (85% and 57.9%, respectively) and localized disease patients (67% and 45.5%, respectively) obtained from a retrospective bio-banked cohort (11). The differences in detection rate are largely due to the fact that exoDNA and ctDNA in the previous study underwent whole genome amplification to increase sensitivity of *KRAS* detection in the context of early detection efforts. Although this was a possibility in the current series, we opted against amplification as this would have distorted the MAFs found through ddPCR and thus effected our clinical endpoints. It is important to note that the use of a tumor gene panel (e.g. *KRAS, TP53, CDKN2A,* and *SMAD4)* may achieve greater sensitivity for detection and monitoring (146, 150). Additionally, the fact that our multigene panel does not cover *KRAS* hotspot mutations in codon 61, may underestimate our true sensitivity as the current panel has theoretical detection rate of up to 80% of known *KRAS* mutations in PDAC. Although our detection rates of *KRAS* mutant molecules are relatively modest at 32% to 41% in baseline treatment naïve metastatic patients based on the liquid biopsy compartment, a fact that may limit the amount of patients that may benefit from such an assay, when looking at general detection in both compartments at once, detection rates increase to 73.1%, which is near the theoretical limit of our assay. This underlines the complementary nature of these biomarkers, especially in setting of low volume disease (such as post-treatment, or monitoring fore recurrence), whereby the absence of mutant detection in one does not preclude the ability to gain valuable genomic information in the other. Additionally, although exoDNA mutant *KRAS* detection levels compared to ctDNA detection levels are not significantly better in the current cohort, exosomes provide the added ability to perform specific enrichment of cancer-derived material, allowing for capture of DNA, RNA, and proteins derived from tumors for mutation, gene expression, and possibly even neoantigen detection (14). The need of a gold standard validation is also important when pursuing liquid biopsy assays such as the one described in this study. As such, recent work has attempted to validate concordance

between mutations found in liquid biopsies and tissue biopsies (166-171). In the context of PDAC, acquiring tissue biopsies for molecular profiling is particularly difficult in the metastatic setting where fine needle aspirates are typically reserved for diagnostic purposes. We thus selected a small cohort of 34 localized disease patients where concordance rates ranged from 66.7% to 95.5% depending on the liquid biopsy and tissue source. Unsurprisingly, surgical tissue specimens saw greater rates of concordance, particularly in exoDNA which is likely associated to the greater sensitivity of mutation detection within exosomes. Overall, *KRAS* mutation detection rates was high within liquid biopsies as a whole, although it remains to be seen if profiling of additional mutations can achieve this sensitivity and specificity.

In conclusion, our study in a relatively large cohort of PDAC patients, comprised of both metastatic and localized disease, reiterates the predictive and prognostic value of liquid biopsies in this malignancy. We demonstrate that while the baseline CA19-9, exoDNA, and ctDNA cargo has prognostic effect, longitudinal monitoring of exoDNA provides unique predictive information on the outcome of neoadjuvant therapy in localized disease, and in anticipating progression in the metastatic setting. In contrast to the challenges of repetitive tissue biopsies for visceral cancers, serial liquid biopsies may provide an attractive alternative strategy to map tumor evolution in real time, providing an unprecedented insight into how the PDAC genome adapts to, and eventually becomes recalcitrant, to therapy.

Chapter 5 – Whole genome, exome, and transcriptome profiling of liquid biopsies with exoDNA

With permission this chapter is based upon "**San Lucas, F. A.*, K. Allenson*, V. Bernard*,** J. Castillo, D. U. Kim, K. Ellis, E. A. Ehli, G. E. Davies, J. L. Petersen, D. Li, R. Wolff, M. Katz, G. Varadhachary, I. Wistuba, A. Maitra, and H. Alvarez. 2015. Minimally invasive genomic and transcriptomic profiling of visceral cancers by next-generation sequencing of circulating exosomes. *Annals of oncology : official journal of the European Society for Medical Oncology / ESMO* (***First authorship shared)**"

Abstract

Background: The ability to perform comprehensive profiling of cancers at high-resolution is essential for precision medicine. Liquid biopsies using shed exosomes provide high-quality nucleic acids to obtain molecular characterization, which may be especially useful for visceral cancers that are not amenable to routine biopsies.

Patients and Methods: We isolated shed exosomes in biofluids from three patients with pancreaticobiliary cancers (two pancreatic, one ampullary). We performed comprehensive profiling of exoDNA and exoRNA by whole genome, exome and transcriptome sequencing using the Illumina HiSeq 2500 sequencer. We assessed the feasibility of calling copy number events, detecting mutational signatures and identifying potentially actionable mutations in exoDNA sequencing data, as well as expressed point mutations and gene fusions in exoRNA sequencing data.

Results: Whole exome sequencing resulted in 95 to 99% of the target regions covered at a mean depth of 133 to 490x. Genome-wide copy number profiles, and high estimates of tumor fractions (ranging from 56 to 82%), suggest robust representation of the tumor DNA within the shed exosomal compartment. Multiple actionable mutations, including alterations in *NOTCH1* and *BRCA2,* were found in patient exoDNA samples. Further, RNA sequencing of shed exosomes identified the presence of expressed fusion genes, representing an avenue for elucidation of tumor neoantigens.

Conclusions: We have demonstrated high-resolution profiling of the genomic and transcriptomic landscapes of visceral cancers. A wide range of cancer-derived biomarkers could be detected within the nucleic acid cargo of shed exosomes, including copy number profiles, point mutations, insertions, deletions, gene fusions and mutational signatures. Liquid biopsies using shed exosomes has the potential to be used as a clinical tool for cancer

diagnosis, therapeutic stratification, and treatment monitoring, precluding the need for direct

tumor sampling.

Patients and samples

Three patients with pancreatobiliary cancers were included in our comprehensive liquid biopsy study (supplementary Table S1), and each was consented following institutional review board approval (PA15-014). Case LBx01 is a 57-year old man who initially presented with stage IIA PDAC. He received neoadjuvant gemcitabine-based chemoradiation therapy with subsequent R0 resection and adjuvant gemcitabine. He was diagnosed with multifocal pulmonary recurrence on surveillance imaging 16 months after completion of adjuvant therapy, and confirmed pathologically by thoracoscopic wedge resection of one dominant lesion. Whole exome and RNA sequencing were performed on the metastatic lung tissue (by Dr. Arul Chinnaiyan at the University of Michigan). Thirteen months subsequent to surgical metastatectomy, the patient then developed evidence of pleural effusion, and therapeutic thoracentesis yielded 800 mL of pleural fluid from which shed exosomes were isolated and downstream whole genome, exome and RNA sequencing analyses were performed. Case LBx02 is a 68-year old woman with PDAC primary and hepatic metastases. Thirty mL of whole blood were collected via standard blood draw prior to initiation of chemotherapy and exosomes were isolated for subsequent tumor profiling analyses. Case LBx03 is a 74-year old man who underwent an upfront pancreaticoduodenectomy for an ampullary mass. Final pathology confirmed a stage IIB pancreatobiliary type adenocarcinoma of the ampulla. He received platinum-based adjuvant chemoradiotherapy and had no evidence of recurrence 5 months after completion of definitive therapy. Thirty mL of peripheral whole blood were collected upon the patient's referral to MD Anderson Cancer Center after resection, but prior to beginning any adjuvant therapy. Plasma exosomes were isolated for tumor profiling analyses.

Introduction

For many visceral cancers, such as pancreatic ductal adenocarcinoma (PDAC), the availability of tissue-based companion diagnostics may be limited or precluded secondary to clinical factors such as tumor location, amount of tumor tissue sampled or procedure-associated risk, hindering the progress of precision medicine (172). Relatively non-invasive liquid biopsies offer a promising alternative for tumor characterization and disease monitoring. To this end, several investigators have identified tumor-specific genetic mutations in patient plasma-derived circulating cell-free DNA (cfDNA) including activating mutations in *KRAS*, *BRAF*, *EGFR* and other cancer genes using highly-sensitive targeted approaches such as digital PCR and targeted amplicon sequencing on cfDNA (173-175). Recently, whole genome and exome sequencing have been performed using the cfDNA of plasma samples in an effort to estimate tumor copy number profiles and identify actionable mutations in a more agnostic manner (45, 176, 177). However, the extensively fragmented nature of cfDNA in circulation makes it difficult for this format to become generalizable in the context of genomic characterization of tumors through current next-generation sequencing (NGS) platforms (85). This limitation is even more profound in the context of circulating RNAs, where profiling is essentially restricted to small microRNAs, due to extensive fragmentation of coding transcripts (86, 87, 178).

Exosomes are 40-150 nanometer-sized membrane-bound extracellular vesicles that arise by specific endosomal biogenesis pathways (179). Functionally, exosomes have been shown to influence the tumor microenvironment as vehicles for cell-cell communication in cancer, harboring a diverse repertoire of molecular cargo that are shielded from degradation in circulation and that are representative of their originating cells (67, 179, 180). Therefore, the quality, diversity and tumor-specific nature of exosomal DNA (exoDNA), and exoRNA provide a potentially favorable alternative compared to cell-free nucleic acids for comprehensive tumor profiling at high-resolution. Indeed, recent publications have shown that exosomes contain

genomic representations of high molecular weight (HMW; >10kb), double-stranded fragments of DNA (70, 71).

We sought to assess the feasibility and potential clinical utility of characterizing the entire genomic and transcriptomic profiles of visceral cancers using the nucleic acid cargo within shed exosomes obtained from a single specimen of patient biofluid. We show, for the first time, that it is possible to perform integrative profiling of tumors from shed exosomes by analyzing the DNA and RNA cargo using standard NGS platforms, and that this approach has the potential to circumvent the need for direct tumor sampling in visceral cancers.

Results

Plasma and pleural effusion exosome isolations are enriched with high molecular weight double-stranded genomic DNA

Shed exosome populations were confirmed by scanning electron microscopy and transmission electron microscopy **(Figures 16A and B).** Nanoparticle-tracking analysis (Particle Metrix Inc.) confirmed the presence of exosome-sized vesicles in the liquid biopsy of all three patients **(Figure 16C).** Expression of canonical exosome surface markers, including the tetraspanin CD63 by flow cytometry and CD9, CD63, CD81 and HSP70 by western blots **(Figure 16D and E)** also established the presence of exosomes in our isolations. Extraction of exoDNA revealed quantifiable HMW double-stranded DNA (dsDNA; >10kb in size) as seen in **Figure 16F**.

Exosomes contain a large fraction of tumor DNA

KRAS mutant allele frequency (MAF) was determined using the *KRAS* multiplex screening assay and droplet digital PCR platform (ddPCR, BioRad Technologies, see Supplementary Methods) demonstrating tumor presence in our exosome isolations **(Figure 16G).** PCR-based analysis of mutant *KRAS* and *BRCA2* pre- and post-whole genome amplification demonstrated conserved MAFs **(Figure 17).** In addition, genome wide copy number profiling identified somatic copy number changes across the genomes of each patient. High estimates of tumor fractions ranging from 56 to 82% for each liquid biopsy sample suggests stout representation of the tumor within the circulating exosomes of each patient.

A

B

C

D

E

F

G
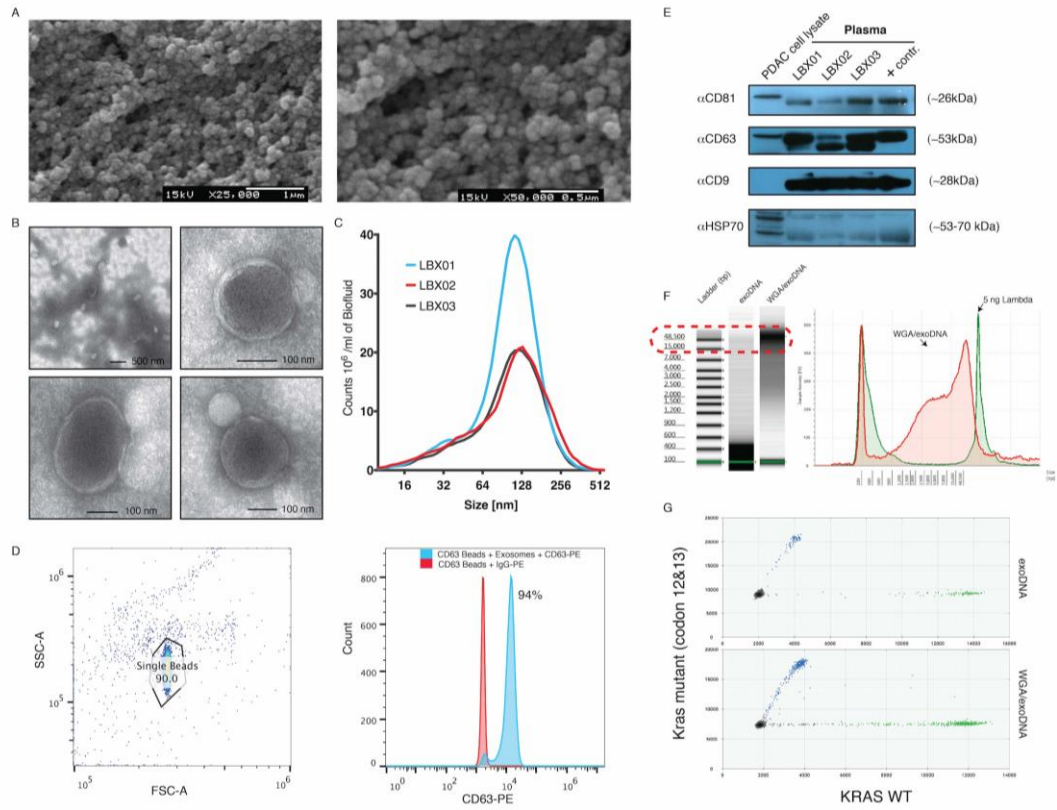
Figure 16 Characterization of exosomes isolated from liquid biopsies

A: Scanning electron microscopy of exosomes from plasma PDAC sample.

B: Illustrates that vesicle diameters are frequently only 5- to 10-fold greater than the bilayer thickness, which is typical of the internal vesicles of multivesicular bodies.

C: Size and counts of particles per ml biofluid (plasma or pleural effusion) as measured by nanoparticle tracking analysis. The size distribution is in the range of exosomes (40-150 nm) and other microvesicles.

D: Enriched exosomes were captured using the CD63+ Dynabeads. Dynabead bound exosomes were stained with PE Mouse Anti-Human CD63. Isotype control was stained by Simultest IgG2a/IgG1. The gating strategy for single beads is shown (left) with effective capture of CD63+ exosomes as demonstrated by the shift in fluorescence (right).

E: Western blots for exosomal markers (CD81, CD63, CD9 and HSP70) show that bands at the expected size were observed for multiple markers. Pa04C protein whole cell lysate is used as a protein expression control and human serum-derived exosomes (+ cont.) is use for the exosomal marker control.

F: Example of an exoDNA obtained from a clinical PDAC patient. Image shows the performance in the electropherogram of a HMW exoDNA pre and post WGA. Exosomes contain HMW DNA (>10kb in size), as determined using an Agilent tape Station 2200. AUC also show HMW DNA concentration higher than 60ng per microliter from a 20 microliter total volume, enough DNA for NGS on clinical samples.

G: ExoDNA was isolated from plasma of an advance case of PDAC. The sample on top comes from an individual with advanced PDAC (LBX03). Using ddPCR on 1µL of exoDNA eluate, we are able to detect mutant KRAS, blue dots (mutant droplets), green dots represent wild type sequences. Allele frequency of KRAS genes is preserved pre- (42%) and post-whole genome amplification (37%) (lower panel).
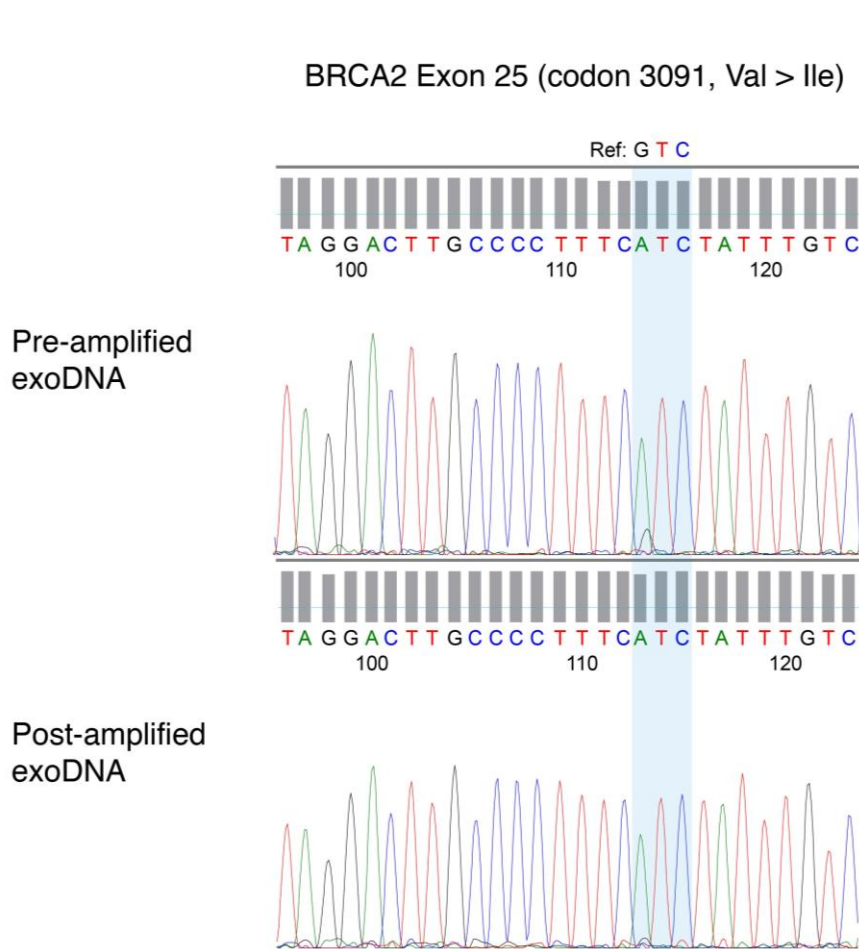
Figure 17 Sanger sequencing validation of exoDNA mutation

BRCA2 Sanger sequencing validation in the pre- and post-amplified exoDNA shows

preservation of allele frequencies approximately 80-90% pre and post-amplification.

ExoDNA is representative of the entire human genome

Whole genome sequencing covered 65 to 91% of the human genome at a mean depth of 12 to 35x at high sequencing quality with 88.2 to 92.5% of bases having greater than or equal to sequencing quality scores of Q30. Exome sequencing covered 95 to 99% of the targeted genome (54 megabases) with at least one read at a mean depth of 133 to 490x with 73 to 96% being covered by at least 10 reads. Ninety to 94.6% of bases represented high quality sequence suggesting that exoDNA in our samples is representative of the entire human genome.

Comprehensive profiling of tumors using exoDNA and mRNA

LBx01: Tumor profiling using pleural effusion exosomes from a patient with pancreatic ductal adenocarcinoma with previously resected lung metastasis

LBx01 is a patient PDAC, who underwent a thoracoscopic resection of a suspicious pulmonary nodule, subsequently confirmed to be metastasis. Fifteen months later, he developed a pleural effusion, which contained less than 1% malignant cells on cytospin, per final cytopathology report. A deep NGS assay performed on the pleural fluid cytospin failed to detect any evidence of tumor DNA. In contrast, abundant cancer-derived exosomes were present in the pleural fluid even with the marked paucity of cancer cells. The pleural effusion exoDNA had a computationally estimated tumor fraction of 82% (95% confidence region (CR) of 81-83%) and a mean genome copy number of 2.57. The exoDNA tumor fraction estimate was higher than that compared to the previously resected metastatic lung tissue (23%, 95% CR, 22-24%). The exoDNA mutation rate was estimated at 341 mutations/Mb compared to 2.06 mutations/Mb in the metastatic lung tissue DNA 15 months prior to the liquid biopsy sampling. This substantially higher mutational load is not surprising given the time between metastectomy and manifestation of pleural effusion, and the multi-drug cytotoxic chemotherapy regimen administered to the patient.

Potentially actionable mutations are listed in **Table 8**. We considered mutations to be potentially actionable if they are either putative drivers (recurrently mutated in COSMIC (100)) that could be monitored over the course of patient management, or COSMIC mutations that reside in genes associated with a clinical trial or cancer drug (see Supplemental Methods). Mutations in *KRAS* and *TP53* were identified in both the lung metastatic tissue and the subsequent pleural effusion. Mutations likely representative of progression include those in *APC* and *CHEK2*. The metastatic lung tissue harbored a mutation signature with peaks at C-to-T base substitutions that are consistent with Signature 1 of the COSMIC mutational signatures (**Figure 18C),** a common cancer signature proposed to be involved in spontaneous deamination of 5-methylcytosine (100, 113). The exoDNA mutational signature deviates from this, which suggests that additional mutational processes may have contributed to tumor progression, possibly driven by cytotoxic chemotherapy.

Table 8 Putative actionable mutations identified in LBc01

Chr	Pos	Ref	Alt	Gene	Amino acid change	Mutation type	COSMIC ID	COSMIC count	ExoRNA MAF	ExoDNA WES MAF	ExoDNA WGS MAF	Lung met WES MAF	Potential actionability
17	7578406	C	T	TP53	R175H	nonsynonymous SNV	COSM99024	91	100.00%	86.29%	80.00%	25.92%	Proteosome and HDAC inhibitor; Wee-1 inhibitors, p53 activator
12	25398284	C	T	KRAS	G12D	nonsynonymous SNV	COSM521	10139	71.43%	44.09%	78.95%	33.33%	MEK inhibitors
5	149459795	C	T	CSF1R	V138I	nonsynonymous SNV	COSM1645517	1	---	16.13%	---	---	CSF1R monoclonal antibody and inhibitors (Quizartinib|Linifanib|Vatalanib)
5	180057572	G	A	FLT4	S128F	nonsynonymous SNV	COSM225226	1	---	8.70%	---	---	FLT4 inhibitors (Ponatinib|Pazopanib|Dovitinib);Tyrosine kinase inhibitor (Sorafenib)
17	7578442	T	C	TP53	Y163C	nonsynonymous SNV	COSM129854	19	---	4.57%	---	---	Proteosome and HDAC inhibitor; Wee-1 inhibitors, p53 activator
5	112175639	C	T	APC	R1450X	stopgain	COSM13127	160	---	4.36%	---	---	---
16	2121535	C	T	TSC2	R622W	nonsynonymous SNV	COSM968407	1	---	4.18%	---	---	Loss of function predicts sensitivity to mTOR inhibitors (Everolimus|Temsirolimus|Sirolimus|BEZ235)
9	80537112	T	A	GNAQ	T96S	nonsynonymous SNV	COSM404628	2	10.53%	3.34%	11.11%	---	Melanoma cell lines with GNAQ mutations are more sensitive to MEK inhibitors (Van Raamsdonk et al., 2009; Ambrosini et al., 2012). The PKC inhibitors AEB071 and AHT956 selectively inhibited cells expressing mutant GNAQ (Chen et al., 2013).
1	65309887	G	A	JAK1	R755X	stopgain	COSM911557	1	---	3.27%	---	---	JAK inhibitors (Ruxolitinib)
22	29091840	T	C	CHEK2	K344E	nonsynonymous SNV	COSM42871	36	---	3.17%	22.22%	---	Loss of function suggests sensitivity to PARP inhibitors

ExoDNA copy number profiling showed that 27% of the genome exhibited copy number variation (**Figure 18A).** This included amplification of *MYC* (copy number (CN)=3; *P-val*=1.3e-72), *KRAS* (CN=6; *P*=2.7e-11), *EGFR* (CN=3; *P*=1.3e-138) and *ERBB2* (CN=5; *P*=6.1e-10). *ERBB2* amplification, in particular, was also identified in the previously resected lung metastasis, albeit at a lower copy number. We confirmed the amplification and overexpression, respectively, *ERBB2* in both exoDNA and exoRNA, where the estimated copy number was 5 and *ERBB2* was over-expressed at 85.13 transcripts per million (TPM) which represents a 3.62 times higher expression compared to normal pancreas tissue (23.52 TPM - the median *ERBB2* expression in normal pancreas tissue identified from the Genotype-Tissue Expression (GTEx) project (181)).

A key advantage of exoRNA (in contrast to cell free nucleic acids) is the preserved quality of transcripts that allows for assessment of an aberrant transcriptome in the same liquid biosample from which the genomic landscape is derived. As exemplified with *ERBB2*, cross comparison of exoDNA and exoRNA data permits precise delineation of the oncogenic targets of genomic copy number aberrations. Another potential clinical benefit of this approach is identification of expressed neoantigens from the tumor, be it missense mutations, or unique cancer-derived fusion transcripts, which can serve as the basis for identification of neoantigen-targeted humoral or cellular immune responses (182, 183). For example, the exoRNA confirmed presence of a *KRAS* G12D mutation in the transcriptome **(Figure 18B).** Furthermore, 87.8% of protein-coding transcripts were expressed (having greater than or equal to 2 TPM) and 40 putative expressed gene fusions were identified **(Figure 18D),** though no delineated cancer signaling pathways were overrepresented in the exoRNA data.
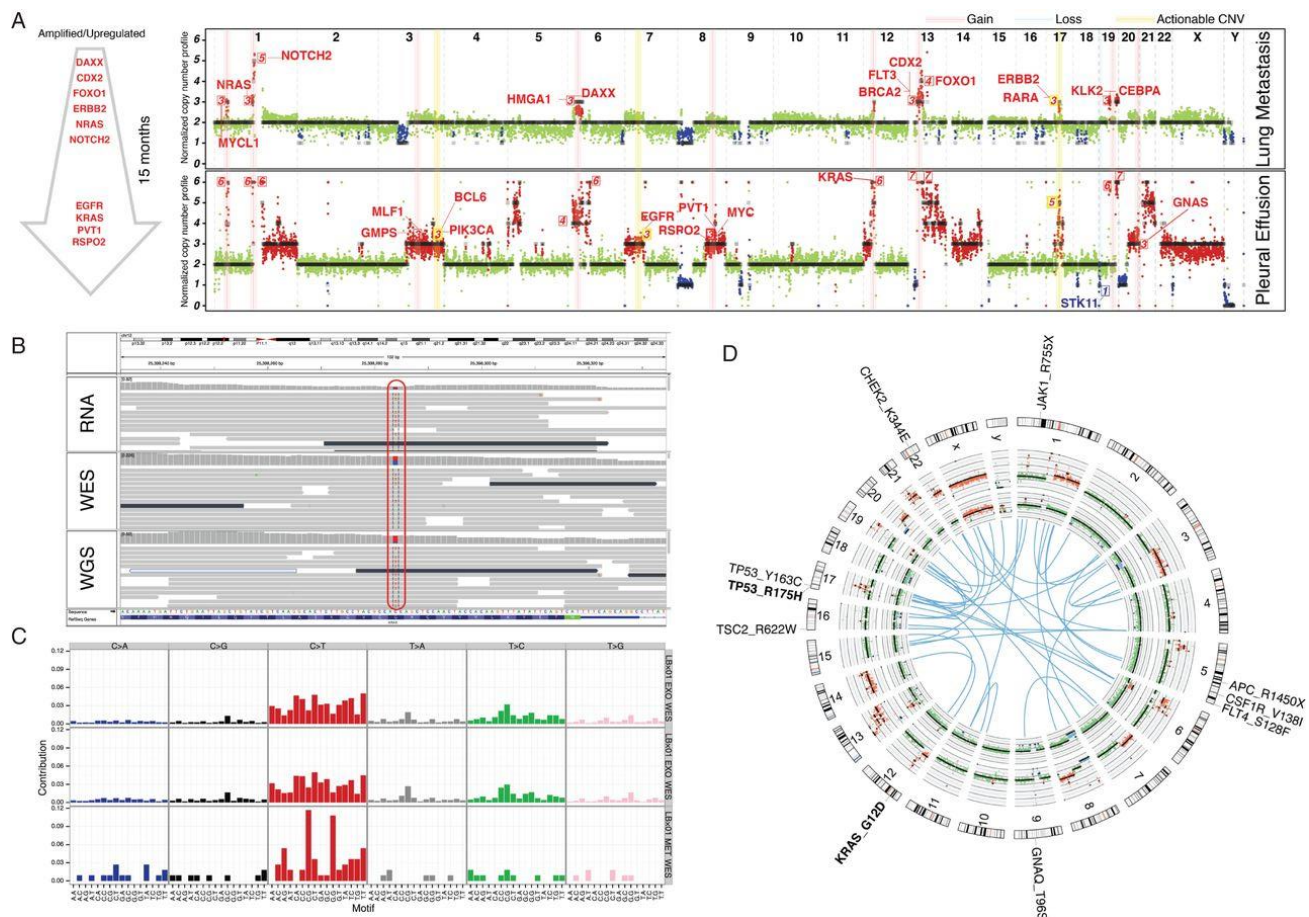
Figure 18 LBx01 tumor profiling

(A) Copy number profile comparison between the metastatic lung tissue (top) sampled 15 months before the pleural effusion exoDNA (bottom). The cancer-related genes on the light-red vertical bars have copy number gains and those on the light-blue vertical bars have copy number losses, where the numbered labels represent the estimated copy numbers. The yellow vertical bar annotates putatively actionable copy number variations (CNVs) (e.g. *ERBB2*). The arrow to the left depicts the progression of cancer-associated CNVs between the 2 time points. These happen to all be amplifications, which were also confirmed to be upregulated in the exoRNA compared with that in the metastatic lung tissue RNA-seq.

(B) Mutant KRAS was identified in the mRNA (RNA sequencing) as well as DNA (exome and genome sequencing) of the pleural effusion exosomes. (C) Mutational signature of the plasma exosomes derived from exome sequencing (top) and genome sequencing (middle) compared with the mutational signature of the metastatic lung tissue (bottom). (D) Circos plot illustrating putative gene fusions (blue), lung metastatic copy number profile (inner-most ring), pleural effusion exosomes copy number profile (second inner-most ring) and gene aberrations. Mutations seen in the pleural effusion are black and those seen in both the metastatic lung tissue and pleural effusion are in bolded black.

LBx02: Tumor profiling using blood-derived exosomes of a pancreatic ductal adenocarcinoma patient

LBx02 is a treatment-naïve patient with PDAC and hepatic metastases. The plasma exoDNA estimated tumor fraction was 56% (95% CR of 54-57%) with a mean genome copy number of 2.12. Copy number profiling showed that 9% of the genome exhibited copy number variation **(Figure 19A).** This included amplification of *MYC* (CN=13; *P*=4.7e-08), *KRAS* (CN=3; *P*=6.5e-24) and loss of *TP53* (CN=1; *P*=3.6e-39). Potential actionable mutations **(Table 9)** include mutations in *ERBB2*, *KRAS*, *NRAS* and *NOTCH1* (in practice, *KRAS or NRAS* mutations are not strictly actionable, although many commercially available or academic center-initiated sequencing panels list them as such). The exoDNA exhibited a mutation rate of 77 mutations/Mb and a profile resembling Signature 1 of the COSMIC mutational signatures **(Figure 19B)** (100, 113).

Approximately 9% of protein-coding transcripts were expressed in the exoRNA and 16 putative expressed fusions were identified (**Figure 19C).** The mTOR signaling pathway was over-represented in the exoRNA transcripts (Benjamini-Hochberg *P*=0.027).

Figure 19 LBx02 tumor profiling

(A) Copy number profile of the plasma exoDNA. (B) Mutational signature of the pleural effusion exosomes derived from exome sequencing (top) and genome sequencing (bottom). (C) Circos plot illustrating putative gene fusions (blue), plasma exoDNA copy number profile (inner-most ring) and potential actionable genes (blue, deletions; red, amplifications; black, somatic point mutations).

ble 9 LBx02 potentially actionable mutations

Chr	Pos	Ref	Alt	Gene	Amino acid change	Mutation type	COSMIC ID	COSMIC count	ExoDNA WES MAF	ExoDNA WGS MAF	Potential actionability
2	212812268	C	T	ERBB4	R103H	nonsynonymous SNV	---	---	51.59%	---	BMS-599626
12	25398284	C	A	KRAS	G12V	nonsynonymous SNV	COSM1140133	152	40.48%	57.14%	MEK inhibitors
1	115258747	C	T	NRAS	G12D	nonsynonymous SNV	COSM564	430	32.33%	30.77%	---
9	139400317	G	A	NOTCH1	T1344M	nonsynonymous SNV	---	---	36.80%	---	gamma secretase inhibitors|BMS-906024|RO4929097|MK-0752
9	35078190	G	C	FANCG	A153G	nonsynonymous SNV	---	---	30.32%	20.00%	Mitomycin
5	180030278	C	T	FLT4	E1336K	nonsynonymous SNV	---	---	25.78%	27.27%	FLT4 inhibitors (Ponatinib|Pazopanib|Dovitinib)
9	135772927	G	C	TSC1	T899S	nonsynonymous SNV	---	---	23.58%	---	Loss of function predicts sensitivity to mTOR inhibitors (Everolimus|Temsirolimus|Sirolimus|BEZ235)
18	60985773	C	T	BCL2	A43T	nonsynonymous SNV	---	---	20.00%	---	ABT-1999
11	108139302	C	G	ATM	T935R	nonsynonymous SNV	---	---	12.18%	---	Inactivation of ATM may predict sensitivity to PARP inhibitors
3	10128832	A	T	FANCD2	Y1117F	nonsynonymous SNV	---	---	11.99%	---	Mitomycin
5	56160742	G	C	MAP3K1	R339P	nonsynonymous SNV	---	---	9.04%	---	JNK1 inhibitor (PGL5001)
9	87325565	A	G	NTRK2	N148D	nonsynonymous SNV	---	---	8.57%	---	PLX7486
3	142257426	A	T	ATR	L1208Q	nonsynonymous SNV	---	---	6.19%	---	Biallelic inactivation predict sensitivity to PARP inhibitors
7	55273294	A	C	EGFR	E1076A	nonsynonymous SNV	---	---	5.12%	---	EGFR inhibitors (Erlotinib|Gefitinib|Afatinib|Lapatinib|Cetuximab|Panitumumab)

LBx03: Tu... carcinoma patient

identifies an unexpected therapeutic vulnerability

LBx03 plasma exoDNA had an estimated tumor fraction of 82% (95% CR of 81-84%) and a mean genome copy number of 2.5. Copy number profiling showed that 53% of the genome exhibited copy number variation **(Figure 20),** which suggests the presence of an "unstable" genome phenotype (40). Copy number aberrations include amplification of *MYC* (CN=4; *P*=6.7e-129) and *KRAS* (CN=3; *P*=3.8e-69). The exoDNA mutation rate is estimated at 125 mutation/Mb exhibiting a relatively large proportion of C-to-A and C-to-T base substitutions **(Figure 20B).** Several potentially actionable mutations were identified (**Table 10**) including an unexpected somatic mutation of *BRCA2*, which was not present in the germline DNA. Specifically, the *BRCA2 V3091I* mutation has previously been reported as conferring a homologous recombination defect in cancer cells (184). Three lines of evidence suggest that this *BRCA2* mutation is indeed pathogenic: *first,* the high MAF in exoDNA, underscoring its "driver" status, *second* the "unstable" genome phenotype on genome-wide copy number assessment (40), and *third,* the exceptional response to a platinum-containing adjuvant regimen that this patient has had to date (although the overall follow-up period remains limited).

In the exoRNA, 16.6% of protein-coding transcripts were expressed, including 40 putative expressed gene fusions **(Figure 20C).** No cancer signaling pathways were overrepresented in the exoRNA data.
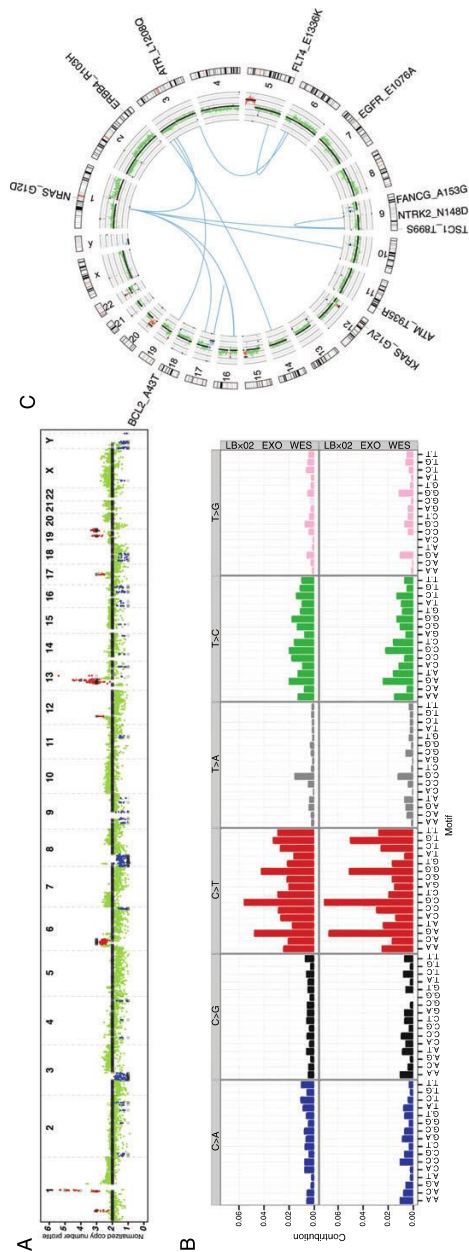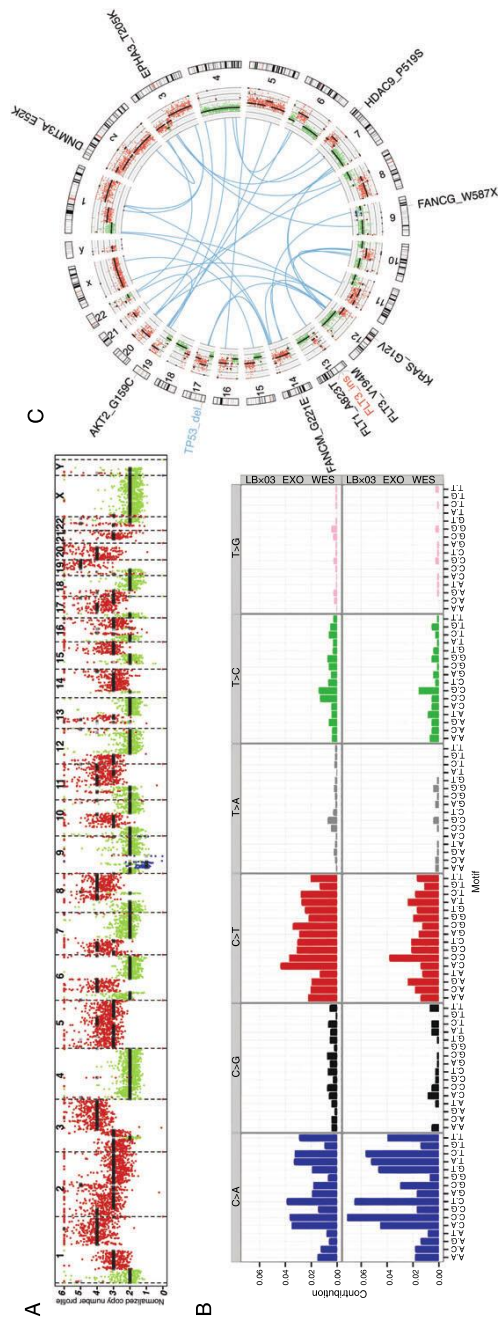
Figure 20 LBx03 tumor profiling

(A) Copy number profile of the plasma exoDNA. (B) Mutational signature of the plasma exosomes derived from exome sequencing (top) and genome sequencing (bottom). (C) Circos plot illustrating putative gene fusions (blue), plasma exoDNA copy number profile (inner-most ring) and potential actionable genes.

Discussion

We have demonstrated the feasibility of using peripheral blood and pleural effusion based liquid biopsies to comprehensively profile the genomes and transcriptomes of deeply located visceral cancers for which traditional tissue biopsies may be difficult, risky, or unachievable in less-specialized centers. In addition, exosome-based liquid biopsy results demonstrate the potential for identifying unexpected therapeutic vulnerabilities. Of particular importance regarding patient LBx03, is the presence of a *BRCA2* mutation, which has been shown to predict responsiveness to platinum-based chemotherapies. Currently, several clinical trials are ongoing that incorporate platinum-based regimens of PARP inhibitors in PDAC patients with such DNA damage repair defects (185). In addition to identifying actionable mutations at the time of presentation, exosome-based liquid biopsies provide an opportunity to identify new therapeutic vulnerabilities that emerge over the course of treatment, or elucidate potential mechanisms of resistance to administered targeted therapies. For example, at the time of metastectomy of the lung metastasis from LBx01, the patient was found to have evidence of *ERBB2* amplification in the pulmonary nodule, leading to subsequent attempt of targeted therapy with Trastuzumab. However, no meaningful response was found to the agent. Two months following completion of this therapy, subsequent liquid biopsy from this patient confirmed the *ERBB2* amplification, as well as the emergence of an *EGFR* amplification, which might represent a clonal selection in response to the trial of a targeted agent (186). Liquid biopsy in this patient far exceeded standard of care lab metrics where less than 1% tumor cells were detected in the pleural effusion, precluding further analysis. Cancer-derived exosomes were able to enrich for the genetic make-up of the local tumor tissue, recapitulating the molecular identity of the diseased lung. It is important to note that such "serial" sampling of the tumor genomic landscape, while possible in superficial cancers like melanomas, is almost unheard of in visceral malignancies, due to logistical or reimbursement limitations.

While cfDNA platforms can certainly elucidate limited panels of genomic abnormalities and even map the emergence of resistance mechanisms during the course of targeted therapies, exosome-based liquid biopsy approaches have the additional benefit of being able to comprehensively profile the cancer transcriptome from the same biosample. In particular, the ability to identify expressed neoantigens (point mutations or fusion transcripts) represents an avenue to interrogate the humoral or cellular responses to such neoantigens in visceral cancers (182, 184). For example, emerging "personalized" adoptive T cell therapies require elucidation of cancer-specific neoantigens that are expressed and processed in an HLA context (187). Typically, this requires a tissue biopsy and RNA profiling of the tumor. Exosome-based liquid biopsy can identify such expressed neoantigens without the need for tissue sampling, and moreover, map the response to immunotherapy through quantitative estimates of neoantigen load in circulation. In addition, since the peripheral blood is a sampling of all body tissues, this genetic analysis presumably has the power to characterize the patient's entire tumor burden: primary tumor and any metastatic disease. This is of particular importance when considering that primary tumors and associated metastases are of a heterogeneous genetic makeup with compounded temporal heterogeneity (188).

Our study is not without limitation. Conceptually, many will desire to see liquid biopsy detected mutations validated in primary tissue. For visceral cancers, the acquisition of such tissues may be limited and localized, thus detection of mutations for validation may not be ideal. Of note, our mutation rates of 341, 77 and 125 mutations/Mb are substantially higher than the average of 2.64 mutations/Mb (range 0.65-28.2) estimated by Waddell et al (40) from PDAC tissue whole genome sequencing. We suspect that a large degree of this discrepancy is due to exoDNA representing tumor heterogeneity at a level that is not attainable through tissue sequencing. A potential strategy to confirm these liquid biopsy findings is to compare serial samples in the same patient, to validate over time the identification of mutations at varying allelic frequency. Such serial profiling is the subject of further study. Nonetheless, our proof of concept results demonstrate

that seamless coordination between clinical and research efforts can produce a workflow from blood draw to sequencing results in a period of 14 days, acquiring results in a clinically relevant timeframe for patients with visceral cancers.

Chapter 6 - Surfaceome profiling enables isolation of cancer-specific exosomal cargo in liquid biopsies from pancreatic cancer patients

With permission this chapter is based upon "**Castillo, J*., V. Bernard*,** F. A. San Lucas, K. Allenson, M. Capello, D. U. Kim, P. Gascoyne, F. C. Mulu, B. M. Stephens, J. Huang, H. Wang, A. A. Momin, R. O. Jacamo, M. Katz, R. Wolff, M. Javle, G. Varadhachary, Wistuba, II, S. Hanash, A. Maitra, and H. Alvarez. 2017. Surfaceome profiling enables isolation of cancer-specific exosomal cargo in liquid biopsies from pancreatic cancer patients. *Annals of oncology : official journal of the European Society for Medical Oncology / ESMO.* (***First authorship shared)**"

Abstract

Background

Detection of circulating tumor DNA (ctDNA) can be limited due to their relative scarcity in circulation, particularly while patients are actively undergoing therapy. Exosomes provide a vehicle through which cancer-specific material can be enriched from the compendium of circulating non-neoplastic tissue-derived nucleic acids. We performed a comprehensive profiling of the pancreatic ductal adenocarcinoma (PDAC) exosomal "surfaceome" in order to identify surface proteins that will render liquid biopsies amenable to cancer-derived exosome enrichment for downstream molecular profiling.

Patients and methods

Surface exosomal proteins were profiled in 13 human PDAC and 2 non-neoplastic cell lines by liquid chromatography-mass spectrometry. A total of 173 prospectively collected blood samples from 103 PDAC patients underwent exosome isolation. Droplet digital PCR (ddPCR) was used on 74 patients (136 total exosome samples) to determine baseline *KRAS* mutation call rates while patients were on therapy. PDAC-specific exosome capture was then performed on additional 29 patients (37 samples) using an antibody cocktail directed against selected proteins, followed by ddPCR analysis. Exosomal DNA in a PDAC patient resistant to therapy were profiled using a molecular barcoded, targeted sequencing panel to determine the utility of enriched nucleic acid material for comprehensive molecular analysis.

Results

Proteomic analysis of the exosome "surfaceome" revealed multiple PDAC specific biomarker candidates: CLDN4, EPCAM, CD151, LGALS3BP, HIST2H2BE and HIST2H2BF. *KRAS* mutations in total exosomes were detected in 44.1% of patients undergoing active therapy compared to 73.0% following exosome capture using the selected biomarkers. Enrichment of

112

exosomal cargo was amenable to molecular profiling, elucidating a putative mechanism of resistance to PARP inhibitor therapy in a patient harboring a *BRCA2* mutation.

Conclusion

Exosomes provide unique opportunities in the context of liquid biopsies for enrichment of tumor-specific material in circulation. We present a comprehensive surfaceome characterization of PDAC exosomes which allows for capture and molecular profiling of tumor-derived DNA.

Introduction

An emerging body of literature demonstrates that comprehensive characterization of cancer genomes has both diagnostic and prognostic utility, and may provide insights into formulating individualized treatment strategies (40, 80). However, even with large scale sequencing efforts, accessibility of tumor tissue is often limited by both patient- and/or system-centered factors. Tissue sampling of pancreatic ductal adenocarcinoma (PDAC) may be limited to an initial diagnostic FNA, while risk of biopsy, locally destructive therapies, cost or facility capabilities may limit further sampling efforts. "Liquid biopsy" is a less invasive strategy for tumor sampling, which may circumvent the need for tissue biopsy while still affording high resolution profiling of the genomic landscapes of visceral cancers. Within the field of liquid biopsy, tumor-derived extracellular vesicles (EVs) such as exosomes, are a source of high-quality nucleic acids for molecular characterization with inherent utility for diagnostic and therapeutic purposes (154).

Exosomes are nanometer-sized membrane-limited extracellular vesicles that arise from endosomal biogenesis pathways and serve as critical means of cell-cell communication (189). Tumor-derived exosomes contain membrane-tethered proteins, microRNAs, and as recently demonstrated, entire genomic complements of DNA (exoDNA) (70, 71, 190, 191). Exosomes are shed from both tumor and non-neoplastic cells into the peripheral circulation. Therefore, one of the potential pitfalls of utilizing exosomes, and essentially any liquid biopsy component including circulating tumor DNA (ctDNA), as a surrogate for the tumor genome is that genetic information obtained from such exosomes will be diluted in large part with the DNA of non-cancer cell-derived exosomes. Exosomal surface biomarkers provide a means to separate cancer from non-cancer derived exosomes through the use of bead-based selection of such markers. While exosomes are known to express tetraspanins such as CD63, CD9, and CD81, these biomarkers are not specific to cancer-derived exosomes. Specific markers to distinguish normal and cancer tissue derived exosomes is an area of active research, particularly in PDAC where the use of such biomarkers have great potential in early disease detection (138, 192). Here, we identify a

panel of PDAC-specific exosomal surface proteins, demonstrate the ability to enrich for PDAC-derived exosomes in circulation using these identified proteins, and then show the feasibility of mutation profiling of enriched exoDNA samples through next-generation sequencing (NGS).

Results

"Surfaceome" profiling of exosomes

Surface and cargo exosomal proteins were profiled in 13 human PDAC cell lines, and 2 non-neoplastic cell lines (HPNE and CAF19) through liquid chromatography-mass spectrometry (MS). Proteomes from exosome surface and cargo were fractionated at an intact protein level and then subjected to trypsin digestion and MS-based analysis. A total of 7086 proteins (corresponding to 3663 gene symbols) were identified. Requiring expression on the surface of at least 3 samples (i.e. the proposed exosomal "surfaceome") demonstrated the presence of canonical proteins universally expressed in exosomal populations including CD81, CD9, and TSG101 resulting in 1057 proteins (corresponding to 482 genes;). In order to identify a panel of PDAC-specific surface exosomal markers, resulting "surfaceome" proteins that were found to be expressed in at least 3 PDAC cell lines with a maximum of 1 spectral count being expressed in non-neoplastic cell lines were considered candidate PDAC-specific exosomal surface markers. In addition, we annotated these candidates using the extracellular vesicle database ExoCarta (database of exosomes proteomics, including data from 160 exosome experiments and 166 samples based on mass spectrometry analyses), which contains human exosome protein profiles from normal and cancer tissue sources to effectively assess the absence of our candidate proteins from vesicles of non-neoplastic origin. Further curation and validation of these biomarkers was prioritized based on biological rationale and availability of targeting antibodies (**Figure 21).**

Figure 21 Cancer-specific exosomal biomarker selection and validation

(A) Heat map representation of proteins that are expressed on the surface of pancreatic ductal adenocarcinoma exosomes that are not expressed (or expressed at very low levels) on the surface of HPNE and CAF19 exosomes. (B) Western blot validation of identified candidate biomarkers: protein expression analysis of cell lysates (left) compared with exosomes (right) of neoplastic (Pa01C, Pa03C, and Pa04C) and non-neoplastic (CAF19 and SC2) cell lines. CD63 and TSG101 are used as antibody controls for identification of exosome populations. Most selected biomarkers show enriched specificity towards being present in cancer exosomes versus normal exosomes.

Biomarker validation

Candidate proteins were validated through western blot analysis of PDAC cell line derived exosomes from Pa01C, Pa03C, and Pa04C (**Figure 21).** Non-neoplastic cell lines CAF19 and SC2 were used as controls. Candidate biomarkers were detected within protein lysates of cell lines with varying degrees of sensitivity and specificity, but were effectively enriched within the exosome protein fractions. In other words, protein biomarkers such as CD151 and HistoneH2B (H2B) are found in the protein lysates from all cell lines, including non-neoplastic cell lines, but are only found within exosomes derived from PDAC cell lines. On the other hand, LGALS3BP is present in all exosomal populations, but is overexpressed in tumor derived exosomes when compared to non-neoplastic sources. In contrast, the recently published PDAC exosomal biomarker glypican-1 (GPC1), did not demonstrate significant expression in tumor-derived exosomes and in fact appeared to be selectively expressed in non-neoplastic sources when four separate GPC1 antibodies were tested, including the originally reported clone (ThermoFisher, PA5-28055) **(Figure 22)** (138). This profiling analysis led to a final antibody cocktail targeting the following candidate biomarkers: anti-CLDN4, EPCAM, CD151, LGALS3BP, HIST2H2BE and HIST2H2BF, respectively used for subsequent enrichment studies.

GPC1 1: Anti-Glypican 1/ **GPC1** antibody **ab137604 (Abcam)**
GPC1 2: Anti-Glypican 1/ **GPC1** antibody **PA5-28055 (Thermo-Scientific)**
GPC1 3:Anti-Glypican 1/ **GPC1** antibody **PA5-24972 (Thermo-Scientific)**
GPC1 4: Anti-Glypican 1/ **GPC1** antibody Sigma-**SAB2700282 (Sigma-Aldrich)**
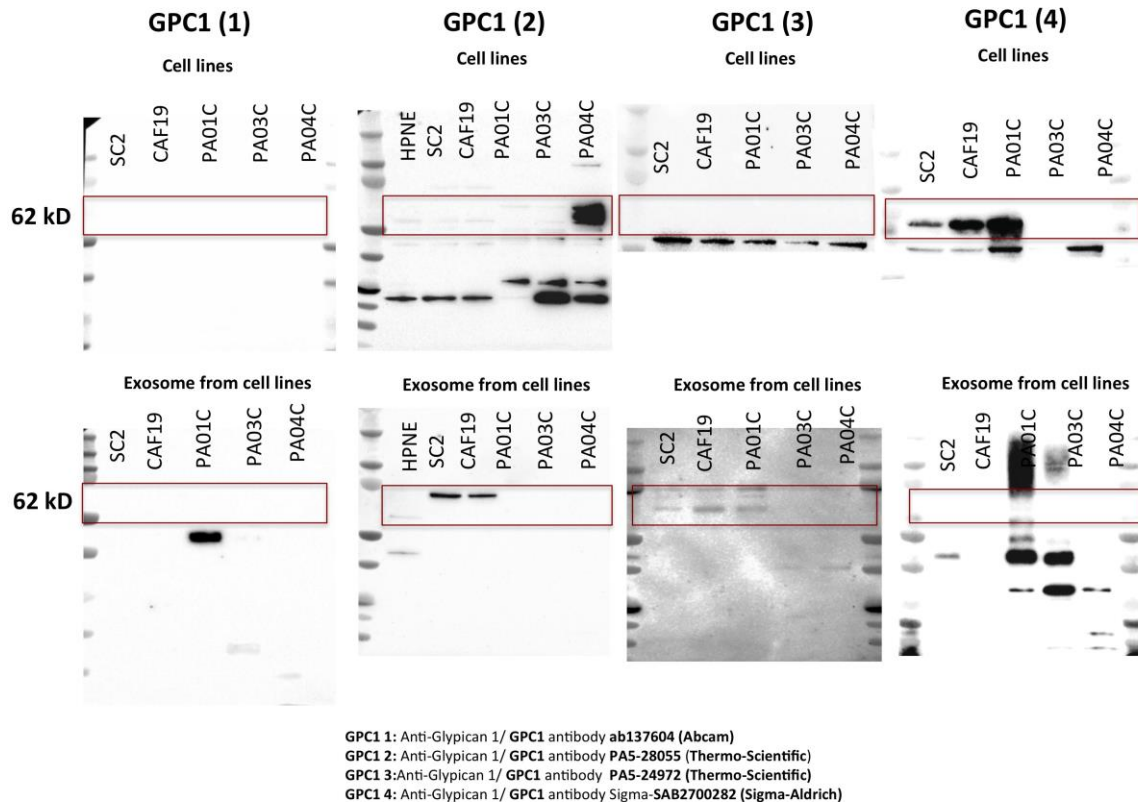
Figure 22 Western blot analysis of GPC1

Western blot analysis of four GPC1 commercially available antibodies which we
attempted to validate for tumor exosome specific detection. No protein was seen at the
expected size range to suggest that this biomarker could be cancer exosome specific.

Validation of capture assay in clinical samples

Following selection of our candidate biomarkers, we designed an immunocapture pulldown assay
to specifically capture enriched populations of cancer-derived exosomes. Aldehyde/sulfate latex
beads were coated with the five antibodies of choice as a cocktail targeting the identified and
validated exosome protein biomarkers. In this fashion, we selectively enriched for cancer derived
exosomes by pulling down only those extracellular vesicles exhibiting the above biomarkers from
the overall shed exosome population. By using PE-CD63 (a pan-exosome marker) fluorescence

118

signal as a surrogate for overall effective exosome capture, we then measured the sensitivity and specificity of the enrichment method. Specifically, by selecting for exosomes using anti-CD63, we are able to detect the presence of exosome populations in all of our cell line isolates **(Figure 23),** but effectively avoid non-specific binding of exosomes using our blocking buffer as shown by the lack of fluorescence **(Figure 23C).** Finally, when the beads are coated with our biomarker antibodies of interest, specific capture of cancer derived exosomes compared to non-neoplastic derived exosomes is apparent **(Figure 23D).**
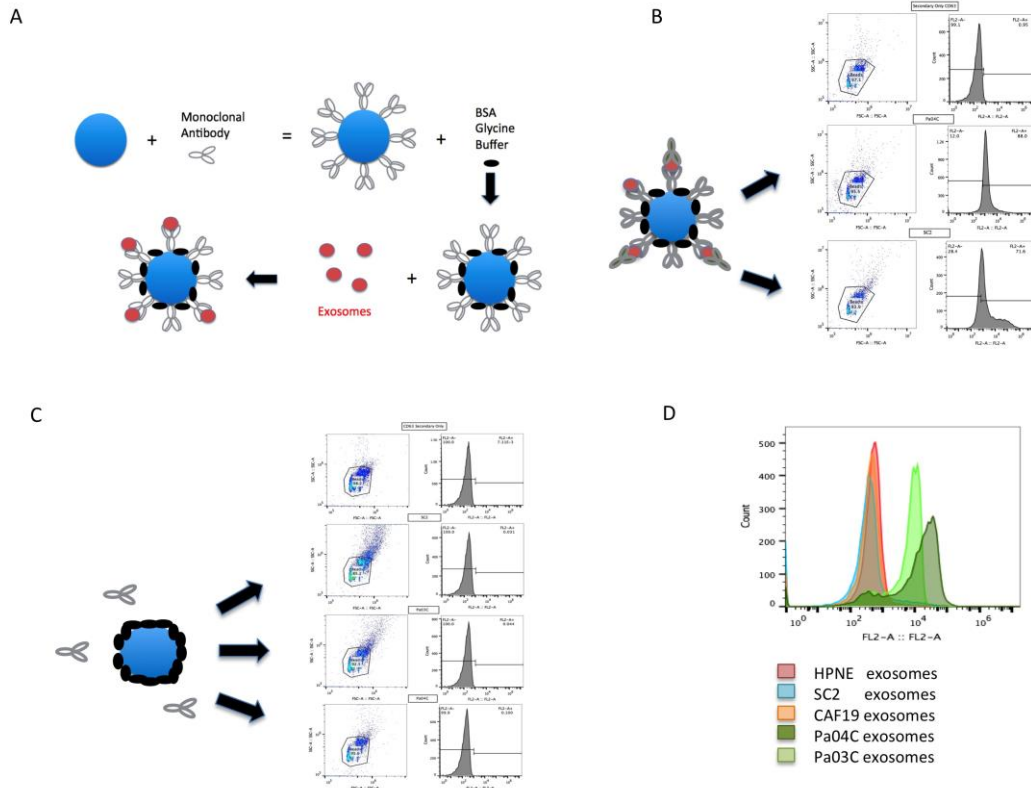
Figure 23 Exosome capture assay methodology

(A) Pulldown assay incubating aldehyde/sulfate latex beads with the cocktail of antibody markers of choice. The aldehyde groups grafted onto the surface of these beads enables facile coupling of proteins to the surface of the particle. Following coating of the bead with the antibody of choice, non-coated surfaces are blocked with a BSA/Glycine buffer to prevent nonspecific binding of exosomes. Beads are then incubated with exosomes overnight resulting in an enriched population of vesicles based on the marker of choice which is amenable to downstream molecular analysis. (B) Pulldown assay is able to capture exosomes with minimal unspecific binding to first determine effective capture of exosomes using our assay, beads coated with CD63 antibody were incubated with either neoplastic (Pa04C) or non-neoplastic (SC2) derived exosomes and subsequently tagged with a CD63-PE conjugated secondary antibody (a pan-exosome marker). Results based on flow cytometry show effective capture of exosome populations using this assay.

(C) To confirm no non-specific binding of exosomes and effective blocking strategy, beads were first incubated with blocking buffer (BSA+Glycine), and then underwent subsequent incubation with the antibody of choice followed by cell line derived exosomes. The resulting beads were then treated with the CD63-PE conjugated secondary antibody and profiled using flow cytometry. This demonstrates that no exosomes were detected being bound to the beads, confirming no non-specific exosome binding. (D) Specific capture of PDAC cell line exosomes using this methodology was then validated in a representative candidate pulldown markers (EPCAM), demonstrating that beads specifically capture exosomes only when incubated with those coming from PDAC cell lines (Pa04C and Pa03C), and not non-neoplastic cell lines (HPNE, SC2, CAF19).

We next aimed to implement our enrichment methodology for PDAC-derived exosomes on patient plasma samples to determine its effectiveness at detecting tumor derived DNA during therapy **(Table 10).**

Table 10 Patient characteristics for exosome capture

Characteristics		Total Exosomes Control Cohort	Captured Exosomes Cohort
Total Samples		136	37
Age (Years)			
Average		61.4	62.4
Median		61	62
Range		(36-88)	(37-88)
Sex			
Male		86	23
Female		50	14
Clinical Staging			
Resectable	Stage IA	7	2
	Stage IB	8	6
	Stage IIA	26	4
	Stage IIB	11	5
Locally Advanced	Stage III	30	8
Metastatic	Stage IV	54	12

Detection rates for mutant *KRAS* exoDNA in a control cohort of 136 prospective samples that did not undergo capture enrichment (total exosomes) taken during active chemotherapeutic intervention was 32.7% (17/52), 50% (15/30), and 51.8% (28/54) in resectable, locally advanced, and metastatic disease, respectively as defined by American Joint Committee on Cancer guidelines (**Figure 24).** In 37 samples that underwent exosome capture as previously described, our mutation detection rate increased to 70.6% (12/17), 71.4% (5/7), and 76.9% (10/13) in resectable, locally advanced, and metastatic disease, respectively. Of note, these
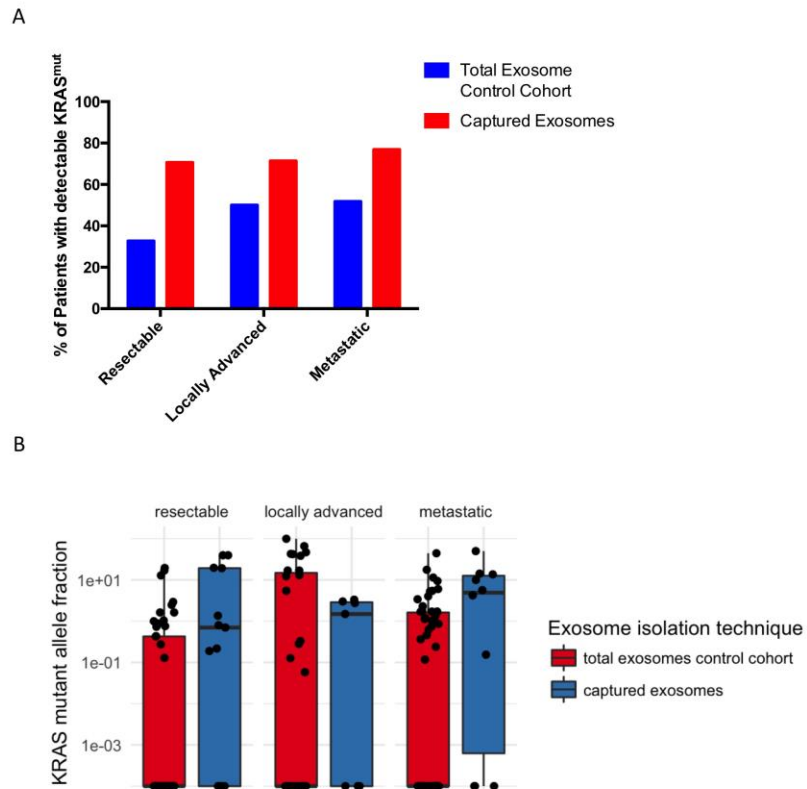
Figure 24 exoDNA *KRAS* mutant detection in circulation

(A) Percent of patients with detectable mutant *KRAS* in exoDNA among those patient samples that did and did not undergo capture enrichment. When comparing the percentages of patients with detectable *KRAS* in the pulldown-cohort versus the total exosome cohort, the pulldown-cohort consistently detects *KRAS* in a higher proportion of patients across stages. This increase in call-rate was statistically significant in resectable patients ($P = 0.024$) where pulldown samples were 4.11 (95% CI: 1.14–17.19) more likely to have *KRAS* detected. (B) *KRAS* mutant allele frequency (MAF) comparisons of captured exosomes versus total exosomes, there was a statistically significant difference showing increased *KRAS* MAFs from the captured exosomes for resectable and metastatic patients ($P = 0.003$ and 0.015, respectively, using one-sided Wilcoxon Rank Sum tests).

detection rates reach the theoretical upper limit of detection of our ddPCR multiplex assay which can detect up to 80% of known *KRAS* mutations found in PDAC (37). This suggests that most patient undergoing therapy have tumor-derived material in circulation that is typically overwhelmed by non-neoplastic tissue derived exosomes. Harvested exoDNA from both protocols yielded an average of 19.17ng (0.11-125.72ng) and 24.13ng (0.12-636.00ng) for captured exosomes and total exosomes, respectively. Overall positive call rate among all combined patients is associated with the pulldown cohort *(p-val = 0.002)* where a pulldown sample is 3.28 (95% CI: 1.41 - 8.19) times more likely to have *KRAS* detected. Importantly, exosome capture not only increases the proportion of cases with detectable mutant alleles, but also leads to a statistically significant increase in *KRAS* MAF within each category, serving as a surrogate for tumor enrichment capability **(Figure 24B).**

Enriched cancer-specific exosomal cargo is amenable to comprehensive molecular profiling by NGS

A metastatic PDAC patient who underwent prior tumor resection, and subsequently developed liver metastasis underwent liquid biopsies for exosome isolation. The emergence of metastasis corresponded with clinically detectable resistance to a Rucaparib (PARP1 inhibitor) clinical trial which the patient was stratified into due a somatic frameshift *BRCA2 (L583*)* mutation with associated loss of heterozygosity. Plasma-derived exosomes were isolated and profiled for *KRAS* mutant detection revealing an increase in *KRAS* mutant burden during disease progression **(Figure 25).** In an on-treatment blood draw where no exoDNA mutant *KRAS* was detected based on ddPCR, we subsequently attempted exoDNA enrichment resulting in an increase in mutational *KRAS* allelic fraction from 0% to 3.2%. More importantly, the amount of DNA material was sufficient for subsequent NGS using a molecular barcoding approach. This resulted in the detection of the known driver mutations that were present in the patient's original primary tumor, and subsequently detected in the metastatic liver tissue, including mutations in

KRAS, TP53, and *BRCA2*. Notably a secondary mutation in *BRCA2* was also detected in liquid biopsies which was not present in the original primary tissue, likely arising during PARP inhibitor therapy. This mutation resided immediately prior to exon 10 where the *BRCA2 (L583*)* mutation was present allowing for the entire exon to be spliced out and leading to transcription of a full mRNA molecule. Tumor exosomal DNA enrichment thus allowed us to detect this putative mechanism of resistance to PARP inhibitor, underscoring the utility of liquid biopsies in facilitating therapeutic stratification.
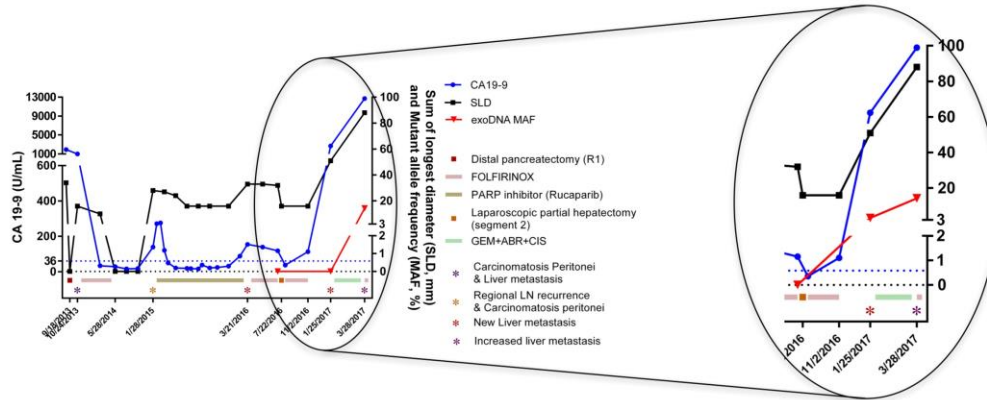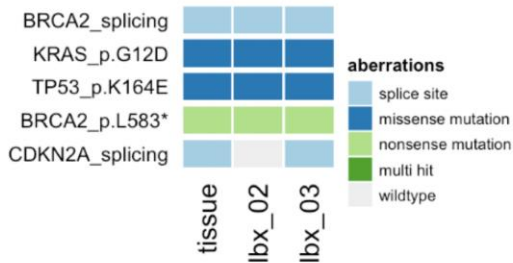
Figure 25 Detection of cancer mutations in capture exosomes through molecular barcodes

(A) Clinical course of a pancreatic ductal adenocarcinoma patient who underwent prior pancreatic tumor resection, and subsequently progressed while on Parp-1 inhibitor therapy. ExoDNA enrichment led to capture of tumor derived material which was not previously detectable. (B) Relevant mutations found in the metastatic tissue and liquid biopsies 6 months (lbx_02) and 9 months (lbx_03) after tissue biopsy. Of note is the presence of a stopgain *BRCA*mutation (L583*) that was correlated to her prolonged response to PARP1 inhibitor therapy. (C) A subsequent mechanism of resistance was detected in the liquid biopsies and confirmed in the tissue in the form of a *BRCA2* splice site variant which splices out the aberrant stopgain mutation. SLD sum of the largest dimension; exoDNA MAF represent the *KRAS* mutant allele fraction. ABR, abraxane (nab-paclitaxel); CIS, cisplatin; GEM, gemcitabine.

26

Discussion

We have performed proteomic profiling of exosomes isolated from a panel of PDAC cells in order to identify a candidate list of cancer-specific surface exosomal proteins (the PDAC exosomal "surfaceome"). We validated the cancer specificity of these exosomal proteins by performing the same proteomic profiling in non-neoplastic pancreatic cell types, and examining which candidate proteins were differentially and preferentially expressed by the collective PDAC exosomal "surfacesome". The resultant PDAC-exosome specific markers can be exploited using an immunocapture assay for enrichment of tumor specific material in liquid biopsies. This allows for subsequent molecular analysis of tumor material with implications for early detection, longitudinal disease monitoring (especially in low tumor volume settings), and therapeutic stratification during targeted therapy.

Since it is possible that the exosome "surfaceome" may evolve throughout disease progression and may, in fact, be a product of the intrinsic heterogeneity found in PDAC, we opted to pursue a multiplexed panel of antibodies against six candidate biomarkers for validation. These included CLDN4, EPCAM, CD151, LGALS3BP, HIST2H2BE and HIST2H2BF. As evidenced by our data, these biomarkers appear to greatly enhance not only the fraction of patients at each PDAC stage with detectable mutant molecules, but also the mutant allelic fraction *per se* at each stage, suggesting enrichment for the tumor-derived nucleic acid component. The latter has direct implications for downstream molecular assessment using NGS that can be pursued in liquid biopsy samples.

Mechanisms of DNA packaging within exosomes remain largely unknown as opposed to the apoptotic/necrotic pathways that are mostly recognized as sources of ctDNA in circulation. In the nucleus, histones are essential for chromatin structure and play a crucial role during gene transcription and silencing. Interestingly, histones have also been found outside the nucleus, in the cytosol, mitochondria and cell membrane (193). Extrachromosomal Histone-H2B has been

identified as a cytosolic DNA sensor for aberrant self and non-self double-stranded DNA, which

mediates an innate immune response and co-localizes within the mitochondrial membrane (194,

195). Upon detection of cytosolic DNA, H2B has been described to partially associate with

mitochondria and co-localize with the late endosome marker CD63 (93). Both mitochondria and

endosomes are known to generate multivesicular bodies that can fuse with the cell membrane

and generate exosomes (196). Therefore the relative enrichment of H2B within the exosome

compartment of cancer cells suggests that this protein may be interacting with mutant DNA that

originated in the nucleus and which subsequently becomes packaged within exosomes for

transport.

Not unexpectedly, the other candidate exosomal "surfaceome" proteins identified in our analysis

have been independently implicated in cancer initiation and progression of PDAC. For example,

the extracellular matrix glycoprotein LGALS3BP is overexpressed by neoplastic cells with a role

in promoting cell viability, migration and metastasis, resulting in its role as a potential biomarker

associated with prognosis and response to therapy (196, 197). Other identified biomarkers such

as the tetraspanin family member CD151 have also been implicated in cancer initiation and

metastasis; in fact, exosomal CD151 *per se* has previously been shown to facilitate metastasis

through induction of epithelial to mesenchymal transition in PDAC cell lines (92). The family of

claudin proteins is involved in the formation of tight junctions, with overexpression of CLDN4

previously described in the context of PDAC (198). Notably, this overexpression was present in

both human archival material and genetically engineered mouse models at the stage of PDAC

precursor lesions (pancreatic intraepithelial neoplasia (PanIN)), with implications for early

detection (199). Finally, expression of epithelial markers in circulation has been best

characterized in the context of circulating tumor cells (CTCs). Specifically, the use of EPCAM to

isolate and quantify CTCs has led to FDA approved prognostic tests in colorectal, breast, and

prostate cancers (200). As the majority of content in circulation is derived from blood components

such as peripheral blood mononuclear cells (PBMCs), the presence of circulating material

expressing epithelial proteins such as EPCAM are postulated to represent tumor-derived origins. This is further supported by our own data, which suggest that EPCAM in circulation may represent a cancer specific exosomal biomarker (201).

Previous work has demonstrated the utility of the biomarker GPC1 as a highly sensitive and specific exosomal biomarker for detection of PDAC (138). While our proteomics data does confirm that GPC1 is expressed on the PDAC-derived exosomal "surfaceome", upon incorporation of public extracellular vesicle databases, this protein appears to be also enriched in exosomes originating from normal tissues. Further, our experimental data confirms the presence of GPC1 in non-neoplastic cell lines including CAF19 and SC2, while not being expressed within the exosomes of three representative PDAC cell lines following attempted validation using multiple commercially available antibodies. A recent study by Yang et al also found that GPC1 as a single exosome marker was not optimal in PDAC plasma samples, although it could potentially be used as a component of a multi-analyte panel (192). Thus, the significance of GPC1 in PDAC liquid biopsies will require future clarification.

Among limitations of this study are the fact that we were unable to obtain matched captured and non-captured total exosome samples from the same patient due to the volumes of plasma required to pursue both protocols. The purpose of utilizing these volumes (~11.7ml of plasma) was to have sufficient nucleic acid material for downstream NGS analysis. Additionally, our relatively small sample size which underwent exosome capture may limit the generalization of our conclusions and would require further validation in larger cohorts. It would also be prudent to perform this analysis on a cohort of healthy controls in order to effectively validate the specificity of our cancer derived exosome capture approach for KRAS mutation detection. Finally, it is important to note the feasibility of implementing such a protocol in the clinics. Whereas plasma processing and DNA isolation for ctDNA can be performed within a day, the need to isolate exosomes using a bead immunocapture based approach followed by DNA isolation would

require four days in addition to the required infrastructure needed for ultracentrifugation. Although it is not a significant processing time difference, new exosome isolation approaches are being developed to decrease cost and increase efficiency of specific exosome capture without the need for ultracentrifugation. This includes the use of antibody coated chips and microfluidic based approaches which can capture specific exosome populations of interest (202, 203)

The need to enrich for tumor derived material in circulation is underlined by the difficulties in detecting rare circulating mutant molecules in a heterogeneous milieu that is typically overwhelmed by non-neoplastic tissue derived DNA. This is particularly compounded in the context of patients undergoing therapy where mutant DNA might be at levels that are undetectable with conventional ultra-sensitive digital PCR techniques. The ability to detect latent mutant molecules has implications in uncovering emerging mechanisms of resistance or vulnerability nodes before these become clinically evident, thus allowing for more effective therapeutic stratification. As typical circulating biomarkers such as ctDNA are not amenable to enrichment methodologies, we present exosomes as a viable alternative to capture tumor specific material. This can come in the form of not only DNA, but also mRNA and proteins that are sourced from the originating tumor cell. Indeed, we have demonstrated how a tumor enrichment platform can lead to detectable tumor material in those patients initially thought to be free of circulating mutant molecules. But more importantly, specific tumor exosome enrichment leads to an augmentation of mutant genomic equivalents that are subsequently amenable to NGS. For example, in our cohort of resectable patients, 44% of patient samples from total exosomes had sufficient quantity and quality of DNA to undergo downstream molecular barcoding (as defined by >1% *KRAS* mutant AF and >1ng of isolated DNA), compared to 67% of patient samples that were subject to exosome capture. This enrichment then permits elucidation of emerging mechanisms of resistance, such as a secondary BRCA2 mutation that reverts PARP sensitivity, as we have demonstrated in our study.

Chapter 7 – Discussion and Future Directions

Chapter 7 – Discussion and Future Directions

Throughout this work, we have demonstrated that both circulating tumor DNA and exosomal derived DNA are amendable to detection through digital PCR and NGS based methods. Exosomes provide an interesting alternative and complementary approach to conventional liquid biopsy compartments such as cfDNA as the surface composition of these extracellular vesicles can give us information of the type of cell where they came from while their content can give us insight into the functional state of that cell of origin. Although much work has been done describing the cargo of these microvesicles including proteins and RNA, the existence of DNA and how it becomes packaged within the vesicles still remains an area of debate. As opposed to ctDNA which is a product of rapid cell turnover following apoptosis and necrosis, packaging of exoDNA would need to occur in viable cells through unknown functional mechanisms. Based on our observations of the presence of histone components in our exosome proteomics, we had hypothesized that these were byproducts of extrachromosomal DNA. Histones in themselves would then serve as cytosolic DNA sensors for aberrant self and non-self double-stranded DNA, which can co-localize with CD63, a known exosomal marker (93). A related mechanism to exosomal DNA packaging was more recently elucidated whereby cells utilize exosomes as a means to eliminate harmful cytosolic DNA and thus preventing activation of DNA damage response pathways (204). Specifically, Takahash, et al., found that inhibiting exosome secretion of cells resulted in an increase of cytosolic DNA which was recognized by STING and provoked a reactive oxygen species dependent DNA damage response. This effect was rescued through overexpression of cytoplasmic DNases which inhibited STING activity. These results suggest that exosomes play an important role in maintaining cellular homeostasis by removing aberrant cytoplasmic DNA. Based on this data, one can then hypothesize that exosomes in general may contain an enriched pool of aberrant or mutated DNA from cells, suggesting that they may represent an enriched source of tumor derived material in circulation when compared to cell-free DNA. This seems to be supported by our work presented in Chapter 3 where presence of *KRAS*

mutations was more readily detectable in exosomes compared to cfDNA of matched patient samples. Additionally, our data in Chapter 4 further demonstrates that in addition to higher sensitivity of detection of *KRAS* in circulation, these mutant molecules contained within exosomes are of higher variant allele frequency when compared to matched ctDNA. Although this data is of course correlative, it would further support the role of exoDNA as another putative biomarker amongst liquid biopsies.

The role of liquid biopsies as a field lies in its potential for early detection, prognostication, tumor monitoring, and therapy guidance. Among this, early detection remains the greatest endeavor, particularly in pancreatic cancer, where identification of those patients at high risk of developing or having localized disease can lead to potential curative surgical resection, which would result in a significant impact on survival in this disease. Unfortunately, several issues must be considered in developing an early detection assay such as the one proposed for liquid biopsies. These include: *1. Sensitivity and specificity, 2. Organ specificity, 3. A numbers problem, 4. Lethality problems, 5. Lead time problem.*

In regards to sensitivity and specificity, we've demonstrated in Chapter 3 that a significant hurdle in regards to specificity is that apparently healthy individuals can carry known "driver" mutant molecules in circulation possibly originating from non-clinically relevant lesions. Thus, the current strategy used in this work of detecting a single point mutation would not be optimal in the setting of an early detection screening methodology as a significant number of false positives would arise. One potential solution for this would be to determine the utility of a panel of gene mutations or genomic signature that may predict the presence of cancer. In the context of PDAC for example, this can involve using a panel of the top 4 mutated genes, *KRAS, TP53, SMAD4,* and *CDKN2A.* Detection of 3 or more of these as related to potential driver status may thus increase the specificity of such an assay. Commercial efforts are currently underway to perform such analysis on large sets of patients. Most recently, GRAIL has raised more than $950 million to recruit 120,000 women to perform liquid biopsies at the time of mammography. Their goal is to develop a signature related to breast cancer that involves gene panel sequencing, whole genome

sequencing, and methylation status through bisulfite genomic sequencing. If successful, studies such as these would greatly advance the field of liquid biopsies, as it would support further clinical utility of these biomarkers, unfortunately, performing such studies will not be feasible among other cancer types. Additionally, even if successful, implementing such assays in general populations may not be possible due to cost and suboptimal sensitivity/specificity. Thus, at least in the case of pancreatic cancer, high risk populations would be best stratified for such studies including those with a family history of cancer, genetic predisposition syndromes (e.g. BRCA2 mutant status), chronic pancreatitis, smokers, and new onset diabetes.

In the context of organ specificity, utilizing *KRAS* as an early detection marker will not yield much information considering it is prevalent in many other cancers including lung, colon, and pancreatic. Again, the GRAIL study is attempting to overcome this issue by finding a specific signature correlated to breast cancer through their sequencing strategy. But development of such tools in other cancers may again not be possible due to cost.

In the numbers problem, it is important to consider that hundreds, maybe thousands of biomarkers exist today, so how do we go about validating them? We cannot perform $1 billion experiments every time a new attractive biomarker shows up, so what would be the best strategy to select those most likely to become effective and through which trials? Additionally, even with ctDNA, there are many methodologies available today to profile this liquid biopsy compartment, including digital PCR, whole genome sequencing, and numerous gene panels coupled with molecular barcodes with undisclosed targeting strategies.

In regards to the lethality problem, it's of course important to note that even if we can detect cancer early in general, not all cancers will be lethal. An example being that of prostate cancer, where most men would die with prostate cancer but not of prostate cancer. But even in the case of studies such as those by GRAIL, not all ductal carcinomas in situ (DCIS) will develop an invasive component. In that case, how can we best stratify those patients that are likely to benefit most from surgical resection in order to circumvent morbidity and costs.

Finally, by lead time problem we mean, what is the difference in time between a positive test on a liquid biopsy and a positive result on imaging such as CT or mammography. In the context of breast cancer, if this is just 1-2 weeks, then is there any real benefit to this new biomarker? In Chapter 4 we describe an average lead time of 50 days, but considering the rapid clinical deterioration of pancreatic cancer, can a biomarker such as this be relevant and result in significant survival benefits? Several studies have attempted to report clinically relevant lead times such as Tie et al., who describe a lead time to radiological recurrence of colon cancer of 5 months compared to CEA following resection, and Chaudhuri, et al., who describe a lead time of 5.2 months for localized lung cancer which they attribute to the presence of minimally residual disease (149, 205). Regardless of these findings, a prospective randomized trial validating the utility of these lead times would need to be conducted.

Ultimately, it is the personal view of this author, that liquid biopsies in the form of circulating tumor DNA or exosomal DNA are not optimal for their use in early detection. The cost and specificity needed to implement such assays today are likely not possible and would most likely be better suited for the proteomic field where biosample requirements are not as strenuous.

It is not to say that liquid biopsies have no use at all. It is the opinion of the author that such assays are better suited for tumor monitoring and therapy selection. Yet certain caveats remain regarding the use of liquid biopsies for these purposes today. As many studies on the clinical significance of circulating nucleic acids have been retrospective in nature, few evidence exists of the utility of such assays in a randomized prospective clinical trial setting. While the current data in this dissertation may suggest clinical validity in context of prediction when certain biomarker thresholds have been met, we believe that one of the greatest barriers to clinical implementation will rely on establishing clinical utility through prospective trials. Although it is important to note the requirements to establish pre-analytical and analytical validity, several methodologies and assays have been able to establish this, but still with a lack of evidence of clinical utility. Parameters of pre-analytic and analytical validity rely on the reproducibility of results. This begins to incorporate variability related to time of draws, needles and blood tubes used, time to

processing, and other standard operating procedures of the blood processing and assay itself. Within our own studies we attempt to use only acid citrate dextrose (ACD) tubes for plasma collection and process blood within one hour of time of collection, but the latter is not always feasible, particularly outside of the clinical trial realm. This requires clinical studies infrastructure which include a clinical coordinator and respective personnel. Next clinical, validation must be established through Clinical Laboratory Improvement Amendments (CLIA) certification in order to establish a quality standard of accuracy, reliability, and timeliness of results. Again this has been established in certain scenarios for ctDNA, but the current nature of the isolation and processing of exosomes would likely make it difficult for such SOPs and validation to become viable. Due to the complexity and user variability involved in exosome isolation through ultracentrifugation, the exosome field may find more success with microfluidic based methods which can become more standardized. Similar to the immune-capture approach presented in Chapter 6, one can envision a microfluidic chip coated with antibodies of interest similar to methodologies established for circulating tumor cells (206). In regards to clinical utility, in this current study, we attempt to provide retrospective evidence for disease monitoring in the context of pancreatic cancer, but we envision establishing clinical utility through a prospective clinical trial with the same intended use. This could involve monitoring of metastatic pancreatic cancer patients through serial liquid biopsies, where detection of exoDNA MAF >1% would stratify patients into receiving early follow-up imaging for detection of progression and a change to second-line chemotherapy.

In summary, as an emerging biomarker in the field of solid cancers, the potential of liquid biopsies as being a minimally invasive means of prognostication and tumor monitoring can bring about significant survival benefits. These benefits would likely be better leveraged when using complementary biomarkers such as presented in this work including standard clinical biomarkers (CA19-9) as well as liquid biopsy sources of nucleic acid material (cfDNA and exosomes).

Bibliography

1.	Rahib, L., B. D. Smith, R. Aizenberg, A. B. Rosenzweig, J. M. Fleshman, and L. M. Matrisian. 2014. Projecting cancer incidence and deaths to 2030: the unexpected burden of thyroid, liver, and pancreas cancers in the United States. *Cancer research* 74: 2913-2921.

2.	Siegel, R., J. Ma, Z. Zou, and A. Jemal. 2014. Cancer statistics, 2014. *CA: a cancer journal for clinicians* 64: 9-29.

3.	Yachida, S., S. Jones, I. Bozic, T. Antal, R. Leary, B. Fu, M. Kamiyama, R. H. Hruban, J. R. Eshleman, M. A. Nowak, V. E. Velculescu, K. W. Kinzler, B. Vogelstein, and C. A. Iacobuzio-Donahue. 2010. Distant metastasis occurs late during the genetic evolution of pancreatic cancer. *Nature* 467: 1114-1117.

4.	Hruban, R. H., N. V. Adsay, J. Albores-Saavedra, C. Compton, E. S. Garrett, S. N. Goodman, S. E. Kern, D. S. Klimstra, G. Kloppel, D. S. Longnecker, J. Luttges, and G. J. Offerhaus. 2001. Pancreatic intraepithelial neoplasia: a new nomenclature and classification system for pancreatic duct lesions. *The American journal of surgical pathology* 25: 579-586.

5.	Wu, J., Y. Jiao, M. Dal Molin, A. Maitra, R. F. de Wilde, L. D. Wood, J. R. Eshleman, M. G. Goggins, C. L. Wolfgang, M. I. Canto, R. D. Schulick, B. H. Edil, M. A. Choti, V. Adsay, D. S. Klimstra, G. J. Offerhaus, A. P. Klein, L. Kopelovich, H. Carter, R. Karchin, P. J. Allen, C. M. Schmidt, Y. Naito, L. A. Diaz, Jr., K. W. Kinzler, N. Papadopoulos, R. H. Hruban, and B. Vogelstein. 2011. Whole-exome sequencing of neoplastic cysts of the pancreas reveals recurrent mutations in components of ubiquitin-dependent pathways. *Proceedings of the National Academy of Sciences of the United States of America* 108: 21188-21193.

6.   Iacobuzio-Donahue, C. A., D. S. Klimstra, N. V. Adsay, R. E. Wilentz, P. Argani, T. A. Sohn, C. J. Yeo, J. L. Cameron, S. E. Kern, and R. H. Hruban. 2000. Dpc-4 protein is expressed in virtually all human intraductal papillary mucinous neoplasms of the pancreas: comparison with conventional ductal adenocarcinomas. *The American journal of pathology* 157: 755-761.

7.   Iacobuzio-Donahue, C. A., R. E. Wilentz, P. Argani, C. J. Yeo, J. L. Cameron, S. E. Kern, and R. H. Hruban. 2000. Dpc4 protein in mucinous cystic neoplasms of the pancreas: frequent loss of expression in invasive carcinomas suggests a role in genetic progression. *The American journal of surgical pathology* 24: 1544-1548.

8.   Wu, J., H. Matthaei, A. Maitra, M. Dal Molin, L. D. Wood, J. R. Eshleman, M. Goggins, M. I. Canto, R. D. Schulick, B. H. Edil, C. L. Wolfgang, A. P. Klein, L. A. Diaz, Jr., P. J. Allen, C. M. Schmidt, K. W. Kinzler, N. Papadopoulos, R. H. Hruban, and B. Vogelstein. 2011. Recurrent GNAS mutations define an unexpected pathway for pancreatic cyst development. *Science translational medicine* 3: 92ra66.

9.   Jancik, S., J. Drabek, D. Radzioch, and M. Hajduch. 2010. Clinical relevance of KRAS in human cancers. *Journal of biomedicine & biotechnology* 2010: 150960.

10.   Jones, S., X. Zhang, D. W. Parsons, J. C. Lin, R. J. Leary, P. Angenendt, P. Mankoo, H. Carter, H. Kamiyama, A. Jimeno, S. M. Hong, B. Fu, M. T. Lin, E. S. Calhoun, M. Kamiyama, K. Walter, T. Nikolskaya, Y. Nikolsky, J. Hartigan, D. R. Smith, M. Hidalgo, S. D. Leach, A. P. Klein, E. M. Jaffee, M. Goggins, A. Maitra, C. Iacobuzio-Donahue, J. R. Eshleman, S. E. Kern, R. H. Hruban, R. Karchin, N. Papadopoulos, G. Parmigiani, B. Vogelstein, V. E. Velculescu, and K. W. Kinzler. 2008. Core signaling pathways in human pancreatic cancers revealed by global genomic analyses. *Science (New York, N.Y.)* 321: 1801-1806.

11.   Witkiewicz, A. K., E. A. McMillan, U. Balaji, G. Baek, W. C. Lin, J. Mansour, M. Mollaee, K. U. Wagner, P. Koduru, A. Yopp, M. A. Choti, C. J. Yeo, P. McCue, M. A. White, and E. S. Knudsen. 2015. Whole-exome sequencing of pancreatic cancer defines genetic diversity and therapeutic targets. *Nature communications* 6: 6744.

12.   Campbell, P. J., S. Yachida, L. J. Mudie, P. J. Stephens, E. D. Pleasance, L. A. Stebbings, L. A. Morsberger, C. Latimer, S. McLaren, M. L. Lin, D. J. McBride, I. Varela, S. A. Nik-Zainal, C. Leroy, M. Jia, A. Menzies, A. P. Butler, J. W. Teague, C. A. Griffin, J. Burton, H. Swerdlow, M. A. Quail, M. R. Stratton, C. Iacobuzio-Donahue, and P. A. Futreal. 2010. The patterns and dynamics of genomic instability in metastatic pancreatic cancer. *Nature* 467: 1109-1113.

13.   Caldas, C., S. A. Hahn, L. T. da Costa, M. S. Redston, M. Schutte, A. B. Seymour, C. L. Weinstein, R. H. Hruban, C. J. Yeo, and S. E. Kern. 1994. Frequent somatic mutations and homozygous deletions of the p16 (MTS1) gene in pancreatic adenocarcinoma. *Nature genetics* 8: 27-32.

14.   Schutte, M., R. H. Hruban, J. Geradts, R. Maynard, W. Hilgers, S. K. Rabindran, C. A. Moskaluk, S. A. Hahn, I. Schwarte-Waldhoff, W. Schmiegel, S. B. Baylin, S. E. Kern, and J. G. Herman. 1997. Abrogation of the Rb/p16 tumor-suppressive pathway in virtually all pancreatic carcinomas. *Cancer research* 57: 3126-3130.

15.   Sharpless, N. E. 2005. INK4a/ARF: a multifunctional tumor suppressor locus. *Mutation research* 576: 22-38.

16.   Scarpa, A., P. Capelli, K. Mukai, G. Zamboni, T. Oda, C. Iacono, and S. Hirohashi. 1993. Pancreatic adenocarcinomas frequently show p53 gene mutations. *The American journal of pathology* 142: 1534-1543.

17.   Maitra, A., N. V. Adsay, P. Argani, C. Iacobuzio-Donahue, A. De Marzo, J. L. Cameron, C. J. Yeo, and R. H. Hruban. 2003. Multicomponent analysis of the pancreatic adenocarcinoma progression model using a pancreatic intraepithelial neoplasia tissue microarray. *Modern pathology : an official journal of the United States and Canadian Academy of Pathology, Inc* 16: 902-912.

18.   Siegel, P. M., and J. Massague. 2003. Cytostatic and apoptotic actions of TGF-beta in homeostasis and cancer. *Nature reviews. Cancer* 3: 807-821.

19.   Yachida, S., C. M. White, Y. Naito, Y. Zhong, J. A. Brosnan, A. M. Macgregor-Das, R. A. Morgan, T. Saunders, D. A. Laheru, J. M. Herman, R. H. Hruban, A. P. Klein, S. Jones, V. Velculescu, C. L. Wolfgang, and C. A. Iacobuzio-Donahue. 2012. Clinical significance of the genetic landscape of pancreatic cancer and implications for identification of potential long-term survivors. *Clinical cancer research : an official journal of the American Association for Cancer Research* 18: 6339-6347.

20.   Biankin, A. V., A. L. Morey, C. S. Lee, J. G. Kench, S. A. Biankin, H. C. Hook, D. R. Head, T. B. Hugh, R. L. Sutherland, and S. M. Henshall. 2002. DPC4/Smad4 expression and outcome in pancreatic ductal adenocarcinoma. *Journal of clinical oncology : official journal of the American Society of Clinical Oncology* 20: 4531-4542.

21.   Bardeesy, N., K. H. Cheng, J. H. Berger, G. C. Chu, J. Pahler, P. Olson, A. F. Hezel, J. Horner, G. Y. Lauwers, D. Hanahan, and R. A. DePinho. 2006. Smad4 is dispensable for normal pancreas development yet critical in progression and tumor biology of pancreas cancer. *Genes & development* 20: 3130-3146.

22.   Iacobuzio-Donahue, C. A., B. Fu, S. Yachida, M. Luo, H. Abe, C. M. Henderson, F. Vilardell, Z. Wang, J. W. Keller, P. Banerjee, J. M. Herman, J. L. Cameron, C. J. Yeo, M. K. Halushka, J. R. Eshleman, M. Raben, A. P. Klein, R. H. Hruban, M. Hidalgo, and D.

Laheru. 2009. DPC4 gene status of the primary carcinoma correlates with patterns of failure in patients with pancreatic cancer. *Journal of clinical oncology : official journal of the American Society of Clinical Oncology* 27: 1806-1813.

23. Shi, C., R. H. Hruban, and A. P. Klein. 2009. Familial pancreatic cancer. *Archives of pathology & laboratory medicine* 133: 365-374.

24. Permuth-Wey, J., and K. M. Egan. 2009. Family history is a significant risk factor for pancreatic cancer: results from a systematic review and meta-analysis. *Familial cancer* 8: 109-117.

25. Su, G. H., R. H. Hruban, R. K. Bansal, G. S. Bova, D. J. Tang, M. C. Shekher, A. M. Westerman, M. M. Entius, M. Goggins, C. J. Yeo, and S. E. Kern. 1999. Germline and somatic mutations of the STK11/LKB1 Peutz-Jeghers gene in pancreatic and biliary cancers. *The American journal of pathology* 154: 1835-1840.

26. Witt, H., W. Luck, H. C. Hennies, M. Classen, A. Kage, U. Lass, O. Landt, and M. Becker. 2000. Mutations in the gene encoding the serine protease inhibitor, Kazal type 1 are associated with chronic pancreatitis. *Nature genetics* 25: 213-216.

27. Lowenfels, A. B., P. Maisonneuve, E. P. DiMagno, Y. Elitsur, L. K. Gates, Jr., J. Perrault, and D. C. Whitcomb. 1997. Hereditary pancreatitis and the risk of pancreatic cancer. International Hereditary Pancreatitis Study Group. *Journal of the National Cancer Institute* 89: 442-446.

28. Lowenfels, A. B., P. Maisonneuve, D. C. Whitcomb, M. M. Lerch, and E. P. DiMagno. 2001. Cigarette smoking as a risk factor for pancreatic cancer in patients with hereditary pancreatitis. *Jama* 286: 169-170.

29. Rutter, J. L., C. M. Bromley, A. M. Goldstein, D. E. Elder, E. A. Holly, D. t. Guerry, P. Hartge, J. P. Struewing, D. Hogg, A. Halpern, R. W. Sagebiel, and M. A. Tucker. 2004.

Heterogeneity of risk for melanoma and pancreatic and digestive malignancies: a melanoma case-control study. *Cancer* 101: 2809-2816.

30.   van der Heijden, M. S., C. J. Yeo, R. H. Hruban, and S. E. Kern. 2003. Fanconi anemia gene mutations in young-onset pancreatic cancer. *Cancer research* 63: 2585-2588.

31.   Goggins, M., M. Schutte, J. Lu, C. A. Moskaluk, C. L. Weinstein, G. M. Petersen, C. J. Yeo, C. E. Jackson, H. T. Lynch, R. H. Hruban, and S. E. Kern. 1996. Germline BRCA2 gene mutations in patients with apparently sporadic pancreatic carcinomas. *Cancer research* 56: 5360-5364.

32.   Lynch, H. T., C. A. Deters, C. L. Snyder, J. F. Lynch, P. Villeneuve, J. Silberstein, H. Martin, S. A. Narod, and R. E. Brand. 2005. BRCA1 and pancreatic cancer: pedigree findings and their causal relationships. *Cancer genetics and cytogenetics* 158: 119-125.

33.   Hruban, R. H., M. I. Canto, M. Goggins, R. Schulick, and A. P. Klein. 2010. Update on familial pancreatic cancer. *Advances in surgery* 44: 293-311.

34.   Kastrinos, F., B. Mukherjee, N. Tayob, F. Wang, J. Sparr, V. M. Raymond, P. Bandipalliam, E. M. Stoffel, S. B. Gruber, and S. Syngal. 2009. Risk of pancreatic cancer in families with Lynch syndrome. *Jama* 302: 1790-1795.

35.   Roberts, N. J., Y. Jiao, J. Yu, L. Kopelovich, G. M. Petersen, M. L. Bondy, S. Gallinger, A. G. Schwartz, S. Syngal, M. L. Cote, J. Axilbund, R. Schulick, S. Z. Ali, J. R. Eshleman, V. E. Velculescu, M. Goggins, B. Vogelstein, N. Papadopoulos, R. H. Hruban, K. W. Kinzler, and A. P. Klein. 2012. ATM mutations in patients with hereditary pancreatic cancer. *Cancer discovery* 2: 41-46.

36.   Sausen, M., J. Phallen, V. Adleff, S. Jones, R. J. Leary, M. T. Barrett, V. Anagnostou, S. Parpart-Li, D. Murphy, Q. Kay Li, C. A. Hruban, R. Scharpf, J. R. White, P. J. O'Dwyer,

P. J. Allen, J. R. Eshleman, C. B. Thompson, D. S. Klimstra, D. C. Linehan, A. Maitra, R. H. Hruban, L. A. Diaz, Jr., D. D. Von Hoff, J. S. Johansen, J. A. Drebin, and V. E. Velculescu. 2015. Clinical implications of genomic alterations in the tumour and circulation of pancreatic cancer patients. *Nature communications* 6: 7686.

37.   Biankin, A. V., N. Waddell, K. S. Kassahn, M. C. Gingras, L. B. Muthuswamy, A. L. Johns, D. K. Miller, P. J. Wilson, A. M. Patch, J. Wu, D. K. Chang, M. J. Cowley, B. B. Gardiner, S. Song, I. Harliwong, S. Idrisoglu, C. Nourse, E. Nourbakhsh, S. Manning, S. Wani, M. Gongora, M. Pajic, C. J. Scarlett, A. J. Gill, A. V. Pinho, I. Rooman, M. Anderson, O. Holmes, C. Leonard, D. Taylor, S. Wood, Q. Xu, K. Nones, J. L. Fink, A. Christ, T. Bruxner, N. Cloonan, G. Kolle, F. Newell, M. Pinese, R. S. Mead, J. L. Humphris, W. Kaplan, M. D. Jones, E. K. Colvin, A. M. Nagrial, E. S. Humphrey, A. Chou, V. T. Chin, L. A. Chantrill, A. Mawson, J. S. Samra, J. G. Kench, J. A. Lovell, R. J. Daly, N. D. Merrett, C. Toon, K. Epari, N. Q. Nguyen, A. Barbour, N. Zeps, I. Australian Pancreatic Cancer Genome, N. Kakkar, F. Zhao, Y. Q. Wu, M. Wang, D. M. Muzny, W. E. Fisher, F. C. Brunicardi, S. E. Hodges, J. G. Reid, J. Drummond, K. Chang, Y. Han, L. R. Lewis, H. Dinh, C. J. Buhay, T. Beck, L. Timms, M. Sam, K. Begley, A. Brown, D. Pai, A. Panchal, N. Buchner, R. De Borja, R. E. Denroche, C. K. Yung, S. Serra, N. Onetto, D. Mukhopadhyay, M. S. Tsao, P. A. Shaw, G. M. Petersen, S. Gallinger, R. H. Hruban, A. Maitra, C. A. Iacobuzio-Donahue, R. D. Schulick, C. L. Wolfgang, R. A. Morgan, R. T. Lawlor, P. Capelli, V. Corbo, M. Scardoni, G. Tortora, M. A. Tempero, K. M. Mann, N. A. Jenkins, P. A. Perez-Mancera, D. J. Adams, D. A. Largaespada, L. F. Wessels, A. G. Rust, L. D. Stein, D. A. Tuveson, N. G. Copeland, E. A. Musgrove, A. Scarpa, J. R. Eshleman, T. J. Hudson, R. L. Sutherland, D. A. Wheeler, J. V. Pearson, J. D. McPherson, R. A. Gibbs,

and S. M. Grimmond. 2012. Pancreatic cancer genomes reveal aberrations in axon guidance pathway genes. *Nature* 491: 399-405.

38.   Mehlen, P., C. Delloye-Bourgeois, and A. Chedotal. 2011. Novel roles for Slits and netrins: axon guidance cues as anticancer targets? *Nature reviews. Cancer* 11: 188-197.

39.   Kikuchi, K., A. Kishino, O. Konishi, K. Kumagai, N. Hosotani, I. Saji, C. Nakayama, and T. Kimura. 2003. In vitro and in vivo characterization of a novel semaphorin 3A inhibitor, SM-216289 or xanthofulvin. *The Journal of biological chemistry* 278: 42985-42991.

40.   Waddell, N., M. Pajic, A. M. Patch, D. K. Chang, K. S. Kassahn, P. Bailey, A. L. Johns, D. Miller, K. Nones, K. Quek, M. C. Quinn, A. J. Robertson, M. Z. Fadlullah, T. J. Bruxner, A. N. Christ, I. Harliwong, S. Idrisoglu, S. Manning, C. Nourse, E. Nourbakhsh, S. Wani, P. J. Wilson, E. Markham, N. Cloonan, M. J. Anderson, J. L. Fink, O. Holmes, S. H. Kazakoff, C. Leonard, F. Newell, B. Poudel, S. Song, D. Taylor, N. Waddell, S. Wood, Q. Xu, J. Wu, M. Pinese, M. J. Cowley, H. C. Lee, M. D. Jones, A. M. Nagrial, J. Humphris, L. A. Chantrill, V. Chin, A. M. Steinmann, A. Mawson, E. S. Humphrey, E. K. Colvin, A. Chou, C. J. Scarlett, A. V. Pinho, M. Giry-Laterriere, I. Rooman, J. S. Samra, J. G. Kench, J. A. Pettitt, N. D. Merrett, C. Toon, K. Epari, N. Q. Nguyen, A. Barbour, N. Zeps, N. B. Jamieson, J. S. Graham, S. P. Niclou, R. Bjerkvig, R. Grutzmann, D. Aust, R. H. Hruban, A. Maitra, C. A. Iacobuzio-Donahue, C. L. Wolfgang, R. A. Morgan, R. T. Lawlor, V. Corbo, C. Bassi, M. Falconi, G. Zamboni, G. Tortora, M. A. Tempero, I. Australian Pancreatic Cancer Genome, A. J. Gill, J. R. Eshleman, C. Pilarsky, A. Scarpa, E. A. Musgrove, J. V. Pearson, A. V. Biankin, and S. M. Grimmond. 2015. Whole genomes redefine the mutational landscape of pancreatic cancer. *Nature* 518: 495-501.

41. Jiang, X., H. X. Hao, J. D. Growney, S. Woolfenden, C. Bottiglio, N. Ng, B. Lu, M. H. Hsieh, L. Bagdasarian, R. Meyer, T. R. Smith, M. Avello, O. Charlat, Y. Xie, J. A. Porter, S. Pan, J. Liu, M. E. McLaughlin, and F. Cong. 2013. Inactivating mutations of RNF43 confer Wnt dependency in pancreatic ductal adenocarcinoma. *Proceedings of the National Academy of Sciences of the United States of America* 110: 12649-12654.

42. Bettegowda, C., M. Sausen, R. J. Leary, I. Kinde, Y. Wang, N. Agrawal, B. R. Bartlett, H. Wang, B. Luber, R. M. Alani, E. S. Antonarakis, N. S. Azad, A. Bardelli, H. Brem, J. L. Cameron, C. C. Lee, L. A. Fecher, G. L. Gallia, P. Gibbs, D. Le, R. L. Giuntoli, M. Goggins, M. D. Hogarty, M. Holdhoff, S. M. Hong, Y. Jiao, H. H. Juhl, J. J. Kim, G. Siravegna, D. A. Laheru, C. Lauricella, M. Lim, E. J. Lipson, S. K. Marie, G. J. Netto, K. S. Oliner, A. Olivi, L. Olsson, G. J. Riggins, A. Sartore-Bianchi, K. Schmidt, M. Shih l, S. M. Oba-Shinjo, S. Siena, D. Theodorescu, J. Tie, T. T. Harkins, S. Veronese, T. L. Wang, J. D. Weingart, C. L. Wolfgang, L. D. Wood, D. Xing, R. H. Hruban, J. Wu, P. J. Allen, C. M. Schmidt, M. A. Choti, V. E. Velculescu, K. W. Kinzler, B. Vogelstein, N. Papadopoulos, and L. A. Diaz, Jr. 2014. Detection of circulating tumor DNA in early- and late-stage human malignancies. *Sci Transl Med* 6: 224ra224.

43. Newman, A. M., S. V. Bratman, J. To, J. F. Wynne, N. C. Eclov, L. A. Modlin, C. L. Liu, J. W. Neal, H. A. Wakelee, R. E. Merritt, J. B. Shrager, B. W. Loo, Jr., A. A. Alizadeh, and M. Diehn. 2014. An ultrasensitive method for quantitating circulating tumor DNA with broad patient coverage. *Nature medicine* 20: 548-554.

44. Ting, D. T., B. S. Wittner, M. Ligorio, N. Vincent Jordan, A. M. Shah, D. T. Miyamoto, N. Aceto, F. Bersani, B. W. Brannigan, K. Xega, J. C. Ciciliano, H. Zhu, O. C. MacKenzie, J. Trautwein, K. S. Arora, M. Shahid, H. L. Ellis, N. Qu, N. Bardeesy, M. N. Rivera, V. Deshpande, C. R. Ferrone, R. Kapur, S. Ramaswamy, T. Shioda, M. Toner, S.

Maheswaran, and D. A. Haber. 2014. Single-cell RNA sequencing identifies extracellular matrix gene expression by pancreatic circulating tumor cells. *Cell reports* 8: 1905-1918.

45.   Murtaza, M., S. J. Dawson, D. W. Tsui, D. Gale, T. Forshew, A. M. Piskorz, C. Parkinson, S. F. Chin, Z. Kingsbury, A. S. Wong, F. Marass, S. Humphray, J. Hadfield, D. Bentley, T. M. Chin, J. D. Brenton, C. Caldas, and N. Rosenfeld. 2013. Non-invasive analysis of acquired resistance to cancer therapy by sequencing of plasma DNA. *Nature* 497: 108-112.

46.   Yu, K. H., M. Ricigliano, M. Hidalgo, G. K. Abou-Alfa, M. A. Lowery, L. B. Saltz, J. F. Crotty, K. Gary, B. Cooper, R. Lapidus, M. Sadowska, and E. M. O'Reilly. 2014. Pharmacogenomic modeling of circulating tumor and invasive cells for prediction of chemotherapy response and resistance in pancreatic cancer. *Clinical cancer research : an official journal of the American Association for Cancer Research* 20: 5281-5289.

47.   Misale, S., R. Yaeger, S. Hobor, E. Scala, M. Janakiraman, D. Liska, E. Valtorta, R. Schiavo, M. Buscarino, G. Siravegna, K. Bencardino, A. Cercek, C. T. Chen, S. Veronese, C. Zanon, A. Sartore-Bianchi, M. Gambacorta, M. Gallicchio, E. Vakiani, V. Boscaro, E. Medico, M. Weiser, S. Siena, F. Di Nicolantonio, D. Solit, and A. Bardelli. 2012. Emergence of KRAS mutations and acquired resistance to anti-EGFR therapy in colorectal cancer. *Nature* 486: 532-536.

48.   Barrett, M. T., E. Lenkiewicz, L. Evers, T. Holley, C. Ruiz, L. Bubendorf, A. Sekulic, R. K. Ramanathan, and D. D. Von Hoff. 2013. Clonal evolution and therapeutic resistance in solid tumors. *Frontiers in pharmacology* 4: 2.

49.   Haeno, H., M. Gonen, M. B. Davis, J. M. Herman, C. A. Iacobuzio-Donahue, and F. Michor. 2012. Computational modeling of pancreatic cancer reveals kinetics of metastasis suggesting optimum treatment strategies. *Cell* 148: 362-375.

50.   Xia, B., Q. Sheng, K. Nakanishi, A. Ohashi, J. Wu, N. Christ, X. Liu, M. Jasin, F. J. Couch, and D. M. Livingston. 2006. Control of BRCA2 cellular and clinical functions by a nuclear partner, PALB2. *Molecular cell* 22: 719-729.

51.   Villarroel, M. C., N. V. Rajeshkumar, I. Garrido-Laguna, A. De Jesus-Acosta, S. Jones, A. Maitra, R. H. Hruban, J. R. Eshleman, A. Klein, D. Laheru, R. Donehower, and M. Hidalgo. 2011. Personalizing cancer treatment in the age of global genomic analyses: PALB2 gene mutations and the response to DNA damaging agents in pancreatic cancer. *Molecular cancer therapeutics* 10: 3-8.

52.   van der Heijden, M. S., J. R. Brody, D. A. Dezentje, E. Gallmeier, S. C. Cunningham, M. J. Swartz, A. M. DeMarzo, G. J. Offerhaus, W. H. Isacoff, R. H. Hruban, and S. E. Kern. 2005. In vivo therapeutic responses contingent on Fanconi anemia/BRCA2 status of the tumor. *Clinical cancer research : an official journal of the American Association for Cancer Research* 11: 7508-7515.

53.   Farmer, H., N. McCabe, C. J. Lord, A. N. Tutt, D. A. Johnson, T. B. Richardson, M. Santarosa, K. J. Dillon, I. Hickson, C. Knights, N. M. Martin, S. P. Jackson, G. C. Smith, and A. Ashworth. 2005. Targeting the DNA repair defect in BRCA mutant cells as a therapeutic strategy. *Nature* 434: 917-921.

54.   McCabe, N., C. J. Lord, A. N. Tutt, N. M. Martin, G. C. Smith, and A. Ashworth. 2005. BRCA2-deficient CAPAN-1 cells are extremely sensitive to the inhibition of Poly (ADP-Ribose) polymerase: an issue of potency. *Cancer biology & therapy* 4: 934-936.

55.   McLornan, D. P., A. List, and G. J. Mufti. 2014. Applying synthetic lethality for the selective targeting of cancer. *The New England journal of medicine* 371: 1725-1735.

56.   Marcotte, R., K. R. Brown, F. Suarez, A. Sayad, K. Karamboulas, P. M. Krzyzanowski, F. Sircoulomb, M. Medrano, Y. Fedyshyn, J. L. Koh, D. van Dyk, B. Fedyshyn, M. Luhova, G. C. Brito, F. J. Vizeacoumar, F. S. Vizeacoumar, A. Datti, D. Kasimer, A. Buzina, P. Mero, C. Misquitta, J. Normand, M. Haider, T. Ketela, J. L. Wrana, R. Rottapel, B. G. Neel, and J. Moffat. 2012. Essential gene profiles in breast, pancreatic, and ovarian cancer cells. *Cancer discovery* 2: 172-189.

57.   Ward, A. F., B. S. Braun, and K. M. Shannon. 2012. Targeting oncogenic Ras signaling in hematologic malignancies. *Blood* 120: 3397-3406.

58.   Collisson, E. A., C. L. Trejo, J. M. Silva, S. Gu, J. E. Korkola, L. M. Heiser, R. P. Charles, B. A. Rabinovich, B. Hann, D. Dankort, P. T. Spellman, W. A. Phillips, J. W. Gray, and M. McMahon. 2012. A central role for RAF-->MEK-->ERK signaling in the genesis of pancreatic ductal adenocarcinoma. *Cancer discovery* 2: 685-693.

59.   Shimizu, T., A. W. Tolcher, K. P. Papadopoulos, M. Beeram, D. W. Rasco, L. S. Smith, S. Gunn, L. Smetzer, T. A. Mays, B. Kaiser, M. J. Wick, C. Alvarez, A. Cavazos, G. L. Mangold, and A. Patnaik. 2012. The clinical effect of the dual-targeting strategy involving PI3K/AKT/mTOR and RAS/MEK/ERK pathways in patients with advanced cancer. *Clinical cancer research : an official journal of the American Association for Cancer Research* 18: 2316-2325.

60.   Desrochers, L. M., M. A. Antonyak, and R. A. Cerione. 2016. Extracellular Vesicles: Satellites of Information Transfer in Cancer and Stem Cell Biology. *Dev Cell* 37: 301-309.

61. Teis, D., S. Saksena, and S. D. Emr. 2009. SnapShot: the ESCRT machinery. *Cell* 137: 182-182 e181.

62. Cocucci, E., and J. Meldolesi. 2011. Ectosomes. *Curr Biol* 21: R940-941.

63. Lo Cicero, A., P. D. Stahl, and G. Raposo. 2015. Extracellular vesicles shuffling intercellular messages: for good or for bad. *Curr Opin Cell Biol* 35: 69-77.

64. Chiba, M., M. Kimura, and S. Asari. 2012. Exosomes secreted from human colorectal cancer cell lines contain mRNAs, microRNAs and natural antisense RNAs, that can transfer into the human hepatoma HepG2 and lung cancer A549 cell lines. *Oncol Rep* 28: 1551-1558.

65. Cocucci, E., and J. Meldolesi. 2015. Ectosomes and exosomes: shedding the confusion between extracellular vesicles. *Trends Cell Biol* 25: 364-372.

66. Muralidharan-Chari, V., J. W. Clancy, A. Sedgwick, and C. D'Souza-Schorey. 2010. Microvesicles: mediators of extracellular communication during cancer progression. *J Cell Sci* 123: 1603-1611.

67. Skog, J., T. Wurdinger, S. van Rijn, D. H. Meijer, L. Gainche, M. Sena-Esteves, W. T. Curry, Jr., B. S. Carter, A. M. Krichevsky, and X. O. Breakefield. 2008. Glioblastoma microvesicles transport RNA and proteins that promote tumour growth and provide diagnostic biomarkers. *Nat Cell Biol* 10: 1470-1476.

68. Ludwig, A. K., and B. Giebel. 2012. Exosomes: small vesicles participating in intercellular communication. *Int J Biochem Cell Biol* 44: 11-15.

69. Cai, J., Y. Han, H. Ren, C. Chen, D. He, L. Zhou, G. M. Eisner, L. D. Asico, P. A. Jose, and C. Zeng. 2013. Extracellular vesicle-mediated transfer of donor genomic DNA to recipient cells is a novel mechanism for genetic influence between cells. *J Mol Cell Biol* 5: 227-238.

70.   Kahlert, C., S. A. Melo, A. Protopopov, J. Tang, S. Seth, M. Koch, J. Zhang, J. Weitz, L. Chin, A. Futreal, and R. Kalluri. 2014. Identification of double-stranded genomic DNA spanning all chromosomes with mutated KRAS and p53 DNA in the serum exosomes of patients with pancreatic cancer. *The Journal of biological chemistry* 289: 3869-3875.

71.   Thakur, B. K., H. Zhang, A. Becker, I. Matei, Y. Huang, B. Costa-Silva, Y. Zheng, A. Hoshino, H. Brazier, J. Xiang, C. Williams, R. Rodriguez-Barrueco, J. M. Silva, W. Zhang, S. Hearn, O. Elemento, N. Paknejad, K. Manova-Todorova, K. Welte, J. Bromberg, H. Peinado, and D. Lyden. 2014. Double-stranded DNA in exosomes: a novel biomarker in cancer detection. *Cell Res* 24: 766-769.

72.   San Lucas, F. A., K. Allenson, V. Bernard, J. Castillo, D. U. Kim, K. Ellis, E. A. Ehli, G. E. Davies, J. L. Petersen, D. Li, R. Wolff, M. Katz, G. Varadhachary, I. Wistuba, A. Maitra, and H. Alvarez. 2016. Minimally invasive genomic and transcriptomic profiling of visceral cancers by next-generation sequencing of circulating exosomes. *Annals of oncology : official journal of the European Society for Medical Oncology / ESMO* 27: 635-641.

73.   Jin, Y., K. Chen, Z. Wang, Y. Wang, J. Liu, L. Lin, Y. Shao, L. Gao, H. Yin, C. Cui, Z. Tan, L. Liu, C. Zhao, G. Zhang, R. Jia, L. Du, Y. Chen, R. Liu, J. Xu, X. Hu, and Y. Wang. 2016. DNA in serum extracellular vesicles is stable under different storage conditions. *BMC Cancer* 16: 753.

74.   Castillo, J., et al. 2017. Surfaceome profiling enables isolation of cancer-specific exosomal cargo in liquid biopsies from pancreatic cancer patients. *Annals of Oncology*.

75.   Lazaro-Ibanez, E., A. Sanz-Garcia, T. Visakorpi, C. Escobedo-Lucea, P. Siljander, A. Ayuso-Sacido, and M. Yliperttula. 2014. Different gDNA content in the subpopulations of prostate cancer extracellular vesicles: apoptotic bodies, microvesicles, and exosomes. *Prostate* 74: 1379-1390.

76.   Ronquist, G. K., A. Larsson, A. Stavreus-Evers, and G. Ronquist. 2012. Prostasomes are heterogeneous regarding size and appearance but affiliated to one DNA-containing exosome family. *Prostate* 72: 1736-1745.

77.   Lasser, C., V. S. Alikhani, K. Ekstrom, M. Eldh, P. T. Paredes, A. Bossios, M. Sjostrand, S. Gabrielsson, J. Lotvall, and H. Valadi. 2011. Human saliva, plasma and breast milk exosomes contain RNA: uptake by macrophages. *J Transl Med* 9: 9.

78.   Sergeant, G., R. van Eijsden, T. Roskams, V. Van Duppen, and B. Topal. 2012. Pancreatic cancer circulating tumour cells express a cell motility gene signature that predicts survival after surgery. *BMC cancer* 12: 527.

79.   Bryant, K. L., J. D. Mancias, A. C. Kimmelman, and C. J. Der. 2014. KRAS: feeding pancreatic cancer proliferation. *Trends Biochem Sci* 39: 91-100.

80.   Bailey, P., D. K. Chang, K. Nones, A. L. Johns, A. M. Patch, M. C. Gingras, D. K. Miller, A. N. Christ, T. J. Bruxner, M. C. Quinn, C. Nourse, L. C. Murtaugh, I. Harliwong, S. Idrisoglu, S. Manning, E. Nourbakhsh, S. Wani, L. Fink, O. Holmes, V. Chin, M. J. Anderson, S. Kazakoff, C. Leonard, F. Newell, N. Waddell, S. Wood, Q. Xu, P. J. Wilson, N. Cloonan, K. S. Kassahn, D. Taylor, K. Quek, A. Robertson, L. Pantano, L. Mincarelli, L. N. Sanchez, L. Evers, J. Wu, M. Pinese, M. J. Cowley, M. D. Jones, E. K. Colvin, A. M. Nagrial, E. S. Humphrey, L. A. Chantrill, A. Mawson, J. Humphris, A. Chou, M. Pajic, C. J. Scarlett, A. V. Pinho, M. Giry-Laterriere, I. Rooman, J. S. Samra, J. G. Kench, J. A. Lovell, N. D. Merrett, C. W. Toon, K. Epari, N. Q. Nguyen, A. Barbour, N. Zeps, K.

Moran-Jones, N. B. Jamieson, J. S. Graham, F. Duthie, K. Oien, J. Hair, R. Grutzmann, A. Maitra, C. A. Iacobuzio-Donahue, C. L. Wolfgang, R. A. Morgan, R. T. Lawlor, V. Corbo, C. Bassi, B. Rusev, P. Capelli, R. Salvia, G. Tortora, D. Mukhopadhyay, G. M. Petersen, I. Australian Pancreatic Cancer Genome, D. M. Munzy, W. E. Fisher, S. A. Karim, J. R. Eshleman, R. H. Hruban, C. Pilarsky, J. P. Morton, O. J. Sansom, A. Scarpa, E. A. Musgrove, U. M. Bailey, O. Hofmann, R. L. Sutherland, D. A. Wheeler, A. J. Gill, R. A. Gibbs, J. V. Pearson, N. Waddell, A. V. Biankin, and S. M. Grimmond. 2016. Genomic analyses identify molecular subtypes of pancreatic cancer. *Nature* 531: 47-52.

81.   Bernard, V., J. Fleming, and A. Maitra. 2016. Molecular and Genetic Basis of Pancreatic Carcinogenesis: Which Concepts May be Clinically Relevant? *Surgical oncology clinics of North America* 25: 227-238.

82.   Allenson, K., J. Castillo, F. A. San Lucas, G. Scelo, D. U. Kim, V. Bernard, G. Davis, T. Kumar, M. Katz, M. J. Overman, L. Foretova, E. Fabianova, I. Holcatova, V. Janout, F. Meric-Bernstam, P. Gascoyne, I. Wistuba, G. Varadhachary, P. Brennan, S. Hanash, D. Li, A. Maitra, and H. Alvarez. 2017. High prevalence of mutant KRAS in circulating exosome-derived DNA from early-stage pancreatic cancer patients. *Annals of oncology : official journal of the European Society for Medical Oncology / ESMO* 28: 741-747.

83.   Kidess, E., and S. S. Jeffrey. 2013. Circulating tumor cells versus tumor-derived cell-free DNA: rivals or partners in cancer care in the era of single-cell analysis? *Genome Med* 5: 70.

84.   Chantrill, L. A., A. M. Nagrial, C. Watson, A. L. Johns, M. Martyn-Smith, S. Simpson, S. Mead, M. D. Jones, J. S. Samra, A. J. Gill, N. Watson, V. T. Chin, J. L. Humphris, A. Chou, B. Brown, A. Morey, M. Pajic, S. M. Grimmond, D. K. Chang, D. Thomas, L. Sebastian,

K. Sjoquist, S. Yip, N. Pavlakis, R. Asghari, S. Harvey, P. Grimison, J. Simes, A. V. Biankin, I. Australian Pancreatic Cancer Genome, and G. Individualized Molecular Pancreatic Cancer Therapy Trial Management Committee of the Australasian Gastrointestinal Trials. 2015. Precision Medicine for Advanced Pancreas Cancer: The Individualized Molecular Pancreatic Cancer Therapy (IMPaCT) Trial. *Clin Cancer Res* 21: 2029-2037.

85.   Mouliere, F., B. Robert, E. Arnau Peyrotte, M. Del Rio, M. Ychou, F. Molina, C. Gongora, and A. R. Thierry. 2011. High fragmentation characterizes tumour-derived circulating DNA. *PloS one* 6: e23418.

86.   El-Hefnawy, T., S. Raja, L. Kelly, W. L. Bigbee, J. M. Kirkwood, J. D. Luketich, and T. E. Godfrey. 2004. Characterization of amplifiable, circulating RNA in plasma and its potential as a tool for cancer diagnostics. *Clin Chem* 50: 564-573.

87.   Mitchell, P. S., R. K. Parkin, E. M. Kroh, B. R. Fritz, S. K. Wyman, E. L. Pogosova-Agadjanyan, A. Peterson, J. Noteboom, K. C. O'Briant, A. Allen, D. W. Lin, N. Urban, C. W. Drescher, B. S. Knudsen, D. L. Stirewalt, R. Gentleman, R. L. Vessella, P. S. Nelson, D. B. Martin, and M. Tewari. 2008. Circulating microRNAs as stable blood-based markers for cancer detection. *Proceedings of the National Academy of Sciences of the United States of America* 105: 10513-10518.

88.   Kang, Y., R. Zhang, R. Suzuki, S. Q. Li, D. Roife, M. J. Truty, D. Chatterjee, R. M. Thomas, J. Cardwell, Y. Wang, H. Wang, M. H. Katz, and J. B. Fleming. 2015. Two-dimensional culture of human pancreatic adenocarcinoma cells results in an irreversible transition from epithelial to mesenchymal phenotype. *Lab Invest* 95: 207-222.

89.   Yu, J., K. Walter, N. Omura, S. M. Hong, A. Young, A. Li, A. Vincent, and M. Goggins. 2012. Unlike pancreatic cancer cells pancreatic cancer associated fibroblasts display minimal gene induction after 5-aza-2'-deoxycytidine. *PLoS One* 7: e43456.

90.   Lee, K. M., C. Nguyen, A. B. Ulrich, P. M. Pour, and M. M. Ouellette. 2003. Immortalization with telomerase of the Nestin-positive cells of the human pancreas. *Biochem Biophys Res Commun* 301: 1038-1044.

91.   2015. NCI Dictionaries. U.S. Department of Health and Human Services. National Institutes of Health. National Cancer Institute.

92.   Yue, S., W. Mu, U. Erb, and M. Zoller. 2015. The tetraspanins CD151 and Tspan8 are essential exosome components for the crosstalk between cancer initiating cells and their surrounding. *Oncotarget* 6: 2366-2384.

93.   Shen, Y. J., N. Le Bert, A. A. Chitre, C. X. Koo, X. H. Nga, S. S. Ho, M. Khatoo, N. Y. Tan, K. J. Ishii, and S. Gasser. 2015. Genome-derived cytosolic DNA mediates type I interferon-dependent rejection of B cell lymphoma cells. *Cell reports* 11: 460-473.

94.   Li, H., and R. Durbin. 2009. Fast and accurate short read alignment with Burrows-Wheeler transform. *Bioinformatics* 25: 1754-1760.

95.   Li, H., B. Handsaker, A. Wysoker, T. Fennell, J. Ruan, N. Homer, G. Marth, G. Abecasis, R. Durbin, and S. Genome Project Data Processing. 2009. The Sequence Alignment/Map format and SAMtools. *Bioinformatics* 25: 2078-2079.

96.   McKenna, A., M. Hanna, E. Banks, A. Sivachenko, K. Cibulskis, A. Kernytsky, K. Garimella, D. Altshuler, S. Gabriel, M. Daly, and M. A. DePristo. 2010. The Genome Analysis Toolkit: a MapReduce framework for analyzing next-generation DNA sequencing data. *Genome Res* 20: 1297-1303.

97.   Li, B., and C. N. Dewey. 2011. RSEM: accurate transcript quantification from RNA-Seq data with or without a reference genome. *BMC Bioinformatics* 12: 323.

98.   Cibulskis, K., M. S. Lawrence, S. L. Carter, A. Sivachenko, D. Jaffe, C. Sougnez, S. Gabriel, M. Meyerson, E. S. Lander, and G. Getz. 2013. Sensitive detection of somatic point mutations in impure and heterogeneous cancer samples. *Nat Biotechnol* 31: 213-219.

99.   San Lucas, F. A., G. Wang, P. Scheet, and B. Peng. 2012. Integrated annotation and analysis of genetic variants from next-generation sequencing studies with variant tools. *Bioinformatics* 28: 421-422.

100.   Forbes, S. A., D. Beare, P. Gunasekaran, K. Leung, N. Bindal, H. Boutselakis, M. Ding, S. Bamford, C. Cole, S. Ward, C. Y. Kok, M. Jia, T. De, J. W. Teague, M. R. Stratton, U. McDermott, and P. J. Campbell. 2015. COSMIC: exploring the world's knowledge of somatic mutations in human cancer. *Nucleic Acids Res* 43: D805-811.

101.   Liu, X., X. Jian, and E. Boerwinkle. 2013. dbNSFP v2.0: a database of human non-synonymous SNVs and their functional predictions and annotations. *Hum Mutat* 34: E2393-2402.

102.   Genomes Project, C., A. Auton, L. D. Brooks, R. M. Durbin, E. P. Garrison, H. M. Kang, J. O. Korbel, J. L. Marchini, S. McCarthy, G. A. McVean, and G. R. Abecasis. 2015. A global reference for human genetic variation. *Nature* 526: 68-74.

103.   Fu, W., T. D. O'Connor, G. Jun, H. M. Kang, G. Abecasis, S. M. Leal, S. Gabriel, M. J. Rieder, D. Altshuler, J. Shendure, D. A. Nickerson, M. J. Bamshad, N. E. S. Project, and J. M. Akey. 2013. Analysis of 6,515 exomes reveals the recent origin of most human protein-coding variants. *Nature* 493: 216-220.

104. Landrum, M. J., J. M. Lee, G. R. Riley, W. Jang, W. S. Rubinstein, D. M. Church, and D. R. Maglott. 2014. ClinVar: public archive of relationships among sequence variation and human phenotype. *Nucleic Acids Res* 42: D980-985.

105. Jones, S., V. Anagnostou, K. Lytle, S. Parpart-Li, M. Nesselbush, D. R. Riley, M. Shukla, B. Chesnick, M. Kadan, E. Papp, K. G. Galens, D. Murphy, T. Zhang, L. Kann, M. Sausen, S. V. Angiuoli, L. A. Diaz, Jr., and V. E. Velculescu. 2015. Personalized genomic analyses for cancer mutation discovery and interpretation. *Sci Transl Med* 7: 283ra253.

106. Iyer, M. K., A. M. Chinnaiyan, and C. A. Maher. 2011. ChimeraScan: a tool for identifying chimeric transcription in sequencing data. *Bioinformatics* 27: 2903-2904.

107. Robinson, J. T., H. Thorvaldsdottir, W. Winckler, M. Guttman, E. S. Lander, G. Getz, and J. P. Mesirov. 2011. Integrative genomics viewer. *Nat Biotechnol* 29: 24-26.

108. Boeva, V., T. Popova, K. Bleakley, P. Chiche, J. Cappo, G. Schleiermacher, I. Janoueix-Lerosey, O. Delattre, and E. Barillot. 2012. Control-FREEC: a tool for assessing copy number and allelic content using next-generation sequencing data. *Bioinformatics* 28: 423-425.

109. Rosenbloom, K. R., J. Armstrong, G. P. Barber, J. Casper, H. Clawson, M. Diekhans, T. R. Dreszer, P. A. Fujita, L. Guruvadoo, M. Haeussler, R. A. Harte, S. Heitner, G. Hickey, A. S. Hinrichs, R. Hubley, D. Karolchik, K. Learned, B. T. Lee, C. H. Li, K. H. Miga, N. Nguyen, B. Paten, B. J. Raney, A. F. Smit, M. L. Speir, A. S. Zweig, D. Haussler, R. M. Kuhn, and W. J. Kent. 2015. The UCSC Genome Browser database: 2015 update. *Nucleic Acids Res* 43: D670-681.

110. Favero, F., T. Joshi, A. M. Marquard, N. J. Birkbak, M. Krzystanek, Q. Li, Z. Szallasi, and A. C. Eklund. 2015. Sequenza: allele-specific copy number and mutation profiles from tumor sequencing data. *Ann Oncol* 26: 64-70.

111. Huang da, W., B. T. Sherman, and R. A. Lempicki. 2009. Systematic and integrative analysis of large gene lists using DAVID bioinformatics resources. *Nat Protoc* 4: 44-57.

112. Gehring, J. S., B. Fischer, M. Lawrence, and W. Huber. 2015. SomaticSignatures: inferring mutational signatures from single-nucleotide variants. *Bioinformatics*.

113. Alexandrov, L. B., S. Nik-Zainal, D. C. Wedge, S. A. Aparicio, S. Behjati, A. V. Biankin, G. R. Bignell, N. Bolli, A. Borg, A. L. Borresen-Dale, S. Boyault, B. Burkhardt, A. P. Butler, C. Caldas, H. R. Davies, C. Desmedt, R. Eils, J. E. Eyfjord, J. A. Foekens, M. Greaves, F. Hosoda, B. Hutter, T. Ilicic, S. Imbeaud, M. Imielinski, N. Jager, D. T. Jones, D. Jones, S. Knappskog, M. Kool, S. R. Lakhani, C. Lopez-Otin, S. Martin, N. C. Munshi, H. Nakamura, P. A. Northcott, M. Pajic, E. Papaemmanuil, A. Paradiso, J. V. Pearson, X. S. Puente, K. Raine, M. Ramakrishna, A. L. Richardson, J. Richter, P. Rosenstiel, M. Schlesner, T. N. Schumacher, P. N. Span, J. W. Teague, Y. Totoki, A. N. Tutt, R. Valdes-Mas, M. M. van Buuren, L. van 't Veer, A. Vincent-Salomon, N. Waddell, L. R. Yates, I. Australian Pancreatic Cancer Genome, I. B. C. Consortium, I. M.-S. Consortium, I. PedBrain, J. Zucman-Rossi, P. A. Futreal, U. McDermott, P. Lichter, M. Meyerson, S. M. Grimmond, R. Siebert, E. Campo, T. Shibata, S. M. Pfister, P. J. Campbell, and M. R. Stratton. 2013. Signatures of mutational processes in human cancer. *Nature* 500: 415-421.

114. Li, H., and R. Durbin. 2010. Fast and accurate long-read alignment with Burrows-Wheeler transform. *Bioinformatics (Oxford, England)* 26: 589-595.

115.   Xu, C., M. R. Nezami Ranjbar, Z. Wu, J. DiCarlo, and Y. Wang. 2017. Detecting very low allele fraction variants using targeted DNA sequencing and a novel molecular barcode-aware variant caller. *BMC genomics* 18: 5.

116.   Ryan, D. P., T. S. Hong, and N. Bardeesy. 2014. Pancreatic adenocarcinoma. *N Engl J Med* 371: 1039-1049.

117.   Yeo, T. P. 2015. Demographics, epidemiology, and inheritance of pancreatic ductal adenocarcinoma. *Semin Oncol* 42: 8-18.

118.   Warner, E. 2011. Clinical practice. Breast-cancer screening. *N Engl J Med* 365: 1025-1032.

119.   Arteaga, C. L. 2013. Progress in breast cancer: overview. *Clin Cancer Res* 19: 6353-6359.

120.   Lieberman, D. A. 2009. Clinical practice. Screening for colorectal cancer. *N Engl J Med* 361: 1179-1187.

121.   Lee, M. S., and S. Kopetz. 2015. Current and Future Approaches to Target the Epidermal Growth Factor Receptor and Its Downstream Signaling in Metastatic Colorectal Cancer. *Clin Colorectal Cancer* 14: 203-218.

122.   Zhou, C., Y. L. Wu, G. Chen, J. Feng, X. Q. Liu, C. Wang, S. Zhang, J. Wang, S. Zhou, S. Ren, S. Lu, L. Zhang, C. Hu, C. Hu, Y. Luo, L. Chen, M. Ye, J. Huang, X. Zhi, Y. Zhang, Q. Xiu, J. Ma, L. Zhang, and C. You. 2011. Erlotinib versus chemotherapy as first-line treatment for patients with advanced EGFR mutation-positive non-small-cell lung cancer (OPTIMAL, CTONG-0802): a multicentre, open-label, randomised, phase 3 study. *Lancet Oncol* 12: 735-742.

123.   Smith, R. A., D. Manassaram-Baptiste, D. Brooks, M. Doroshenk, S. Fedewa, D. Saslow, O. W. Brawley, and R. Wender. 2015. Cancer screening in the United States,

2015: a review of current American cancer society guidelines and current issues in cancer screening. *CA Cancer J Clin* 65: 30-54.

124. Katz, M. H., H. Wang, J. B. Fleming, C. C. Sun, R. F. Hwang, R. A. Wolff, G. Varadhachary, J. L. Abbruzzese, C. H. Crane, S. Krishnan, J. N. Vauthey, E. K. Abdalla, J. E. Lee, P. W. Pisters, and D. B. Evans. 2009. Long-term survival after multidisciplinary management of resected pancreatic adenocarcinoma. *Ann Surg Oncol* 16: 836-847.

125. Howlader N, N. A., Krapcho M, Miller D, Bishop K, Altekruse SF, Kosary CL, Yu M, Ruhl J, Tatalovich Z, Mariotto A, Lewis DR, Chen HS, Feuer EJ, Cronin KA (eds). 2016. SEER Cancer Statistics Review, 1975-2013. National Cancer Institute. Bethesda, MD.

126. Siegel, R. L., K. D. Miller, and A. Jemal. 2016. Cancer statistics, 2016. *CA Cancer J Clin* 66: 7-30.

127. Chakraborty, S., M. J. Baine, A. R. Sasson, and S. K. Batra. 2011. Current status of molecular markers for early detection of sporadic pancreatic cancer. *Biochim Biophys Acta* 1815: 44-64.

128. Vietsch, E. E., C. H. van Eijck, and A. Wellstein. 2015. Circulating DNA and Micro-RNA in Patients with Pancreatic Cancer. *Pancreat Disord Ther* 5.

129. Mulcahy, H. E., J. Lyautey, C. Lederrey, X. qi Chen, P. Anker, E. M. Alstead, A. Ballinger, M. J. Farthing, and M. Stroun. 1998. A prospective study of K-ras mutations in the plasma of pancreatic cancer patients. *Clin Cancer Res* 4: 271-275.

130. Dianxu, F., Z. Shengdao, H. Tianquan, J. Yu, L. Ruoqing, Y. Zurong, and W. Xuezhi. 2002. A prospective study of detection of pancreatic carcinoma by combined plasma K-ras mutations and serum CA19-9 analysis. *Pancreas* 25: 336-341.

131. Maire, F., S. Micard, P. Hammel, H. Voitot, P. Levy, P. H. Cugnenc, P. Ruszniewski, and P. L. Puig. 2002. Differential diagnosis between chronic pancreatitis and pancreatic cancer: value of the detection of KRAS2 mutations in circulating DNA. *British journal of cancer* 87: 551-554.

132. Uemura, T., K. Hibi, T. Kaneko, S. Takeda, S. Inoue, O. Okochi, T. Nagasaka, and A. Nakao. 2004. Detection of K-ras mutations in the plasma DNA of pancreatic cancer patients. *J Gastroenterol* 39: 56-60.

133. Dabritz, J., R. Preston, J. Hanfler, and H. Oettle. 2009. Follow-up study of K-ras mutations in the plasma of patients with pancreatic cancer: correlation with clinical features and carbohydrate antigen 19-9. *Pancreas* 38: 534-541.

134. Chen, H., H. Tu, Z. Q. Meng, Z. Chen, P. Wang, and L. M. Liu. 2010. K-ras mutational status predicts poor prognosis in unresectable pancreatic cancer. *Eur J Surg Oncol* 36: 657-662.

135. Castells, A., P. Puig, J. Mora, J. Boadas, L. Boix, E. Urgell, M. Sole, G. Capella, F. Lluis, L. Fernandez-Cruz, S. Navarro, and A. Farre. 1999. K-ras mutations in DNA extracted from the plasma of patients with pancreatic carcinoma: diagnostic utility and prognostic significance. *J Clin Oncol* 17: 578-584.

136. Diaz, L. A., Jr., and A. Bardelli. 2014. Liquid biopsies: genotyping circulating tumor DNA. *J Clin Oncol* 32: 579-586.

137. Lu, L., and H. A. Risch. 2016. Exosomes: potential for early detection in pancreatic cancer. *Future Oncol* 12: 1081-1090.

138. Melo, S. A., L. B. Luecke, C. Kahlert, A. F. Fernandez, S. T. Gammon, J. Kaye, V. S. LeBleu, E. A. Mittendorf, J. Weitz, N. Rahbari, C. Reissfelder, C. Pilarsky, M. F. Fraga,

D. Piwnica-Worms, and R. Kalluri. 2015. Glypican-1 identifies cancer exosomes and detects early pancreatic cancer. *Nature* 523: 177-182.

139. Sluijter, J. P., V. Verhage, J. C. Deddens, F. van den Akker, and P. A. Doevendans. 2014. Microvesicles and exosomes for intracardiac communication. *Cardiovasc Res* 102: 302-311.

140. Demory Beckler, M., J. N. Higginbotham, J. L. Franklin, A. J. Ham, P. J. Halvey, I. E. Imasuen, C. Whitwell, M. Li, D. C. Liebler, and R. J. Coffey. 2013. Proteomic analysis of exosomes from mutant KRAS colon cancer cells identifies intercellular transfer of mutant KRAS. *Mol Cell Proteomics* 12: 343-355.

141. Jahr, S., H. Hentze, S. Englisch, D. Hardt, F. O. Fackelmayer, R. D. Hesch, and R. Knippers. 2001. DNA fragments in the blood plasma of cancer patients: quantitations and evidence for their origin from apoptotic and necrotic cells. *Cancer Res* 61: 1659-1665.

142. Diamandis, E. P. 2016. A Word of Caution on New and Revolutionary Diagnostic Tests. *Cancer Cell* 29: 141-142.

143. Krimmel, J. D., M. W. Schmitt, M. I. Harrell, K. J. Agnew, S. R. Kennedy, M. J. Emond, L. A. Loeb, E. M. Swisher, and R. A. Risques. 2016. Ultra-deep sequencing detects ovarian cancer cells in peritoneal fluid and reveals somatic TP53 mutations in noncancerous tissues. *Proceedings of the National Academy of Sciences of the United States of America* 113: 6005-6010.

144. Poruk, K. E., D. Z. Gay, K. Brown, J. D. Mulvihill, K. M. Boucher, C. L. Scaife, M. A. Firpo, and S. J. Mulvihill. 2013. The clinical utility of CA 19-9 in pancreatic adenocarcinoma: diagnostic and prognostic updates. *Curr Mol Med* 13: 340-351.

145. Katz, M. H., P. W. Pisters, D. B. Evans, C. C. Sun, J. E. Lee, J. B. Fleming, J. N. Vauthey, E. K. Abdalla, C. H. Crane, R. A. Wolff, G. R. Varadhachary, and R. F. Hwang. 2008. Borderline resectable pancreatic cancer: the importance of this emerging stage of disease. *J Am Coll Surg* 206: 833-846; discussion 846-838.

146. Chaudhuri, A. A., J. J. Chabon, A. F. Lovejoy, A. M. Newman, H. Stehr, T. D. Azad, M. S. Khodadoust, M. S. Esfahani, C. L. Liu, L. Zhou, F. Scherer, D. M. Kurtz, C. Say, J. N. Carter, D. J. Merriott, J. C. Dudley, M. S. Binkley, L. Modlin, S. K. Padda, M. F. Gensheimer, R. B. West, J. B. Shrager, J. W. Neal, H. A. Wakelee, B. W. Loo, A. A. Alizadeh, and M. Diehn. 2017. Early detection of molecular residual disease in localized lung cancer by circulating tumor DNA profiling. *Cancer Discov*.

147. Beaver, J. A., D. Jelovac, S. Balukrishna, R. L. Cochran, S. Croessmann, D. J. Zabransky, H. Y. Wong, P. Valda Toro, J. Cidado, B. G. Blair, D. Chu, T. Burns, M. J. Higgins, V. Stearns, L. Jacobs, M. Habibi, J. Lange, P. J. Hurley, J. Lauring, D. A. VanDenBerg, J. Kessler, S. Jeter, M. L. Samuels, D. Maar, L. Cope, A. Cimino-Mathews, P. Argani, A. C. Wolff, and B. H. Park. 2014. Detection of cancer DNA in plasma of patients with early-stage breast cancer. *Clinical cancer research : an official journal of the American Association for Cancer Research* 20: 2643-2650.

148. Garcia-Murillas, I., G. Schiavon, B. Weigelt, C. Ng, S. Hrebien, R. J. Cutts, M. Cheang, P. Osin, A. Nerurkar, I. Kozarewa, J. A. Garrido, M. Dowsett, J. S. Reis-Filho, I. E. Smith, and N. C. Turner. 2015. Mutation tracking in circulating tumor DNA predicts relapse in early breast cancer. *Science translational medicine* 7: 302ra133.

149. Tie, J., Y. Wang, C. Tomasetti, L. Li, S. Springer, I. Kinde, N. Silliman, M. Tacey, H. L. Wong, M. Christie, S. Kosmider, I. Skinner, R. Wong, M. Steel, B. Tran, J. Desai, I. Jones, A. Haydon, T. Hayes, T. J. Price, R. L. Strausberg, L. A. Diaz, Jr., N.

Papadopoulos, K. W. Kinzler, B. Vogelstein, and P. Gibbs. 2016. Circulating tumor DNA analysis detects minimal residual disease and predicts recurrence in patients with stage II colon cancer. *Sci Transl Med* 8: 346ra392.

150. Abbosh, C., N. J. Birkbak, G. A. Wilson, M. Jamal-Hanjani, T. Constantin, R. Salari, J. Le Quesne, D. A. Moore, S. Veeriah, R. Rosenthal, T. Marafioti, E. Kirkizlar, T. B. K. Watkins, N. McGranahan, S. Ward, L. Martinson, J. Riley, F. Fraioli, M. Al Bakir, E. Gronroos, F. Zambrana, R. Endozo, W. L. Bi, F. M. Fennessy, N. Sponer, D. Johnson, J. Laycock, S. Shafi, J. Czyzewska-Khan, A. Rowan, T. Chambers, N. Matthews, S. Turajlic, C. Hiley, S. M. Lee, M. D. Forster, T. Ahmad, M. Falzon, E. Borg, D. Lawrence, M. Hayward, S. Kolvekar, N. Panagiotopoulos, S. M. Janes, R. Thakrar, A. Ahmed, F. Blackhall, Y. Summers, D. Hafez, A. Naik, A. Ganguly, S. Kareht, R. Shah, L. Joseph, A. Marie Quinn, P. A. Crosbie, B. Naidu, G. Middleton, G. Langman, S. Trotter, M. Nicolson, H. Remmen, K. Kerr, M. Chetty, L. Gomersall, D. A. Fennell, A. Nakas, S. Rathinam, G. Anand, S. Khan, P. Russell, V. Ezhil, B. Ismail, M. Irvin-Sellers, V. Prakash, J. F. Lester, M. Kornaszewska, R. Attanoos, H. Adams, H. Davies, D. Oukrif, A. U. Akarca, J. A. Hartley, H. L. Lowe, S. Lock, N. Iles, H. Bell, Y. Ngai, G. Elgar, Z. Szallasi, R. F. Schwarz, J. Herrero, A. Stewart, S. A. Quezada, K. S. Peggs, P. Van Loo, C. Dive, C. J. Lin, M. Rabinowitz, H. Aerts, A. Hackshaw, J. A. Shaw, B. G. Zimmermann, T. R. consortium, P. consortium, and C. Swanton. 2017. Phylogenetic ctDNA analysis depicts early-stage lung cancer evolution. *Nature* 545: 446-451.

151. Calvez-Kelm, F. L., M. Foll, M. B. Wozniak, T. M. Delhomme, G. Durand, P. Chopard, M. Pertesi, E. Fabianova, Z. Adamcakova, I. Holcatova, L. Foretova, V. Janout, M. P. Vallee, S. Rinaldi, P. Brennan, J. D. McKay, G. B. Byrnes, and G. Scelo. 2016. KRAS

mutations in blood circulating cell-free DNA: a pancreatic cancer case-control. *Oncotarget*.

152.   Pietrasz, D., N. Pecuchet, F. Garlan, A. Didelot, O. Dubreuil, S. Doat, F. Imbert-Bismut, M. Karoui, J. C. Vaillant, V. Taly, P. Laurent-Puig, and J. B. Bachet. 2017. Plasma Circulating Tumor DNA in Pancreatic Cancer Patients Is a Prognostic Marker. *Clin Cancer Res* 23: 116-123.

153.   Takai, E., Y. Totoki, H. Nakamura, M. Kato, T. Shibata, and S. Yachida. 2016. Clinical Utility of Circulating Tumor DNA for Molecular Assessment and Precision Medicine in Pancreatic Cancer. *Advances in experimental medicine and biology* 924: 13-17.

154.   San Lucas, F. A., K. Allenson, V. Bernard, J. Castillo, D. U. Kim, K. Ellis, E. A. Ehli, G. E. Davies, J. L. Petersen, D. Li, R. Wolff, M. Katz, G. Varadhachary, I. Wistuba, A. Maitra, and H. Alvarez. 2015. Minimally invasive genomic and transcriptomic profiling of visceral cancers by next-generation sequencing of circulating exosomes. *Annals of oncology : official journal of the European Society for Medical Oncology / ESMO*.

155.   Furukawa, T., Y. Kuboki, E. Tanji, S. Yoshida, T. Hatori, M. Yamamoto, N. Shibata, K. Shimizu, N. Kamatani, and K. Shiratori. 2011. Whole-exome sequencing uncovers frequent GNAS mutations in intraductal papillary mucinous neoplasms of the pancreas. *Scientific reports* 1: 161.

156.   Lee, J. H., Y. Kim, J. W. Choi, and Y. S. Kim. 2016. KRAS, GNAS, and RNF43 mutations in intraductal papillary mucinous neoplasm of the pancreas: a meta-analysis. *Springerplus* 5: 1172.

157.   Luttges, J., A. Diederichs, M. A. Menke, I. Vogel, B. Kremer, and G. Kloppel. 2000. Ductal lesions in patients with chronic pancreatitis show K-ras mutations in a

frequency similar to that in the normal pancreas and lack nuclear immunoreactivity for p53. *Cancer* 88: 2495-2504.

158. Le Calvez-Kelm, F., M. Foll, M. B. Wozniak, T. M. Delhomme, G. Durand, P. Chopard, M. Pertesi, E. Fabianova, Z. Adamcakova, I. Holcatova, L. Foretova, V. Janout, M. P. Vallee, S. Rinaldi, P. Brennan, J. D. McKay, G. B. Byrnes, and G. Scelo. 2016. KRAS mutations in blood circulating cell-free DNA: a pancreatic cancer case-control. *Oncotarget* 7: 78827-78840.

159. Mohrmann, L., H. Huang, D. S. Hong, A. M. Tsimberidou, S. Fu, S. Piha-Paul, V. Subbiah, D. D. Karp, A. Naing, A. K. Krug, D. Enderle, T. Priewasser, M. Noerholm, E. Eitan, C. Coticchia, G. Stoll, L. M. Jordan, C. Eng, S. Kopetz, J. Skog, F. Meric-Bernstam, and F. Janku. 2017. Liquid Biopsies Using Plasma Exosomal Nucleic Acids and Plasma Cell-Free DNA compared with Clinical Outcomes of Patients with Advanced Cancers. *Clinical cancer research : an official journal of the American Association for Cancer Research*.

160. Earl, J., S. Garcia-Nieto, J. C. Martinez-Avila, J. Montans, A. Sanjuanbenito, M. Rodriguez-Garrote, E. Lisa, E. Mendia, E. Lobo, N. Malats, A. Carrato, and C. Guillen-Ponce. 2015. Circulating tumor cells (Ctc) and kras mutant circulating free Dna (cfdna) detection in peripheral blood as biomarkers in patients diagnosed with exocrine pancreatic cancer. *BMC cancer* 15: 797.

161. Hadano, N., Y. Murakami, K. Uemura, Y. Hashimoto, N. Kondo, N. Nakagawa, T. Sueda, and E. Hiyama. 2016. Prognostic value of circulating tumour DNA in patients undergoing curative resection for pancreatic cancer. *British journal of cancer* 115: 59-65.

162.   Cohen, J. D., A. A. Javed, C. Thoburn, F. Wong, J. Tie, P. Gibbs, C. M. Schmidt, M. T. Yip-Schneider, P. J. Allen, M. Schattner, R. E. Brand, A. D. Singhi, G. M. Petersen, S. M. Hong, S. C. Kim, M. Falconi, C. Doglioni, M. J. Weiss, N. Ahuja, J. He, M. A. Makary, A. Maitra, S. M. Hanash, M. Dal Molin, Y. Wang, L. Li, J. Ptak, L. Dobbyn, J. Schaefer, N. Silliman, M. Popoli, M. G. Goggins, R. H. Hruban, C. L. Wolfgang, A. P. Klein, C. Tomasetti, N. Papadopoulos, K. W. Kinzler, B. Vogelstein, and A. M. Lennon. 2017. Combined circulating tumor DNA and protein biomarker-based liquid biopsy for the earlier detection of pancreatic cancers. *Proc Natl Acad Sci U S A* 114: 10202-10207.

163.   Cohen, J. D., L. Li, Y. Wang, C. Thoburn, B. Afsari, L. Danilova, C. Douville, A. A. Javed, F. Wong, A. Mattox, R. H. Hruban, C. L. Wolfgang, M. G. Goggins, M. Dal Molin, T. L. Wang, R. Roden, A. P. Klein, J. Ptak, L. Dobbyn, J. Schaefer, N. Silliman, M. Popoli, J. T. Vogelstein, J. D. Browne, R. E. Schoen, R. E. Brand, J. Tie, P. Gibbs, H. L. Wong, A. S. Mansfield, J. Jen, S. M. Hanash, M. Falconi, P. J. Allen, S. Zhou, C. Bettegowda, L. A. Diaz, Jr., C. Tomasetti, K. W. Kinzler, B. Vogelstein, A. M. Lennon, and N. Papadopoulos. 2018. Detection and localization of surgically resectable cancers with a multi-analyte blood test. *Science* 359: 926-930.

164.   Tjensvoll, K., M. Lapin, T. Buhl, S. Oltedal, K. Steen-Ottosen Berry, B. Gilje, J. A. Soreide, M. Javle, O. Nordgard, and R. Smaaland. 2016. Clinical relevance of circulating KRAS mutated DNA in plasma from patients with advanced pancreatic cancer. *Mol Oncol* 10: 635-643.

165.   Cloyd, J. M., H. Wang, M. E. Egger, C. D. Tzeng, L. R. Prakash, A. Maitra, G. R. Varadhachary, R. Shroff, M. Javle, D. Fogelman, R. A. Wolff, M. J. Overman, E. J. Koay, P. Das, J. M. Herman, M. P. Kim, J. N. Vauthey, T. A. Aloia, J. B. Fleming, J. E. Lee, and

M. H. G. Katz. 2017. Association of Clinical Factors With a Major Pathologic Response Following Preoperative Therapy for Pancreatic Ductal Adenocarcinoma. *JAMA Surg* 152: 1048-1056.

166.   Chae, Y. K., A. A. Davis, S. Jain, C. Santa-Maria, L. Flaum, N. Beaubier, L. C. Platanias, W. Gradishar, F. J. Giles, and M. Cristofanilli. 2017. Concordance of Genomic Alterations by Next-Generation Sequencing in Tumor Tissue versus Circulating Tumor DNA in Breast Cancer. *Mol Cancer Ther* 16: 1412-1420.

167.   Schwaederle, M., H. Husain, P. T. Fanta, D. E. Piccioni, S. Kesari, R. B. Schwab, S. P. Patel, O. Harismendy, M. Ikeda, B. A. Parker, and R. Kurzrock. 2016. Use of Liquid Biopsies in Clinical Oncology: Pilot Experience in 168 Patients. *Clin Cancer Res* 22: 5497-5505.

168.   Villaflor, V., B. Won, R. Nagy, K. Banks, R. B. Lanman, A. Talasaz, and R. Salgia. 2016. Biopsy-free circulating tumor DNA assay identifies actionable mutations in lung cancer. *Oncotarget* 7: 66880-66891.

169.   Hahn, A. W., D. M. Gill, B. Maughan, A. Agarwal, L. Arjyal, S. Gupta, J. Streeter, E. Bailey, S. K. Pal, and N. Agarwal. 2017. Correlation of genomic alterations assessed by next-generation sequencing (NGS) of tumor tissue DNA and circulating tumor DNA (ctDNA) in metastatic renal cell carcinoma (mRCC): potential clinical implications. *Oncotarget* 8: 33614-33620.

170.   Kuderer, N. M., K. A. Burton, S. Blau, A. L. Rose, S. Parker, G. H. Lyman, and C. A. Blau. 2017. Comparison of 2 Commercially Available Next-Generation Sequencing Platforms in Oncology. *JAMA Oncol* 3: 996-998.

171.   Toor, O. M., Z. Ahmed, W. Bahaj, U. Boda, L. S. Cummings, M. E. McNally, K. F. Kennedy, T. J. Pluard, A. Hussain, J. Subramanian, and A. Masood. 2018. Correlation

of Somatic Genomic Alterations Between Tissue Genomics and ctDNA Employing

Next Generation Sequencing: Analysis of Lung and Gastrointestinal Cancers. *Mol*

Cancer Ther.

172. Chantrill, L. A., A. M. Nagrial, C. Watson, A. L. Johns, M. Martyn-Smith, S. Simpson, S.

Mead, M. D. Jones, J. S. Samra, A. J. Gill, N. Watson, V. T. Chin, J. L. Humphris, A. Chou,

B. Brown, A. Morey, M. Pajic, S. M. Grimmond, D. K. Chang, D. Thomas, L. Sebastian,

K. Sjoquist, S. Yip, N. Pavlakis, R. Asghari, S. Harvey, P. Grimison, J. Simes, A. V.

Biankin, I. Australian Pancreatic Cancer Genome, and G. the Individualized

Molecular Pancreatic Cancer Therapy Trial Management Committee of the

Australasian Gastrointestinal Trials. 2015. Precision Medicine for Advanced

Pancreas Cancer: The Individualized Molecular Pancreatic Cancer Therapy

(IMPaCT) Trial. *Clinical cancer research : an official journal of the American*

Association for Cancer Research.

173. Taly, V., D. Pekin, L. Benhaim, S. K. Kotsopoulos, D. Le Corre, X. Li, I. Atochin, D. R.

Link, A. D. Griffiths, K. Pallier, H. Blons, O. Bouche, B. Landi, J. B. Hutchison, and P.

Laurent-Puig. 2013. Multiplex picodroplet digital PCR to detect KRAS mutations in

circulating DNA from the plasma of colorectal cancer patients. *Clinical chemistry* 59:

1722-1731.

174. Lanman, R. B., S. A. Mortimer, O. A. Zill, D. Sebisanovic, R. Lopez, S. Blau, E. A.

Collisson, S. G. Divers, D. S. Hoon, E. S. Kopetz, J. Lee, P. G. Nikolinakos, A. M. Baca, B.

G. Kermani, H. Eltoukhy, and A. Talasaz. 2015. Analytical and Clinical Validation of a

Digital Sequencing Panel for Quantitative, Highly Accurate Evaluation of Cell-Free

Circulating Tumor DNA. *PloS one* 10: e0140712.

175.   Zill, O. A., C. Greene, D. Sebisanovic, L. M. Siew, J. Leng, M. Vu, A. E. Hendifar, Z. Wang, C. E. Atreya, R. K. Kelley, K. Van Loon, A. H. Ko, M. A. Tempero, T. G. Bivona, P. N. Munster, A. Talasaz, and E. A. Collisson. 2015. Cell-Free DNA Next-Generation Sequencing in Pancreatobiliary Carcinomas. *Cancer discovery* 5: 1040-1048.

176.   Chan, K. C., P. Jiang, Y. W. Zheng, G. J. Liao, H. Sun, J. Wong, S. S. Siu, W. C. Chan, S. L. Chan, A. T. Chan, P. B. Lai, R. W. Chiu, and Y. M. Lo. 2013. Cancer genome scanning in plasma: detection of tumor-associated copy number aberrations, single-nucleotide variants, and tumoral heterogeneity by massively parallel sequencing. *Clinical chemistry* 59: 211-224.

177.   Butler, T. M., K. Johnson-Camacho, M. Peto, N. J. Wang, T. A. Macey, J. E. Korkola, T. M. Koppie, C. L. Corless, J. W. Gray, and P. T. Spellman. 2015. Exome Sequencing of Cell-Free DNA from Metastatic Cancer Patients Identifies Clinically Actionable Mutations Distinct from Primary Disease. *PloS one* 10: e0136407.

178.   Fleischhacker, M. 2006. Biology of circulating mRNA: still more questions than answers? *Annals of the New York Academy of Sciences* 1075: 40-49.

179.   Thery, C., L. Zitvogel, and S. Amigorena. 2002. Exosomes: composition, biogenesis and function. *Nature reviews. Immunology* 2: 569-579.

180.   Kahlert, C., and R. Kalluri. 2013. Exosomes in tumor microenvironment influence cancer progression and metastasis. *Journal of molecular medicine* 91: 431-437.

181.   Consortium, G. 2015. The Genotype-Tissue Expression (GTEx) pilot analysis: multitissue gene regulation in humans. *Science* 348: 648-660.

182.   Overwijk, W. W., E. Wang, F. M. Marincola, H. G. Rammensee, and N. P. Restifo. 2013. Mining the mutanome: developing highly personalized Immunotherapies based on mutational analysis of tumors. *Journal for immunotherapy of cancer* 1: 11.

183. Schumacher, T. N., and R. D. Schreiber. 2015. Neoantigens in cancer immunotherapy. *Science* 348: 69-74.

184. Balia, C., A. Galli, and M. A. Caligo. 2011. Effect of the overexpression of BRCA2 unclassified missense variants on spontaneous homologous recombination in human cells. *Breast cancer research and treatment* 129: 1001-1009.

185. Lowery, M. A., D. P. Kelsen, Z. K. Stadler, K. H. Yu, Y. Y. Janjigian, E. Ludwig, D. R. D'Adamo, E. Salo-Mullen, M. E. Robson, P. J. Allen, R. C. Kurtz, and E. M. O'Reilly. 2011. An emerging entity: pancreatic adenocarcinoma associated with a known BRCA mutation: clinical descriptors, treatment implications, and future directions. *The oncologist* 16: 1397-1402.

186. Henjes, F., C. Bender, S. von der Heyde, L. Braun, H. A. Mannsperger, C. Schmidt, S. Wiemann, M. Hasmann, S. Aulmann, T. Beissbarth, and U. Korf. 2012. Strong EGFR signaling in cell line models of ERBB2-amplified breast cancer attenuates response towards ERBB2-targeting drugs. *Oncogenesis* 1: e16.

187. Tran, E., S. Turcotte, A. Gros, P. F. Robbins, Y. C. Lu, M. E. Dudley, J. R. Wunderlich, R. P. Somerville, K. Hogan, C. S. Hinrichs, M. R. Parkhurst, J. C. Yang, and S. A. Rosenberg. 2014. Cancer immunotherapy based on mutation-specific CD4+ T cells in a patient with epithelial cancer. *Science* 344: 641-645.

188. Gerlinger, M., S. Horswell, J. Larkin, A. J. Rowan, M. P. Salm, I. Varela, R. Fisher, N. McGranahan, N. Matthews, C. R. Santos, P. Martinez, B. Phillimore, S. Begum, A. Rabinowitz, B. Spencer-Dene, S. Gulati, P. A. Bates, G. Stamp, L. Pickering, M. Gore, D. L. Nicol, S. Hazell, P. A. Futreal, A. Stewart, and C. Swanton. 2014. Genomic architecture and evolution of clear cell renal cell carcinomas defined by multiregion sequencing. *Nature genetics* 46: 225-233.

189. Kalluri, R. 2016. The biology and function of fibroblasts in cancer. *Nature reviews. Cancer* 16: 582-598.

190. Costa-Silva, B., N. M. Aiello, A. J. Ocean, S. Singh, H. Zhang, B. K. Thakur, A. Becker, A. Hoshino, M. T. Mark, H. Molina, J. Xiang, T. Zhang, T. M. Theilen, G. Garcia-Santos, C. Williams, Y. Ararso, Y. Huang, G. Rodrigues, T. L. Shen, K. J. Labori, I. M. Lothe, E. H. Kure, J. Hernandez, A. Doussot, S. H. Ebbesen, P. M. Grandgenett, M. A. Hollingsworth, M. Jain, K. Mallya, S. K. Batra, W. R. Jarnagin, R. E. Schwartz, I. Matei, H. Peinado, B. Z. Stanger, J. Bromberg, and D. Lyden. 2015. Pancreatic cancer exosomes initiate pre-metastatic niche formation in the liver. *Nature cell biology* 17: 816-826.

191. Melo, S. A., H. Sugimoto, J. T. O'Connell, N. Kato, A. Villanueva, A. Vidal, L. Qiu, E. Vitkin, L. T. Perelman, C. A. Melo, A. Lucci, C. Ivan, G. A. Calin, and R. Kalluri. 2014. Cancer exosomes perform cell-independent microRNA biogenesis and promote tumorigenesis. *Cancer cell* 26: 707-721.

192. Yang, K. S., H. Im, S. Hong, I. Pergolini, A. F. Del Castillo, R. Wang, S. Clardy, C. H. Huang, C. Pille, S. Ferrone, R. Yang, C. M. Castro, H. Lee, C. F. Del Castillo, and R. Weissleder. 2017. Multiparametric plasma EV profiling facilitates diagnosis of pancreatic malignancy. *Sci Transl Med* 9.

193. Kobiyama, K., F. Takeshita, N. Jounai, A. Sakaue-Sawano, A. Miyawaki, K. J. Ishii, T. Kawai, S. Sasaki, H. Hirano, N. Ishii, K. Okuda, and K. Suzuki. 2010. Extrachromosomal histone H2B mediates innate antiviral immune responses induced by intracellular double-stranded DNA. *Journal of virology* 84: 822-832.

194. Choi, Y. S., J. Hoon Jeong, H. K. Min, H. J. Jung, D. Hwang, S. W. Lee, and Y. Kim Pak. 2011. Shot-gun proteomic analysis of mitochondrial D-loop DNA binding proteins: identification of mitochondrial histones. *Molecular bioSystems* 7: 1523-1536.

195. Kobiyama, K., A. Kawashima, N. Jounai, F. Takeshita, K. J. Ishii, T. Ito, and K. Suzuki. 2013. Role of Extrachromosomal Histone H2B on Recognition of DNA Viruses and Cell Damage. *Frontiers in genetics* 4: 91.

196. Sugiura, A., G. L. McLelland, E. A. Fon, and H. M. McBride. 2014. A new pathway for mitochondrial quality control: mitochondrial-derived vesicles. *The EMBO journal* 33: 2142-2156.

197. Nigjeh, E. N., R. Chen, Y. Allen-Tamura, R. E. Brand, T. A. Brentnall, and S. Pan. 2017. Spectral library-based glycopeptide analysis-detection of circulating galectin-3 binding protein in pancreatic cancer. *Proteomics Clin Appl*.

198. Nichols, L. S., R. Ashfaq, and C. A. Iacobuzio-Donahue. 2004. Claudin 4 protein expression in primary and metastatic pancreatic cancer: support for use as a therapeutic target. *American journal of clinical pathology* 121: 226-230.

199. Neesse, A., A. Hahnenkamp, H. Griesmann, M. Buchholz, S. A. Hahn, A. Maghnouj, V. Fendrich, J. Ring, B. Sipos, D. A. Tuveson, C. Bremer, T. M. Gress, and P. Michl. 2013. Claudin-4-targeted optical imaging detects pancreatic cancer and its precursor lesions. *Gut* 62: 1034-1043.

200. Ligthart, S. T., F. A. Coumans, F. C. Bidard, L. H. Simkens, C. J. Punt, M. R. de Groot, G. Attard, J. S. de Bono, J. Y. Pierga, and L. W. Terstappen. 2013. Circulating Tumor Cells Count and Morphological Features in Breast, Colorectal and Prostate Cancer. *PloS one* 8: e67148.

201.   Kalra, H., R. J. Simpson, H. Ji, E. Aikawa, P. Altevogt, P. Askenase, V. C. Bond, F. E. Borras, X. Breakefield, V. Budnik, E. Buzas, G. Camussi, A. Clayton, E. Cocucci, J. M. Falcon-Perez, S. Gabrielsson, Y. S. Gho, D. Gupta, H. C. Harsha, A. Hendrix, A. F. Hill, J. M. Inal, G. Jenster, E. M. Kramer-Albers, S. K. Lim, A. Llorente, J. Lotvall, A. Marcilla, L. Mincheva-Nilsson, I. Nazarenko, R. Nieuwland, E. N. Nolte-'t Hoen, A. Pandey, T. Patel, M. G. Piper, S. Pluchino, T. S. Prasad, L. Rajendran, G. Raposo, M. Record, G. E. Reid, F. Sanchez-Madrid, R. M. Schiffelers, P. Siljander, A. Stensballe, W. Stoorvogel, D. Taylor, C. Thery, H. Valadi, B. W. van Balkom, J. Vazquez, M. Vidal, M. H. Wauben, M. Yanez-Mo, M. Zoeller, and S. Mathivanan. 2012. Vesiclepedia: a compendium for extracellular vesicles with continuous community annotation. *PLoS biology* 10: e1001450.

202.   Liang, K., F. Liu, J. Fan, D. Sun, C. Liu, C. J. Lyon, D. W. Bernard, Y. Li, K. Yokoi, M. H. Katz, E. J. Koay, Z. Zhao, and Y. Hu. 2017. Nanoplasmonic Quantification of Tumor-derived Extracellular Vesicles in Plasma Microsamples for Diagnosis and Treatment Monitoring. *Nat Biomed Eng* 1.

203.   Kanwar, S. S., C. J. Dunlay, D. M. Simeone, and S. Nagrath. 2014. Microfluidic device (ExoChip) for on-chip isolation, quantification and characterization of circulating exosomes. *Lab Chip* 14: 1891-1900.

204.   Takahashi, A., R. Okada, K. Nagao, Y. Kawamata, A. Hanyu, S. Yoshimoto, M. Takasugi, S. Watanabe, M. T. Kanemaki, C. Obuse, and E. Hara. 2017. Exosomes maintain cellular homeostasis by excreting harmful DNA from cells. *Nat Commun* 8: 15287.

205.   Chaudhuri, A. A., J. J. Chabon, A. F. Lovejoy, A. M. Newman, H. Stehr, T. D. Azad, M. S. Khodadoust, M. S. Esfahani, C. L. Liu, L. Zhou, F. Scherer, D. M. Kurtz, C. Say, J. N.

Carter, D. J. Merriott, J. C. Dudley, M. S. Binkley, L. Modlin, S. K. Padda, M. F. Gensheimer, R. B. West, J. B. Shrager, J. W. Neal, H. A. Wakelee, B. W. Loo, Jr., A. A. Alizadeh, and M. Diehn. 2017. Early Detection of Molecular Residual Disease in Localized Lung Cancer by Circulating Tumor DNA Profiling. *Cancer Discov* 7: 1394-1403.

206.   Cristofanilli, M., G. T. Budd, M. J. Ellis, A. Stopeck, J. Matera, M. C. Miller, J. M. Reuben, G. V. Doyle, W. J. Allard, L. W. Terstappen, and D. F. Hayes. 2004. Circulating tumor cells, disease progression, and survival in metastatic breast cancer. *N Engl J Med* 351: 781-791.

VITA

Vincent Bernard Pagan was born in San Juan, Puerto Rico, the son of Victor Bernard and Lillibeth Pagan. After completed his high school education at Colegio San Ignacio de Loyola, San Juan, PR in 2005, he entered Johns Hopkins University in Baltimore, MD. He received a degree of Bachelor in Science with a major in Chemical and Biomolecular Engineering from JHU in May, 2009. He then went on the complete a Master in Science in Biotechnology from JHU in May, 2010. On August of 2011 he entered into a MD/PhD program through a U54 Partnership in Excellence grant between the University of Puerto Rico School of Medicine and The University of Texas MD Anderson Cancer Center UTHealth Graduate School of Biomedical Sciences.